

Eko Adhi Setiawan

Concept and Controllability of Virtual Power Plant

This work has been accepted by the faculty of electrical engineering / computer science of the University of Kassel as a thesis for acquiring the academic degree of Doktor der Ingenieurwissenschaften (Dr.-Ing.).

Supervisor: Prof. Dr.-Ing Jürgen Schmid
Co-Supervisor: Dr. rer. nat Thomas Degner

Defense day:

27th April 2007

The publication was funded by Deutscher Akademischer Austausch Dienst
Gedruckt mit Unterstützung des Deutschen Akademischen Austausch Dienstes

Bibliographic information published by Deutsche Nationalbibliothek
Die Deutsche Nationalbibliothek lists this publication in the Deutsche Nationalbibliografie;
detailed bibliographic data is available in the Internet at <http://dnb.ddb.de>

Zugl.: Kassel, Univ., Diss. 2007
ISBN: 978-3-89958-309-0
URN: urn:nbn:de:0002-3096

© 2007, kassel university press GmbH, Kassel
www.upress.uni-kassel.de

Printed by: Unidruckerei, University of Kassel
Printed in Germany

Abstract / Zusammenfassung

Keywords: Virtual Power Plant, Aggregation Control, Distributed Generation, Communication, Optimum Efficiency

In the end of 20th century the conception of electrical power supply is morphing gradually from centralized into decentralized system, indicated by increasing the installation of distributed generation on the main grid. With emerging of advanced communication and information technology, the aggregation control of several DG units can be developed as virtual power plant in order to provide added-value to the electric power system.

This thesis presents definitions and types of Virtual Power Plants (VPP), then developing control through numerical simulation. The thesis proposes three DG controls namely Basic Autocontrol System (BAS), Smart Autocontrol System (SAS) and Tracking Efficiency Autocontrol System (TEAS). The BAS controls the DG output power with the objective to cover the local load demand. The drawback of this system is that the coordination among DG units is not established yet. In contrast to the BAS, the SAS has a control coordination centre which is responsible of controlling a certain number of DG units. The SAS controls and coordinates the operation of the dedicated DG units in order to minimize power exchange with the superior grid. However the efficiency issue is not considered at two previous control systems, therefore the TEAS was developed. Principally this system is similar to the SAS in terms of information exchange but additionally optimizes the operation efficiency of DG units. This is accomplished by tracking the systems' most efficient operation point. All control systems have been implemented into a simulation environment. The simulation results show that all developed control systems are capable to minimize the power exchange with the superior grid. The systems are able to follow changing load conditions. Furthermore the simulation results prove the ability of TEAS to optimize the system efficiency.

Finally the contribution of VPP to voltage regulation is investigated with several scenarios. The influence of both, active and reactive power injection by DG units on the voltage profile is studied in a test network.

List of Contents

Abstract / Zusammenfassung

List of contents	i
List of figures	iv
List of tables	vii
1. Chapter 1. Introduction	
1.1 Motivation	1
1.2 Research objectives	5
1.3 Research approach	5
1.4 Thesis overview	6
2. Chapter 2. Concept of Virtual Power Plant (VPP)	
2.1 Short history and evolution of electrical supply	7
2.2 A review of Virtual Power Plant definition	8
2.3 Components of ideal Virtual Power Plant	9
2.4 Interfaces and interconnection configuration	13
2.5 Types of Virtual Power Plant	16
3. Chapter 3. Developing model of Virtual Power Plant	
3.1 Components of the VPP in simulation	21
3.1.1 Main grid model	21
3.1.2 Distributed generation model	24
3.1.3 Three phase dynamic load model	30
3.1.4 Measurement unit (data acquisition)	32
4. Chapter 4. Virtual Power Plant under Autocontrol System	
4.1 Concept of Basic Autocontrol System	34
4.2 Simulation scenarios	41
4.3 The concept of Smart Autocontrol System	46
4.4 The analysis of dispatching DG power under SAS	48
4.4.1 Dispatching power in 1 st sequence	48
4.4.2 Dispatching power in 2 nd sequence	50
4.4.3 Dispatching power in 3 rd sequence	51
5. Chapter 5. Tracking optimum efficiency of VPP	
5.1 Efficiency curve of distributed generation	54

List of Contents

5.2 Developing logic algorithms	57
5.2.1 Formulation of power output of DG1 according to the logic algorithm	57
5.2.2 Formulation of power output of DG2 according to the logic algorithm	59
5.2.3 Formulation of power output of DG3 according to the logic algorithm	60
5.3 The analysis of tracking efficiency and dispatching power according to TEAS algorithm	61
5.3.1 Tracking efficiency and dispatching power in 1 st sequence	61
5.3.2 Tracking efficiency and dispatching power in 2 nd sequence	62
5.3.3 Tracking efficiency and dispatching power in 3 rd sequence	64
5.4 Comparison result of BAS, SAS and TEAS according to efficiency of VPP	70
5.4.1 Comparison at load 1	70
5.4.2 Comparison at load 2	71
5.4.3 Comparison at load 3	72
5.5 General equation of Tracking Autocontrol System	74
5.6 Conclusion	76
6. Chapter 6. VPP contribution to voltage regulation	
6.1 Introduction	78
6.2 The simulation and scenarios	79
6.2.1 Simulation one DG unit parallel with main grid	80
6.2.2 Simulation two DG units parallel with main grid	83
6.2.3 Simulation three DG units parallel with main grid	87
6.2.4 The voltage profile of three DG units under BAS, SAS and TEAS	90
6.3. Conclusion	92
7. Conclusion	
7.1 Conclusion	93
7.2 Relevant contribution and further work	94
9. List of references	95
10. Appendixes	
10.1 Appendix A. Calculation of R-L-C	98
10.2 Appendix B. Resistance and Inductance of Transformer	99
10.3 Appendix C.VPP under SAS (Matlab Simulink Environment)	100
10.4 Appendix D. SAS Logic Algorithm	101
10.5 Appendix E. VPP under TEAS	102

List of Contents

10.6 Appendix F. TEAS Logic Algorithm and flow chart at LC 1	103
10.7 Appendix G. TEAS Logic Algorithm and flow chart at LC 2	104
10.8 Appendix H. TEAS Logic Algorithm and flow chart at LC 3	105
10.9 Appendix I. Relation equation (1),(2),(3) and (4)	106
10.10 Appendix J. Three DG units with three variation of efficiency curves	107
10.11 Appendix K. Setting of DG power parameter at LIL, LEL, TIL and TEL blocks (case DG1)	108
10.12 Appendix K. Setting of DG power parameter at LIL, LEL, TIL and TEL blocks (case DG2)	109
10.13 Appendix K. Setting of DG power parameter at LIL, LEL, TIL and TEL blocks (case DG3)	110

List of Figures

Figure 1.Continuous growth of energy consumption	2
Figure 2.Projected global carbon emission	2
Figure 3.Traditional conception	3
Figure 4.New conception	3
Figure 5.Power flow from main supply with and without DG	4
Figure 6.Evolution of electrical power supply	7
Figure 7.DG interfaces	13
Figure 8.Configuration 1	15
Figure 9.Configuration 2	15
Figure 10.Configuration 3	15
Figure 11.Configuration 4	16
Figure 12.Centralised control of Virtual Power Plant	18
Figure 13.Decentralised control of Virtual Power Plant	18
Figure 14.Types of VPP concerning the control topology	20
Figure 15.Centralised VPP and main grid	21
Figure 16.Three phase block	21
Figure 17.Medium voltage transmission and distribution line	22
Figure 18.Transformer step down	23
Figure 19.Fix load model	24
Figure 20.DG unit and controller model	24
Figure 21.Input and output of Distributed Generation Control	25
Figure 22.The input and output of hydraulic turbine and governor system	26
Figure 23.The hydraulic turbine block	27
Figure 24.The gate servo motor block	27
Figure 25.Droop governor block diagram	28
Figure 26.Excitation system block	30
Figure 27.Dynamics load model	30
Figure 28.Profile of active power demand of load 1	31
Figure 29.Profile of active power demand of load 2	31
Figure 30.Profile of active power demand of load 3	32
Figure 31.Measurement block and data acquisition	32

Figure 32.The illustration of Basic Autocontrol System (BAS)	34
Figure 33.Schematic diagram of Basic Autocontrol System	35
Figure 34.The BAS in Matlab Simulink environment	35
Figure 35.Ramp down test result	36
Figure 36.Active power vs Speed reference	36
Figure 37.Active power vs gate characteristics	37
Figure 38.The schematic block of Basic Autocontrol System in detail	38
Figure 39.The active power output follows the dynamic load	39
Figure 40.Electromagnetic torque and Load angle	40
Figure 41.Frequency	40
Figure 42.Profile of three dynamics loads	41
Figure 43.Grid power import to cover the total loads	42
Figure 44.Total three loads demand vs Total power of three DG units with constant full power output	42
Figure 45.Power output and demand of three DG units at constant full power output	43
Figure 46.Power output and demand of three DG units under BAS	45
Figure 47.Total three loads demand and total power output of three DG units with BAS	46
Figure 48.Smart Autocontrol System (SAS)	47
Figure 49.Simplicity logic algorithm in CCC	47
Figure 50.Power output and demand of DG 1 under SAS	48
Figure 51.Power output and demand of DG 2 under SAS	49
Figure 52.Power output and demand of DG 3 under SAS	49
Figure 53.Dispatching power of three DG units in 1 st sequence	50
Figure 54.Dispatching power of three DG units in 2 nd and 3 rd sequences	51
Figure 55.A.Total loads demand and total power of VPP under SAS, B. Power metering (from main grid side)	52
Figure 56.Efficiency curve of the DG	54
Figure 57.The simplicity diagram of decentralised VPP	55
Figure 58.TEAS logic algorithm of local controller 1	56
Figure 59.Power dispatching of three DG units under TEAS in 1 st sequence	61
Figure 60.Power dispatching of three DG units under TEAS in 2 nd sequence	62
Figure 61.Power dispatching of three DG units under TEAS in 3 rd sequence	64

List of Figures

Figure 62.Power sharing and tracking efficiency at load 1	66
Figure 63.Power sharing and tracking efficiency at load 2	67
Figure 64.Power sharing and tracking efficiency at load 3	68
Figure 65.A. Total loads demand and total power of VPP under TEAS, b. Power metering (from main grid side)	69
Figure 66.Comparison of efficiency at load 1	70
Figure 67.Comparison of efficiency at load 2	71
Figure 68.Comparison of efficiency at load 3	72
Figure 69.Summary of efficiency comparison under BAS, SAS and TEAS	74
Figure 70.Principle of signal exchange under TEAS for three local controllers	75
Figure 71.Profile of load 1 and load 3	79
Figure 72.Profile of load 2	79
Figure 73.Installation one DG unit at variation location	80
Figure 74.Voltage profile after installation one DG unit at location A	81
Figure 75.Voltage profile after installation one DG unit at location B	81
Figure 76.Voltage profile after installation one DG unit at location C	82
Figure 77.Reactive power from DG unit at location A or C	83
Figure 78.Reactive power from DG unit at location B	83
Figure 79.Location of two DG units with three variation combination	84
Figure 80.Voltage profile after installation two DG unit (combination A)	85
Figure 81.Voltage profile after installation two DG unit (combination B)	85
Figure 82.Voltage profile after installation two DG unit (combination C)	86
Figure 83.Reactive power behaviour of DG 1 and DG 2 (combination A)	86
Figure 84.Reactive power behaviour of DG 1 and DG 2 (combination B)	86
Figure 85.Reactive power behaviour of DG 1 and DG 2 (combination C)	87
Figure 86.Three DG units parallel with main grid	87
Figure 87.Reactive power behaviour and voltage profile of three DG units with gain variation	88
Figure 88.Voltage profile of three DG units with gain excitation variation	89
Figure 89.The correlation between DG units installation and increasing voltage profile	90
Figure 90. Voltage profile without Virtual Power Plant	90
Figure 91. Comparison voltage profile under BAS, SAS and TEAS	91

List of Tables

Table 1.Distribution Generation capabilities and utility interfaces	10
Table 2.Overview of the characteristic of selected decentralized energy technologies	10
Table 3.The important technologies for decentralize electrical supply in application area	11
Table 4.Cycle life and efficiency of different storage system	12
Table 5.Classification of communication Needs and Requirements	12
Table 6.Physical and market interfaces	14
Table 7.Data lines parameters	22
Table 8.Transformer data	23
Table 9.The (m) signals in simulation	26
Table 10.Component of VPP system in simulation	33
Table 11.The DG priority to cover remaining loads	48
Table 12.Power output and DG efficiency	55
Table 13.Detail DG comparison efficiency under BAS, SAS and TEAS	73
Table 14.The summary of comparison result of different types DG control	77

Chapter 1

Introduction

1.1 MOTIVATION

The need for electrical power is never ending as shown in figure 1, because the electrical power is a large part of energy consumption. The world's energy consumption is projected to be nearly double by 2010 in comparison with that in 1990 due to population increases and economic growth in developing countries. World energy reserves are not sufficient to meet such rapidly growing energy demands. The demand for this new energy will be met in the largest part through the burning of fossil fuels, the major source of CO₂ emissions. Ninety percent of the world's fuel is carbonaceous and results in CO₂ emissions. Current CO₂ emissions levels are bad but the real crisis will arrive in the next 100 years as CO₂ emissions rise sharply and largely as shown in figure 2. Therefore the increasing of energy needs is bringing concern about sustainable development and environmental issue, such as the effort to reduce gas emission and greenhouse effect.

Renewable energy systems already reduce GHG emissions from the energy sector, although on a modest scale. Most long-term energy projections show that renewable energy will play a major role in the global energy supply in the second half of the century, with capacity increasing gradually in the first three decades. The analysis of the role of renewable energy in a carbon constrained world had been presented by [1]. The conclusions based on the analysis are:

- Global energy demand will continue to grow, increasing by approximately 60% by 2030 unless major efforts are successful at increasing energy efficiency and reducing overall energy use.
- The domination of fossil fuels in current energy supplies will not automatically change in the next decades unless renewable energy becomes more cost competitive.

A limit to global warming of 2°C above pre-industrial levels can avoid the most serious climate change threats. This level can only be reached with major long-term emission reductions from many different and combined options, including larger renewable energy markets, efficiency improvements, and cleaner fossil fuels [1].

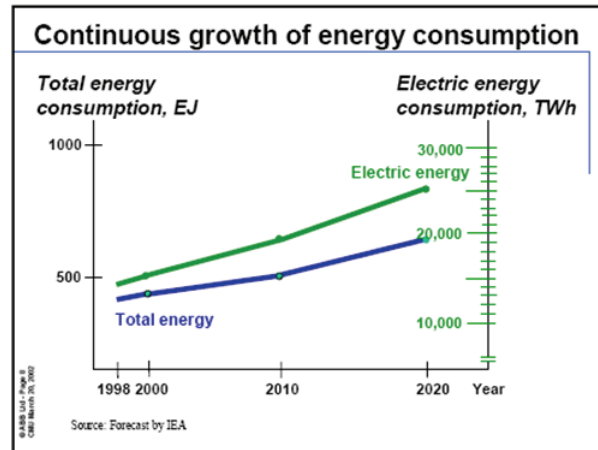


Figure 1. Continuous growth of energy consumption [2]

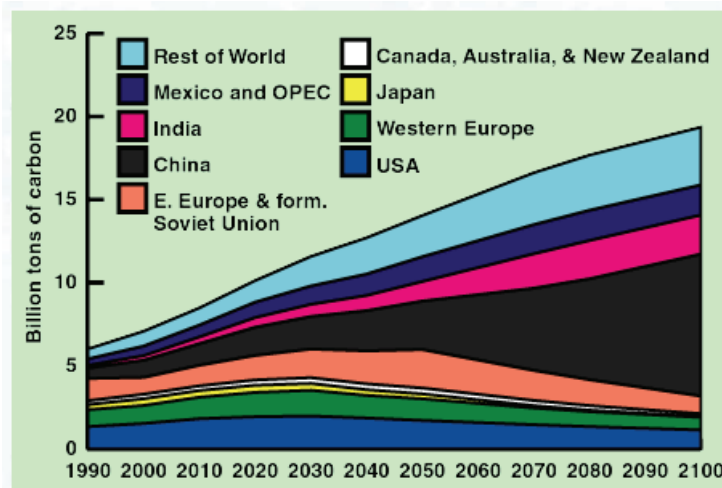


Figure 2. Projected Global Carbon Emission [3]

The share of electricity generated from renewable energy sources for the European Union is targeted to increase from the current 14% to 21% by 2010 (EU, 2002). Policies and actions aimed at increasing the use of renewable energy have been successful in some EU Member States, contributing to growth in electricity generated from renewable energy of 2.8% per year. However, since electricity consumption grew by almost the same rate, the share of renewable energy in electricity generation remained almost constant during the 1990s. Current BAU “Business As Usual” projections for the EU Commission Directorate- General Energy and Transport indicate that the share of renewable energy in power generation will only increase to around 18% by 2030. Consequently, more vigorous policies strongly supporting renewable energy are required to meet the 2010 target, combined with measures to increase energy efficiency and energy conservation [1].

The small scale power generating technology, such as microhydro, photovoltaic, wind turbine and microturbine are gradually replacing conventional / traditional technologies in various applications. They are identified as distributed generation (DG), the DG technology is often lumped with distributed storage and their combination is referred to as distribution energy resources (DER) that represents a modular electric generation or at storage installed customer site. Dispersed generation, a subsection of DER, refers to smaller generating units that are usually installed at customer sites and isolated from a utility system [4]. Many governments have been supporting renewable energy sources for environmental reasons, and the competition on generation imposed by electricity market liberalization has pushed the development of DG technologies and their connection to grids [5].

This situation brings out new conception of electrical supply industry from traditional conception as shown in figure 3 and 4. In traditional conception, the electricity production consisted of four levels; generation, transmission, distribution and consumption. On the other hand, in new conception, the generation of power is not only at first level, thus energy flux is not unidirectional.

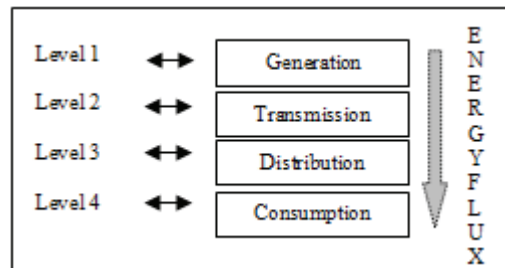


Figure 3. Traditional conception [6]

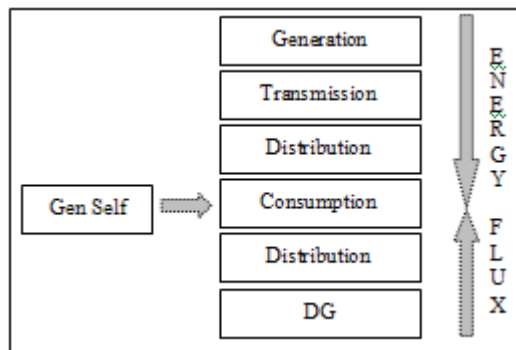


Figure 4. New conception [6]

In recent years with variation of loads and domination of centralized generation with bulk scale capacity, the losses increase and consequently the system reliability decreases.

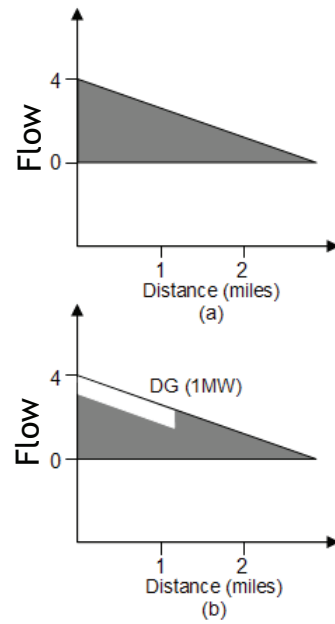


Figure 5. Power flow from main supply with and without DG [7]

Figure 5 shows that the DG units reduce power flow on transmission, and by installing more DG units at distribution level, a part of load can be covered, power import and losses can be reduced. The distributed generations also have many benefits, such as high fuel efficiency [8], short construction lead time, modular installation and low emission, which all contribute to their growing popularity and DG offers great value. It provides a flexible way to choose a wide range of combination of cost and reliability [9] that means it can play a vital role in the impending distributed generation market.

A restructure of electric power supply is likely to include many generators that are not under the direct centralized control of an electric utility. These distributed generations will be operating independently as well as independently owned [8]. Moreover the confluence of deregulating with advanced telecommunications and information technology has straightened new opportunities and penetration of distributed generation. This condition will impact directly the conventional/traditional roles of utilities as energy supplier and consumers as energy users to be morphing rapidly and structure of electrical utility grid will be more complex. For example, power generation is no longer limited to centralized power plants. The technology is available to generate power at all levels, whether at the transmission, distribution, or at the end user levels. Many actors produce and consume power simultaneously, traditional SCADA (Supervisory Control and Data Acquisition) is inadequate to handle, let alone optimize, all possible combinations of power production and consumption [10].

Furthermore, penetration/deployment of DER at main grids emerged new concepts such as Microgrids and Virtual Power Plant (VPP). These concepts are radically different methods for designing and operating power system and also hold the potential for providing the high reliability, quality, security and availability of electrical service required by emerging digital society [11]. Hopefully in the future, coordination and aggregation control of DG units can imply a strengthening of distribution networks, a heterogeneous generation structure, decentralised dispatching and distribution energy network. This is the vision of the concept of virtual power plant.

This thesis presents definition and types of virtual power plant, and demonstrates simulation results of three various controls of distributed generation which is operated parallel with the main grid.

1.2 RESEARCH OBJECTIVES

- The first objective is to make aggregation control of a number of DG units. The first step to achieve this objective is designing concept of virtual power plant through numerical simulation.
- The second objective is to achieve optimum efficiency of VPP and to improve reliability of VPP in term of minimizing import/export power during dynamics load. To achieve these objectives, three types of DG controls (basic autocontrol, smart autocontrol and tracking efficiency autocontrol system) are proposed and implemented in simulation.
- The third objective is to investigate voltage and reactive power behaviour between VPP and main grid. The focus is to know the VPP contribution to voltage regulation.

1.3. RESEARCH APPROACH

The simulation of virtual power plant had been done in Matlab–Simulink environment. The Matlab-Simulink software is widely used in academia and industries for modelling and simulating dynamic system and possible to explore a lot of scenarios. The synchronous machines (SM), hydraulic turbine governor (HTG) and excitation models had been taken from Matlab Simulink library as representation of distributed generation unit. The variation of control system for distributed generation e.g. Basic Autocontrol System (BAS), Smart Autocontrol System (SAS) and Tracking Efficiency Autocontrol System (TEAS) were developed also from toolbox library Matlab Simulink.

I.4 THESIS OVERVIEW

A motivation, research objectives and research approach is discussed in introductory chapter; the subsequent chapters of dissertation are organized as follows:

Chapter 2, *Concept of Virtual Power Plant*, is started with short history and evolution of electrical energy supply from 19th century to 21st century. The chapter then focuses on the reviewing various definition of virtual power plant and continuing description of different kind of interconnection configuration. The last part of this chapter is a summary of definition of virtual power plant and showing two classifications of virtual power plant according to the control topology.

Chapter 3, *Developing Model of Virtual Power Plant*, describes model components of virtual power plant simulation in Matlab Simulink environment. The modelling of component virtual power plant is classified into four major parts: main grid model, distributed generation model, dynamic load model and measurement unit (data acquisition).

Chapter 4, *Virtual Power Plant under Autocontrol System*, introduces and applies in simulation two various control systems of distributed generation. The first control is called basic autocontrol system (BAS). This system is applied to control DG output according to load signal; thereby the DG is enabled to follow the load. The second control is smart autocontrol system (SAS). In contrast with previous control, this system has a control coordination centre (CCC) which is responsible for controlling a several number of DG units. In the last section, the performance of BAS and SAS in following dynamics load is demonstrated by examples.

Chapter 5, *Tracking Optimum Efficiency of Virtual Power Plant*, discusses the controllability of virtual power plant to track the optimum efficiency during dynamics load and improving reliability of VPP in term of minimizing export and import power to the grid. This system is called Tracking Efficiency Autocontrol System (TEAS) which is applied in decentralised topology. By using similarly load profile as in the previous chapter, the comparison performance of BAS, SAS and TEAS is presented in this chapter.

Chapter 6, *Contribution of Virtual Power Plant in Voltage Regulation*, investigates the voltage and reactive power behaviour between VPP and main grid during dynamics load. The focus is to know the contribution of VPP to voltage regulation. To achieve this objective, various scenarios of DG units installation are simulated in this chapter.

Chapter 7 is conclusion of the dissertation.

Chapter 2

Concept of Virtual Power Plant

2.1 Short history and evolution of electrical power supply

The beginning of this chapter is started with summarizes the history and evolution of electric power system. Figure 6 describes the milestone on the evolution.

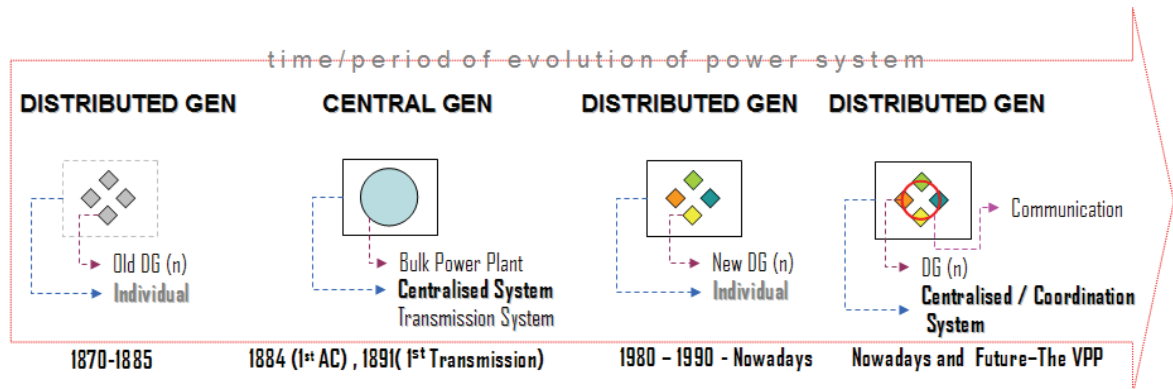


Figure 6. Evolution of electricity power system

From 1870 to 1885 the first electric power systems were distributed with small hydropower and thermal power at capacity under 100 kW [12]. The Grand Rapids Electric Light and Power Company was organized and created the first hydroelectric power plant to furnish arc lighting service in the United States [13].

In 1884 Nikola Tesla invented the electric alternator, an electric generator that produced alternating current. It was beginning of the development of large scale power grids with introduction of three phases AC. The first transmission of three-phase alternating current using high voltage took place in the year 1891 on the occasion of the international electricity exhibition in Frankfurt. In that year, a 25 kV transmission line, approximately 175 kilometres long, was built between Lauffen at the Neckar and Frankfurt [14]. Moreover in 1954 the first atomic power plant was operated to produce more than 5,000 kilowatts of electricity in Russia. Then electrical power plant and transmission gradually enlarged under centralised system. The main tasks of centralized bulk power plant were divided into four issues: a. Transmission of large power/energy quantities, b. Optimisation of the operation, c. Increasing the reliability and d. Make power market possible [12].

In the beginning of 1980 until 1990 the developing and installation of variation distributed generation (e.g. wind and solar) were gradually increasing. In 1941 the first

wind turbine to generate energy for an alternating current central power system was developed and solar cell in 1954. However in the end of the 20th century the evolution of electrical power supply had been changed gradually from centralized into decentralized system. Nowadays the installations of DG units that use renewable or non renewable energy resources are increasing significantly. The drawback of DG at the moment is many DG units are too small to provide value-added benefits to the electric power system [12]. And many of them are operating individually without any coordination with other DG units. With emerging of advanced communication and information technology, the small distributed generation units could to be monitored, controlled and coordinated centrally. Thus the multitude of small DG can be aggregated then treated as a single large power plant.

2.2 A review of Virtual Power Plant definition

The term of Virtual Power Plant (VPP) is interesting, auspicious and also wide; a result of literature review shows that there is no consensus regarding the definition of VPP. Some researchers at electrical company or at research groups have different definition of virtual power plant, even some researchers even used another terminology i.e. virtual utility [11, 15]. Below are some various definitions from several researchers and projects in Europe.

a. Europe Union (EU) Project of Virtual Fuel Cell Power Plant, which supported by several electrical and gas companies defined virtual power plant as a group of interconnected decentralized residential micro CHP (Combined Heat and Power), using fuel cell technology, installed in multi family houses, small enterprises, and public facilities etc., for individual heating, cooling and electricity production [16].

b. Unna public utility company and EUS GmbH Germany with their pilot project virtual power plant described the virtual power plant as overall controlled aggregation of distribution generation resources DER, at different places, if necessary, in distribution networks of different operators network [17].

c. Santjer (Feb.2002) defined VPP as, ein VPP ist eine auf Energie- und Steuerungsebene zusammengeschaltete große Menge an räumlich weit verteilten Energieerzeugern. Das VPP ist in der Lage, Energiemengen und „Vorleistungen zur Bereitstellung von Systemdienstleistungen“ zur Verfügung zu stellen wie ein konventionelles Kraftwerk. Größtes Anlagenteil eines VPP ist das öffentliche Stromversorgungsnetz [18].

d. Koeppel (Nov 2003) wrote that VPP is combining different types of renewable and non renewable generators and storages devices to be able to appear on the market as one power plant with defined hourly output or different power generation and storage devices with diverse weakness (e.g. stochastic output) and strengths (e.g. High energy short term storage) are combined so they cleverly complement [19]

e. The leads to the definition proposed by International Gas Union, the Virtual Power Plant comprises a multitude of decentralized, grid-connected, micro- and mini-CHP (combined heat and power) units using fuel cell, gas turbine, gas engine, steam cell or sterling engine technology, installed in single family or multi-family houses, small enterprises, public facilities, et cetera, for combined individual heating and cooling, and flexible electricity production. The multitude of decentralized units can be centrally controlled and managed as part of an interconnected network, resulting in a virtual power plant that can be operated and act as a distributed large power plant – with great flexibility in terms of fuel choice (natural gas, biogas, LPG, hydrogen) – contributing to meet peaking energy demand in the public electricity sector [20].

The last definition is more comprehensive, it includes technical aspect and economical aspect such as grid connected, central control, electricity production and energy demand. However all definitions as mentioned above do not fully describe VPP in detail yet. Therefore in the following pages the components, types, topology and summarized definition of VPP is presented.

2.3 Components of ideal Virtual Power Plant

The ideal virtual power plant consists of:

a. Generation technology.

The DG specification is useful to broadly mention the range of capabilities for various technologies, generally falling under the distributed generation category as listed in Table 1. The electric power network interface, which plays a major role when considering the network operation aspects related to dispersed generation, is also shown in Table 1. Furthermore, table 2 explains DG technologies connected to loads and bonded to the voltage grids.

Table 1. Distribution generation capabilities and utility interfaces [21]

Technologies	Typical Capability Ranges	Utility interface
Solar / PV	A few to several hundred kW	dc to ac converter
Wind	A few hundred W to a few MW	Asynchronous generator or inverter
Geothermal	A few hundred kW to few MW	Synchronous generator
Ocean	A few hundred kW to few MW	Four-quadr. Synchronous machine
ICE*	A few hundred kW to tens of MW	Synchronous generator or ac to ac converter
Combined cycle	A few tens of MW to several hundred MW	Synchronous generator
Combustion turbine	A few MW to hundreds of MW	Synchronous generator
Micro turbine	A few tens of kW to a few MW	ac to ac converter
Fuel cells	A few tens of kW to a few tens of MW	dc to ac converter

*) Internal Combustion Engine

Table 2. Overview of the characteristic of selected decentralized energy technologies [22]

Technologies	Function in electrical system
Biomass-CHP	Base / medium load bonding with medium / high voltage grid
Geothermal (Hot Dry Rock)	Base / medium load bonding with medium / high voltage grid
Wind energy	Above all substation at medium load bonding with medium voltage grid
Micro gas turbine	Medium or peak load bonding with low voltage grid
Fuel cell unit for house power supply	Medium or peak load bonding with low voltage grid
Large fuel cell	Base/medium load bonding with low and medium voltage grid

Table 3. The important technologies for decentralized electrical supply in application area [23]

Power delivery and distribution	<ul style="list-style-type: none"> • Cable and conductor • Superconducting technologies • High voltage and medium voltage • Switch and electric power station • Semiconductor switch and power electronic • Passive and active grid condition • Grid analyzer • Other power quality techniques • Protection • Energy storage
Network management	<ul style="list-style-type: none"> • Operating systems and software for energy- and network management • systems adapted/lower cost communication : data communication • technology of communication protocols and standard
Energy use	<ul style="list-style-type: none"> • (Interactive) meter • Smart building and intelligent home • uninterruptible power supply

Table 3 listed the important technologies for decentralized electrical supply in three application area: power distribution area, network management area and energy use area.

b. Energy storage technologies

Energy storage systems can be considered today as a new means to adapt the variations of the power demand to the given level of power generation. In context of use renewable energies or other distributed power generation, can be used also as additional sources, or as energy buffers in the case of non schedulable or stochastic generation, e.g. fuel cell and PV technologies especially in weak networks in relation with distributed generation system, and renewable energy sources. The chart of Table 4, gives an introduction of life and efficiency of most used storage technologies.

Table 4. Cycle life and efficiency of different storage system [24], [25]

Storage system	Life (cycles)	Efficiency (%)
Pumped Hydro	75 years	70 - 80
Compressed air	40 years	-
Flow Batteries	1500 – 2500	75 – 85
Metal Air Battery	100 – 200	50
NaS -Sodium Sulfur Battery	2000 – 3000	89
Other advanced batteries	500 – 1500	90 – 95
Lead Acid	300 - 1500	60 - 95
Super capacitors	10000- 100000	93 - 98

c. Information communication technology (ICT).

The important requirement for VPP is communication technologies and infrastructure. The different needs and requirements have been classified into three different main categories reflecting the degree of importance of various communication needs.

Table 5 Classification of communication Needs and Requirements [26]

Real-time Operational Communication	Administrative Operational Communication	Administrative Communication
Real-time operational data communication Tele-protection Power system control Real-time operational voice communication Telephony	Event and disturbances recording Asset management Handling of settlement information Substation camera supervision	Telephony, facsimile Electronic mail

In many different communications media technologies can be considered for communications in Energy Management System (EMS), Supervisory Control and Data Acquisition (SCADA) and Distribution Dispatching Centre Project. And the most appropriate communication technologies available for EMS and SCADA Distributed Dispatching Centre Projects are therefore considered to be priority order [27]:

- Fiber optic cable from the System Master Control Centre to each of the Area Distribution Dispatch Centre (if applicable) and to substations on the fiber optic cable route.
- Microwave or Time Division Multiple Address (TDMA) from the Area Distribution Dispatch Centres to selected substation

- Multiple Address Radio System (MARS) and UHF P-T-P radio in the 450/900 MHz band to remote substations and remote controlled line switches. Some leased circuits for SCADA communication to very remote substations.
- Satellite from the System Master Control Centre (SMC) to each of the ADDCs (if applicable).
- Metallic cable for local or in building application.

2.4 Interfaces and interconnection configuration.

The physical interfaces include a DG unit's interaction with the fuel, electrical infrastructure and a communications interface with a central entity that controls and/or monitors the DG system. Physical interfaces are mainly concerned with issues such as safety, protocols, system impacts, reliability, standards, and metering. The interfaces are not only physical but also in some instances can include a market dimension as well. The market interface covers how the DG unit or its owner interacts or competes with other suppliers in the marketplace. The market interface includes concerns over dispatch, tariffs, pricing signals and business and operational decisions. An overview of the DG interfaces is shown in figure 7.

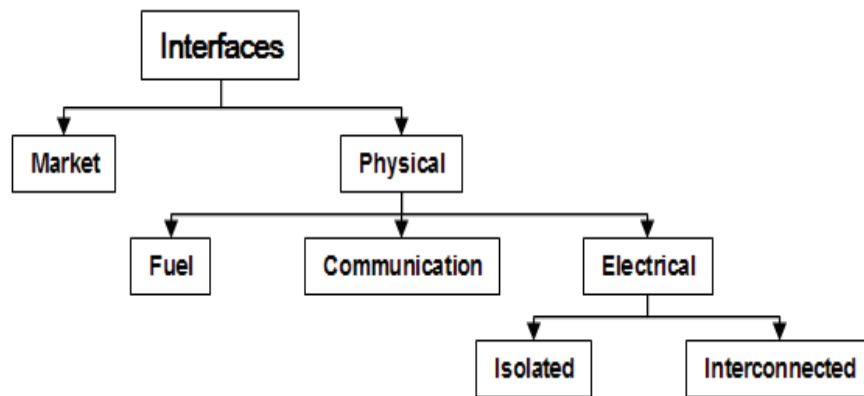


Figure 7. System interfaces of distributed generation [28]

The electrical interface is the means by which the DG unit electrically connects to the power system outside the facility in which the unit is installed. Depending on the application and operation of the DG unit, the interface configuration can range from a complex parallel interconnection, to being non-existent if the DG unit is operated in isolation. The complexity of the interface increases with the level of interaction required between the DG unit/owner and the electrical grid/distribution company. In the future, DG will still need proper interfaces as it does today. However, the kinds of interfaces

are impossible to predict beyond the certainty that they'll most likely change dramatically to facilitate the special characteristics and applications of DG. Table 6 illustrates some possible scenarios for how these interfaces could change.

Table 6. Physical and market interfaces [29]

Interfaces	Today	Possible Future ^(*)
Electrical	<ul style="list-style-type: none"> • Customized interconnection solutions. • Technical requirement vary by utility • Varying levels of complexity in the process and contracts • Process controlled by utility 	<ul style="list-style-type: none"> • Plug and play interconnect solutions <ul style="list-style-type: none"> - Integrated with the DG product - Satisfying all technical standards - Verified and certified by third party • National Standard or state wide standards • Standardized process and contracts that streamlines interconnection making it doable for all customer classes
Fuel	<ul style="list-style-type: none"> • Larger DG units (>1MW) installed upstream in the natural gas distribution system 	<ul style="list-style-type: none"> • Smaller DG units – perhaps to the small commercial or residential level – will be installed further down the natural gas distribution system • Increased throughput and expanded distribution system • Other fuel infrastructure, in addition natural gas, may be developing
Communication	<ul style="list-style-type: none"> • Remote monitoring for O&M purposes 	<ul style="list-style-type: none"> • Development of system, standard and protocols for communication system for: <ul style="list-style-type: none"> - dispatch - control • DG ISO to control and dispatch units
Market	<ul style="list-style-type: none"> • Access through limited tariff only 	<ul style="list-style-type: none"> • Expansion and modification of available tariff to include: <ul style="list-style-type: none"> - sales to grid - ancillary service - choice of back up service • Access to market: <ul style="list-style-type: none"> - real time pricing signals - distribution only tariff

(*) Some points has been realised

The term “interconnection” is often used synonymously with the terms “synchronized operation” or “parallel operation”. In parallel operation, the DG and the grid always connected to the load and hence to each other. Various types of DG interconnection to the utility grids are divided into four configurations:

Configuration 1; *Grid Interconnected with Minimize Power Export and Import*

- DG parallel operation with the grid.
- DG provides peaking or base load power to all or some loads
- DG has no or minimize export of power to the grid and the utility provides supplemental / backup

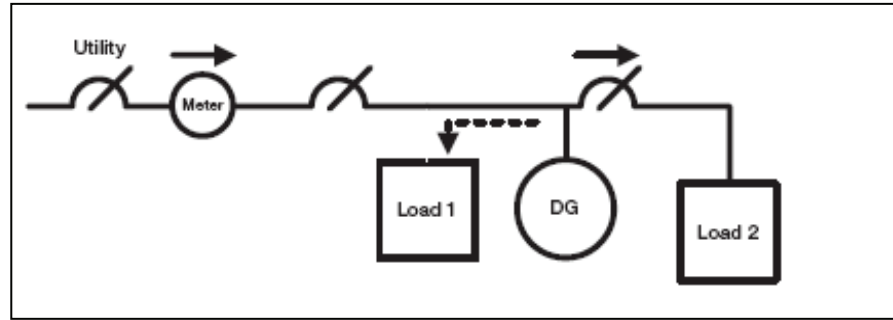


Figure 8.Configuration 1 [29]

Configuration 2; *Grid Interconnection with Power Export – Customer Side*

- DG parallel with the grid
- DG provides peaking or base load power to load and exports power to grid
- Utility may provide supplemental or backup power

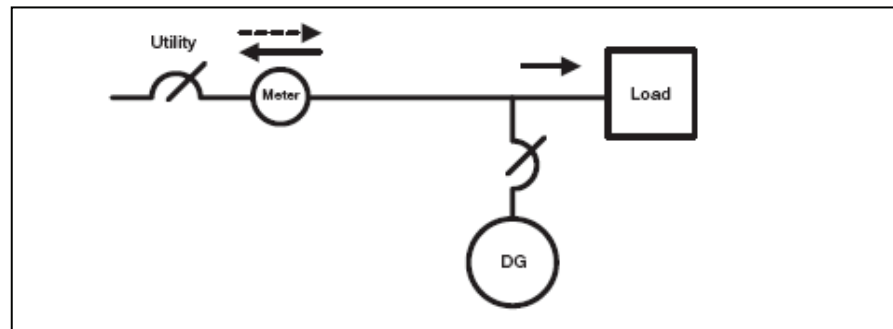


Figure 9.Configuration 2 [29]

Configuration 3; *Grid Interconnection with Power Export – Utility Side*

- DG provides peaking, base load or backup power for utility to provide to customer
- DG operates in parallel with grid

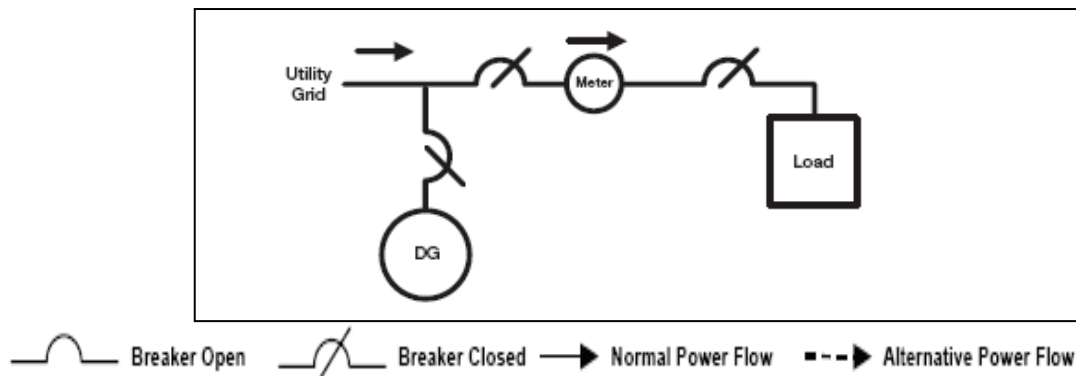


Figure 10.Configuration 3 [29]

Configuration 4; *Roll over operation or isolated with automatic transfer system.*

In rollover design the two sources are never connected together, and only one of the two suppliers is ever connected to the load at any one time. As a result, a brief interruption of service occurs during switching, whenever the main fails and power has to be “rolled over” to the alternate. However, rollover designs require less equipment, simpler and less expensive to operate [9].

- Generator provides power to an isolated customer load (load 2) for peaking, base load or backup power.
- Utility provides power to customer load 1 and occasionally loads 2
- Generator does not operate in parallel.

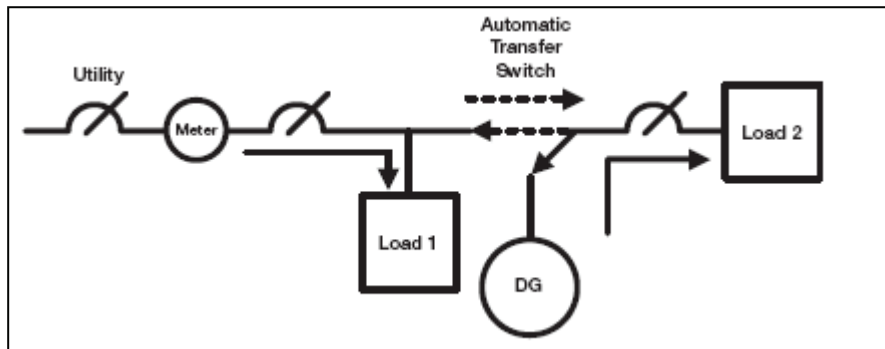


Figure 11. Configuration 4 [29]

2.5 Types of Virtual Power Plant

Due to several definitions of virtual power plant and a review concerning different aspects of distributed generation as mentioned previously, the definition of VPP can be summarized as: **aggregation control of a number of distributed generation units, grid connected and installed near loads. The aggregation control can be centralised or decentralised system supported by logic control algorithm and communication infrastructure, then treated as a single large power plant.**

To clarify the definition some points are explained below:

- The large capacity of DG unit is from a few tens of kW to a few MW.
- The DG units are interconnected to the main grid and installed near the loads.
- The VPP system is supported by fast communication infrastructure in order to guarantee information exchange.
- The control coordination centre/CCC (in centralised system) or local controller/LC (in decentralised system) is the heart of VPP. Both of CCC and

LC are consisted of interface and logic control algorithm which can be developed for some particular purposes. For example tracking optimum efficiency of DG units, controlling DG in order to follow the dynamics load or controlling DG output depends on the dynamics price signal.

Concerning the issue of aggregation control of distributed generations on the electric distribution, Smith et al. [27] wrote some advantages such as:

- Scheduled dispatching power. One advantage of new DER technology is their capability to dispatch power quite rapidly in response to varying utility and local load conditions.
- Load Management – DER can be used to reduce load during peak demand periods. By increasing the power output from these units during high load periods, the stress on central generation as well as local transmission and distribution lines can be relieved.
- Voltage Regulation- by coordinating distribution elements with DER, improved voltage regulation is possible.

In the following paragraphs the types of VPP are divided into two categories according to the control topology:

1. The centralised VPP.

In this category the distributed generation units are centrally controlled by control coordination centre (CCC) which is located right in the centre of DG units. The loads signals are transmitted to the CCC, and processed by means of logic algorithm. Thereafter the signals are dispatched to each DGC (distributed generation controller), and then the active power output is produced according to the CCC signals (see figure 12). With the CCC it is able to execute both technical and economical functions, in order to gain benefit of aggregation distributed generation.

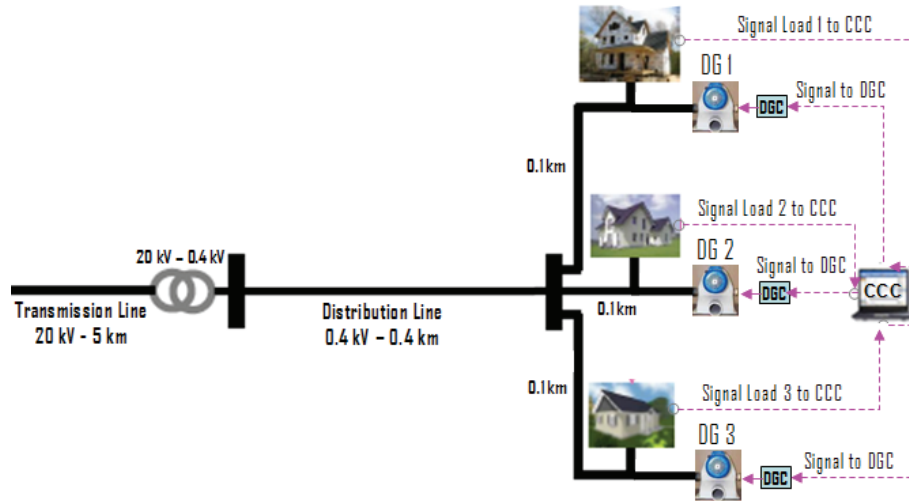


Figure 12. Centralised Virtual Power Plant

2. Decentralised VPP.

In decentralised system topology, each DG unit is locally controlled by local controller (LC). Principally the active power output of DG is controlled by distributed generation controller (DGC) and the DGC is controlled by local controller (LC) which is installed with logic algorithms. To perform an integrated system, the local controllers are connected/linked to each other forming a ring network architecture through communication to allow signals exchange, thereby coordinating and thus treated as single control centre (see figure 13).

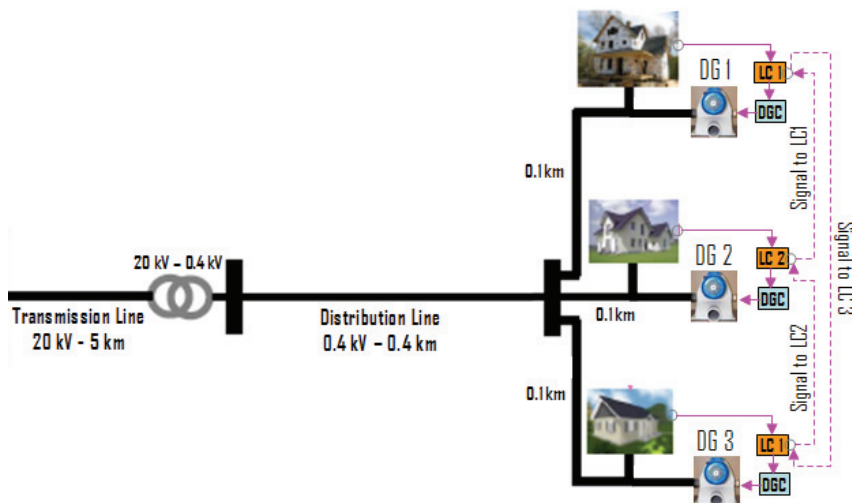


Figure 13. Decentralised Virtual Power Plant

Figure 14 illustrates interconnection of several DG units to the main grids with a different kind of control. In feeder A, two DG units of microturbine and diesel are installed near their loads and interconnected to the main grid. The DG units are operated

individually with full power output setting to supply their loads. In this case, the configuration number 2 and 3 can to be applied (see pages 15 and 16), thus if the loads are decreasing, the DG units export power into the grid and if the loads are increasing over the maximum capacity of DG, thus the loads are compensated by main grid. In feeder B, two fuel cell units and one diesel unit are operated parallel to the main grid and controlled by local controller. As shown in the figure, each local controller is not integrated to each other with communication. In other words, the local controller is responsible only with the control of own DG, thus the DG unit will produce power according to the load signal. In this case, the DG units are suitable to apply configuration 1, 2 or 3 for interconnection.

The centralized VPP is shown in feeder C, where three DG units of microturbine are interconnected to the main grid and placed near the loads. The signals from the loads are transmitted centrally to the CCC. Here the information/signals are controlled and processed according to the logic algorithm which had been programmed. The signal is dispatched to the DG controller afterwards. At feeder D, three units of microhydro which are controlled by their local controller are installed to supply the loads. Even they do not have control centre unit; each local controller is integrated with communication to exchange the signals. This system is representing decentralised VPP. For interconnection to the grid, the DG units at feeder C and D are possible to use configuration no. 1, 2 and 3.

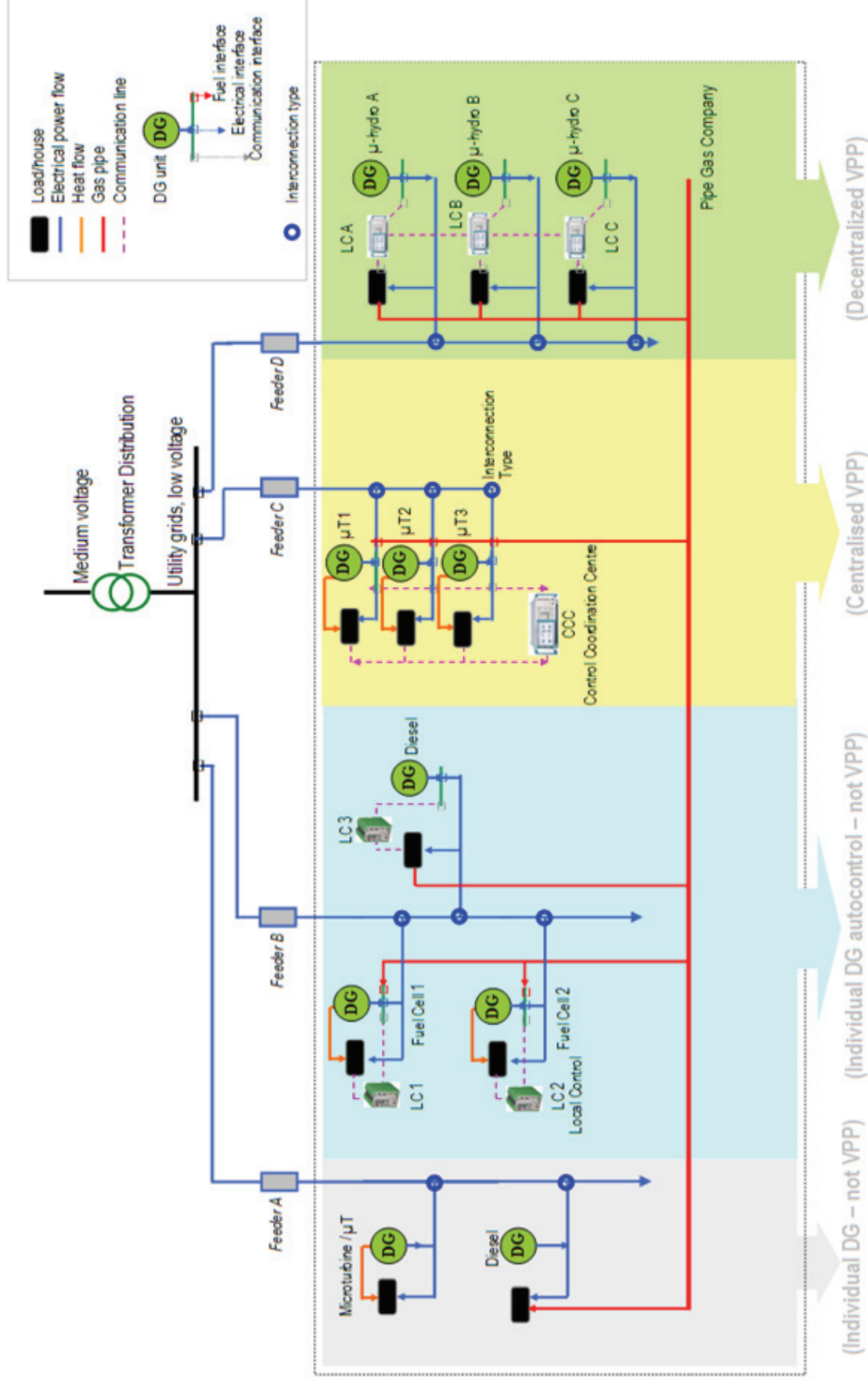


Figure 14.Types of Virtual Power Plant concerning to the control topology

Chapter 3

Developing Model of Virtual Power Plant

3.1 Components of the VPP in simulation

This chapter provides description of model components of VPP which is developed by using library models in Matlab-Simulink in order to simulate the concept of Virtual Power Plant. The components are divided into four major model components: main grid model, distributed generation model, dynamics load model and electrical and mechanical measurement units. The schematic diagram of centralised VPP and main grid is described in figure 15. In simulation, the virtual power plant is consisted of three distributed generation units which operate parallel with the main grid and three dynamics loads. The detailed model description of VPP is presented in following paragraphs.

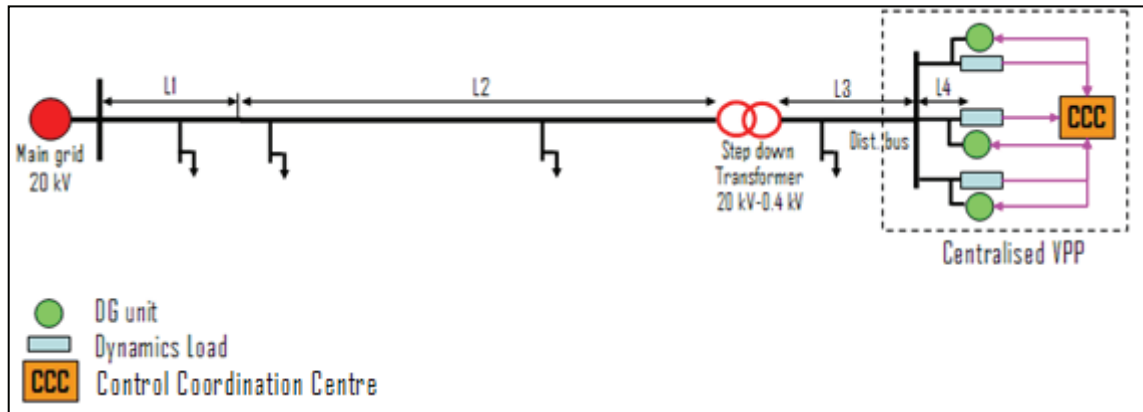


Figure 15. Centralised VPP and main grid

3.1.1 Main Grid model

The main grid model is consisted of a. three phase AC source, b. medium transmission and distribution line, c. step down transformer and d. fix resistive loads. The components are available in power system library in Matlab Simulink and each model parameters are fulfilled with the proper data from grid reference.

a. The three-phase AC source block

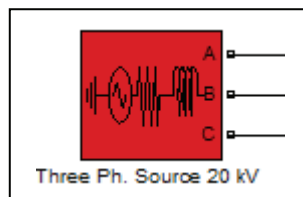


Figure 16. Three phase block

The Three-Phase Source block implements a balanced three-phase voltage source with internal R-L impedance. The three voltage sources are connected in Y with a neutral connection that can be internally grounded or made accessible. The source internal resistance and inductance are either by directly entering R and L values or by indirectly specifying the source inductive short-circuits level and X/R ratio. The internal phase to phase voltage is in volts RMS (V_{rms}). The base voltage is 20 kV (V_{rms} L-L) and the frequency system is 50 Hz.

b. Transmission and distribution line

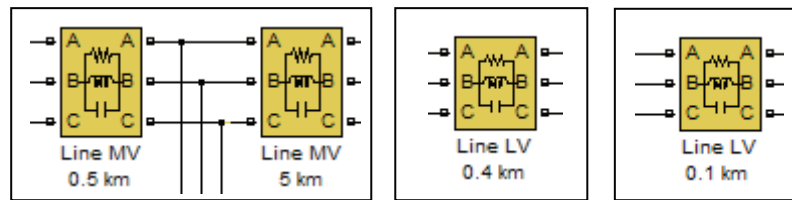


Figure 17. Medium voltage transmission and distribution line

This section describes each of the branches that transmit electrical power. The branches are usually lines or cables. There are aerial lines at the 20 kV and 0.4 kV voltage level which is responsible for distributing power at lower voltage levels. Each branch is described in detail with explanation of the values used for the electrical parameters.

The three-phase parallel RLC branch block implements three balanced branches consisting each of a resistor (in ohms- Ω), an inductor (in henries-H), a capacitor (in farads-F), or a parallel combination of these. Each branch data is described in table 7.

Table 7. Data lines parameters [30]

No	Type	X (ohm/km)	R (ohm/km)	C (nF/km)
1	Overhead line (L1)	0.1226	0.156	235.00
2	Overhead line (L2)	0.3614	0.2426	10.12
3	Distribution line (L3 & L4)	0.302	0.437	10.2

The typical data line parameters as shown above particularly for low voltage line is unusual, normally at low voltage level is predominantly resistive. All branches in simulation are represented by three phase parallel RLC branch. The lengths of overhead lines L1 and L2 are 0.5 km and 5 km respectively. At low voltage level, the length of distribution line (L3) from step down transformer to distribution bus is 0.4 km and

length distance from distribution bus to each loads/DG units are 0.1 km (L4). The calculation to define R-L-C value of each line is presented at appendix A in detail.

c. Step down transformer

As shown in figure 15 the system has only one transformer. The three-phase transformer (two windings) block implements a three-phase transformer using three single-phase transformers. The nominal power rating of the transformer is in volt-amperes (VA), and nominal frequency in hertz (Hz). The primary side busbar is 20 kV, and the secondary busbar is 400 V. The secondary busbar is connected to distribution line 400 V. Table 8 describes data of the transformer.

Table 8. Transformer data

No.	Primary volt (kV)	Secondary volt (kV)	Rating (kVA)	Connection
1	20	0.4	250	D ₁₁ Y _g

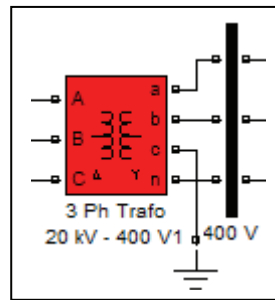


Figure 18. Transformer step down

In order to comply with simulation, the specified resistance and inductance of the windings are in per unit (p.u). The values are based on the transformer rated power P_n , in VA, nominal frequency f_n in Hz, and nominal voltage V_n , in volt, of the corresponding winding. The formulation and calculation of each winding per unit resistance and inductance is in appendix B.

d. The fix loads

The fixed loads are represented by resistive load. The nominal phase to phase voltage of the load is in volts RMS (V_{rms}) and three phase active power of the load is in watts (W). There are some fixed loads connected to medium voltage line e.g. industrial load 1200 kW, trade 400 kW (100 customers @ 4 kW) and house hold 800 kW (50 customers @ 8 kW + 200 customers @ 2kW). And 10 kW fixed load is connected to the distribution line.

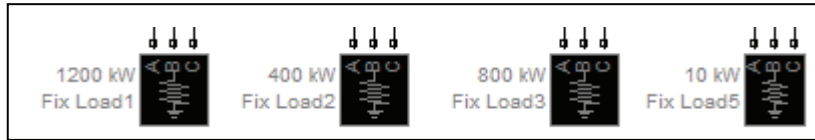


Figure 19. Fix load model

3.1.2 Distributed generation model

The distributed generation model consists of synchronous machine, hydraulic turbine governor and excitation model. In simulation, three DG units which have similar characteristics are interconnected on the distribution grid.

a. Distributed generation

This model consists of a unit synchronous machine (SM) equipped with distributed generation controller (DGC). The DGC is consisted of two important parts: hydraulic turbine governor and excitation. The SM model is a dynamic model of a three-phase round-rotor or salient-pole synchronous machine and operates in generator or motor modes. The operating mode is dictated by the sign of the mechanical power (positive for generator mode, negative for motor mode). The model SM provides a set of predetermined electrical and mechanical parameters for various synchronous machine ratings of power (kVA), phase-to-phase voltage (V), frequency (Hz), and rated speed (rpm) etc. Three DG units are connected at low voltage (400 V), with each capacity 31.3 kVA, 50 Hz and maximum active power output is 29 kW.

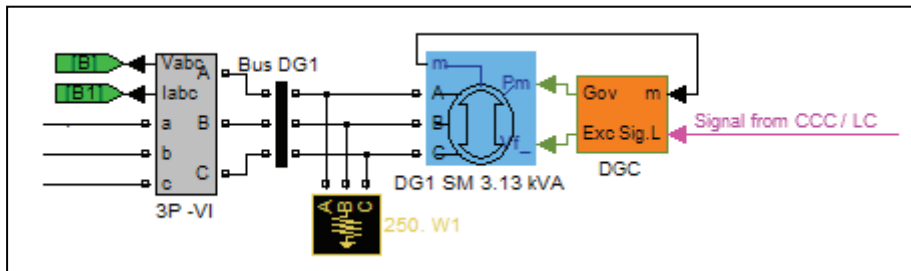


Figure 20. DG unit and controller model

The model of DGC had been taken from hydraulic turbine governor model and an excitation model from Matlab-Simulink library.

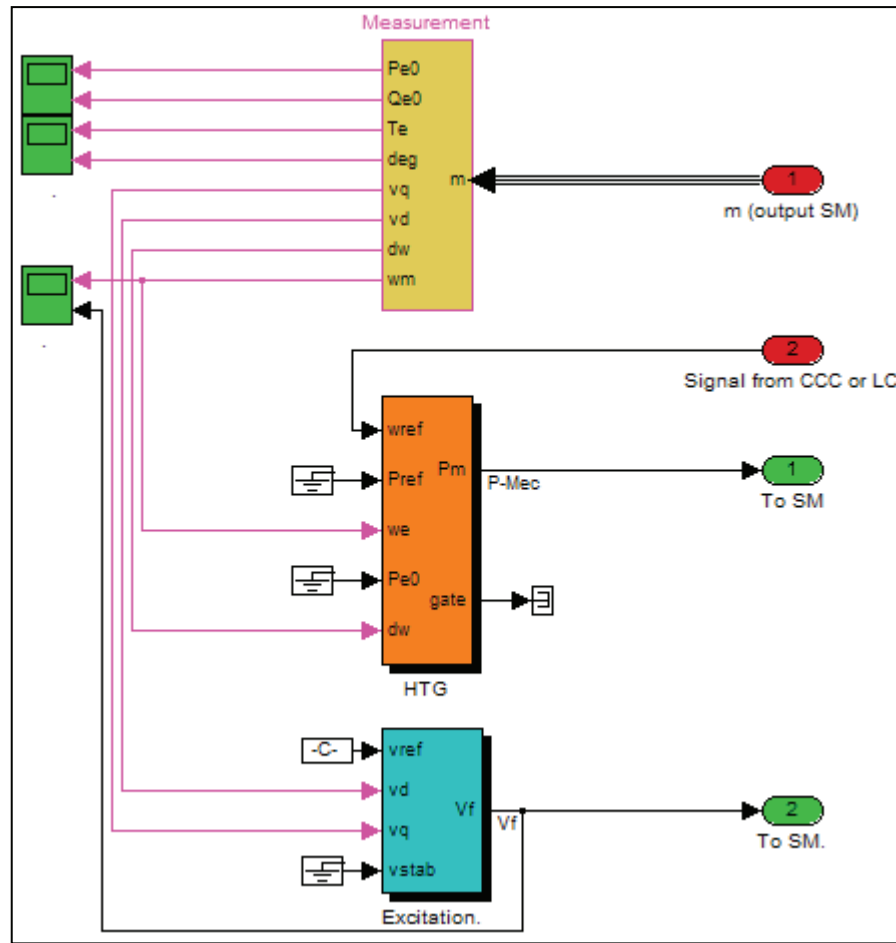


Figure 21. Input and output of Distributed Generation Control

The units of inputs and outputs vary according to block parameters (see figure 21). If the fundamental parameters in SI units are used, the inputs and outputs are in SI units, except for rotating speed deviation (dw) in the vector of internal variables, which is always in p.u., and angle, which is always in radian. Otherwise, the inputs and outputs are in p.u.

The first Simulink input of synchronous machine is the mechanical power (P_m) at the machine's shaft. In generating mode, this input can be a positive constant or function or the output of a prime mover block (see the Hydraulic Turbine and Governor -HTG- blocks). The second Simulink synchronous machine input of the block is the field voltage (V_f). This voltage can be supplied by a voltage regulator in generator mode (see the Excitation System block).

The (m) is the Simulink output of the synchronous machine block; it is a vector containing 22 signals. These signals can be demultiplex by using the Bus Selector block provided in the Simulink library (see table 9 below). The m signals are used as input to HTG block (w_e and d_w) and excitation block (v_d and v_q).

Table 9. The (m) signals in simulation

Signal	Definition	Unit
1	Stator voltage (v_q)	pu
2	Stator voltage (v_d)	pu
3	Rotor speed (w_m or w_e)	pu
4	Electromagnetic torque (T_e)	pu
5	Load angle delta	deg
6	Output active power (P_{e0})	pu
7	Output reactive power (Q_{e0})	pu
8	Rotor speed deviation (d_w)	pu

The Hydraulic Turbine and Governor block implements a nonlinear hydraulic turbine model, a PID governor system, and a servomotor [31], see figure 22 below.

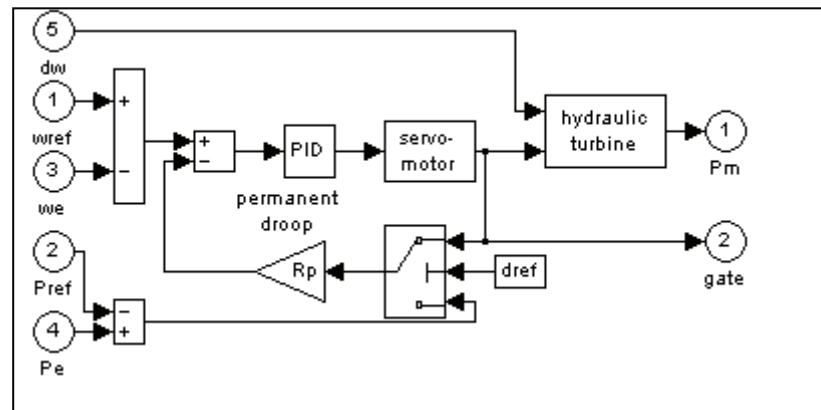


Figure 22. The input and output of the hydraulic turbine and governor system [31]

Inputs and outputs of governor system are:

- 1st input, w_{ref} (reference speed): desired speed (in p.u). In simulation reference speed is varied according to signal from CCC or LC in pu (the detail discussion is shown in chapter 4 and 5).
- 2nd input, P_{ref} (reference mechanical power): desired electrical power in p.u. This input can be left unconnected if the gate position as input to the feedback loop instead of the power deviation will be used.
- 3rd input, w_e or w_m (machine actual speed): SM actual speed in p.u.

- 4th input, P_{e0} (machine actual electrical power) in p.u. This input can be left unconnected, if the gate position as input to the feedback loop instead of the power deviation will be used.
- 5th input, d_w (speed deviation) in p.u.
- the first output is mechanical power P_m for the Synchronous Machine block, in p.u. and the second is gate opening, in p.u. The gate's opening is limited between g_{min} and g_{max} and its speed is limited between vg_{min} and vg_{max} .

The static gain of the governor is equal to the inverse of the permanent droop R_p in the feedback loop. The PID regulator has a proportional gain (K_p), an integral gain (K_i), and a derivative gain (K_d). The high-frequency gain of the PID is limited by a first-order low-pass filter with time constant T_d (s). During simulation the proportional gain is set by specific value, the integral and derivative gains are set to zero.

The hydraulic turbine is modelled by the following nonlinear system.

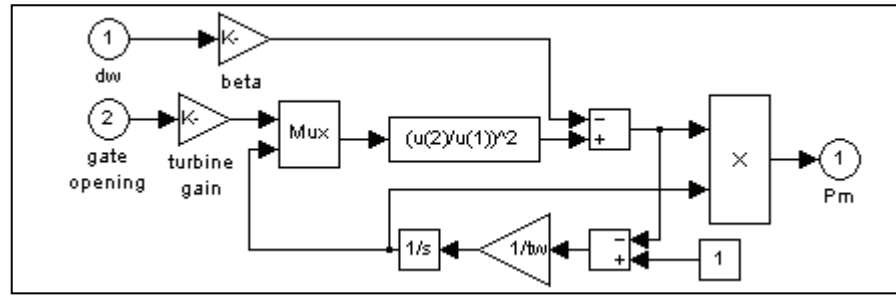


Figure 23. The hydraulic turbine block [31]

The gate servomotor is modelled by a second-order system.

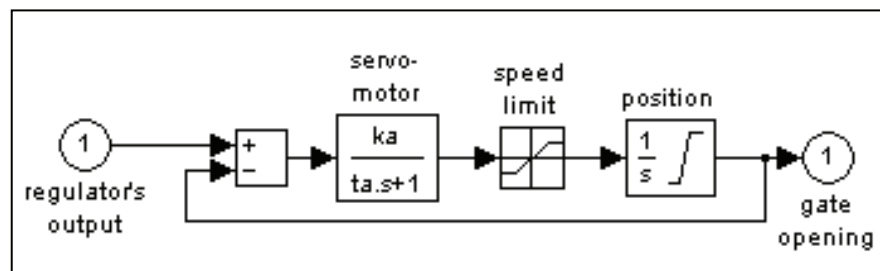


Figure 24. The gate servo motor block [31]

b. Speed governors

Direct speed governing and the supplemental adjustment of speed governor set points are the methods used on present day power systems for matching generation to load, for the allocation of generation output among generation sources, and for the achievement of desired system frequency.

- *Speed governors for synchronous generators*

Speed governors [32] vary prime mover output (torque) automatically for changes in system speed (frequency). The speed sensing device is usually a fly ball assembly for mechanical-hydraulic governors and a frequency transducer for electro-hydraulic governors. The output of the speed sensor passes through signal conditioning and amplification and operates a control mechanism to adjust the prime mover output until the system frequency change is arrested.

- *Speed droop*

The definition of droop is the amount of frequency change that is necessary to cause the main prime mover control mechanism to move from fully closed to fully open. A governor tuned with speed droop will open the control valve a specified amount for a given disturbance. This is accomplished by using feedback from the main prime mover control mechanism. A simplified block diagram of a droop governor is shown in figure 25. If 1% change in speed occurs, the main control mechanism must move enough to cause the feedback through the droop element to cancel this speed change. Thus, for 1% speed change, the percent movement of the main control mechanism will be the reciprocal of the droop (i.e. if the droop is 5% the movement will be $1/0.05 = 20$).

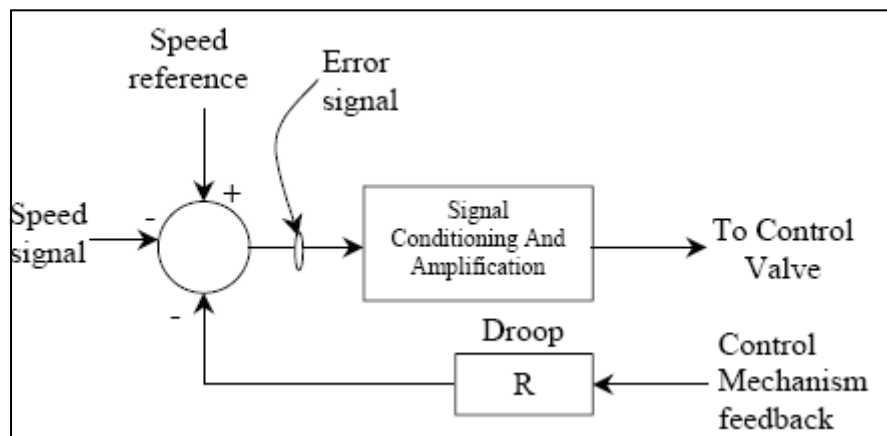


Figure 25. Droop governor block diagram [32]

If the governor is tuned to be “isochronous” (i.e. zero droop), it will keep opening the valve until the frequency is restored to the original value. This type of tuning is used on small, isolated power systems, but would result in excess governor movement on large, interconnected systems. Governors using speed droop or speed regulation requires a sustained change in system frequency to produce a sustained change in prime mover

control mechanism or generator power output. Therefore, governors alone cannot restore the power system frequency to the pre-disturbance level.

- Secondary regulation

The term speed regulation refers to the amount of speed or frequency change that is necessary to cause the output of the synchronous generator to change from zero output to full output. In contrast with droop, this term focuses on the output of the generator, rather than the position of its valves.

- Supplementary regulation

An important feature of a governor system is the device by which the main prime movers control mechanism, and hence the generator power output, can be changed without requiring a change in system speed. This adjustment can be made by local action of plant control operator, or remotely from the dispatch centre automatic generation control system. In mechanical governors, a "speeder motor" drives a linkage that is added to the output of the ball head linkage and the droop feedback linkage by a system of floating levers. In analogue or digital electro hydraulic governors, a motor-operated potentiometer or digital reference setter provides the reference signal to the electronic circuits.

The effect of the speed reference input is to produce a family of parallel speed-load characteristic curves. Increasing the speed reference of a generator that is connected to a large power system will result in more power being produced by the unit. Therefore, the power output of particular generators can be adjusted at will to allow for economic dispatch of generation sources. In addition, supplementary regulation of several generator speed reference inputs after a disturbance permits the restoration of system frequency. Increasing the speed reference of a generator connected to a small or isolated power system will increase the speed of the system, but not necessarily increase the power produced by the unit.

c. Excitation

The excitation provides an excitation system for the synchronous machine and regulates its terminal voltage in generating mode. The Excitation System block is a Simulink system implementing a DC exciter described in [33], without the exciter's saturation function. The SM excitation is performed by the standard excitation block provided in the machine library. The basic elements that form the Excitation System block are the voltage regulator and the exciter.

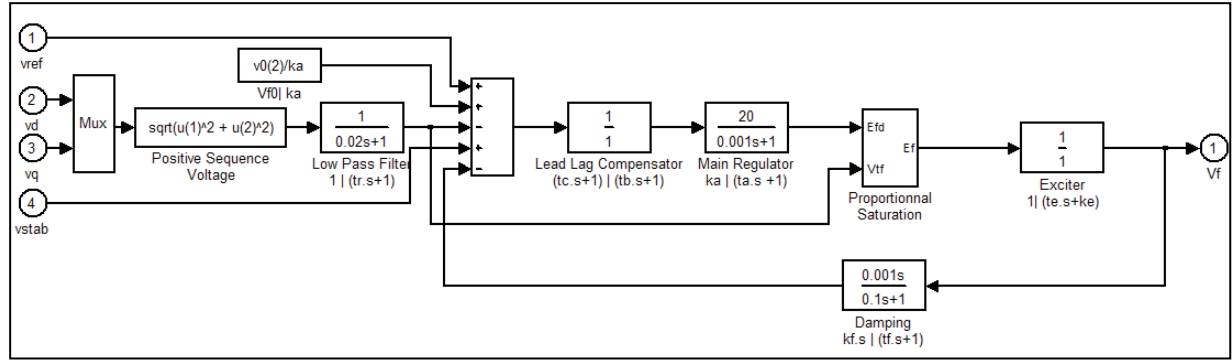


Figure 26. Excitation system block [33]

The excitation system block implements of an IEEE type 1 synchronous machine voltage regulator combined to an exciter.

The first input : V_{ref} , the desired stator terminal voltage (p.u). In simulation the V_{ref} is set constant 1 p.u.

The second input: V_d component of terminal voltage (p.u).

The third input: V_q component of terminal voltage (p.u).The V_d and V_q are output of m signal from synchronous machine.

The forth input: V_{stab} stabilization voltage from user-supplied power system stabilizer (p.u).

The output: field voltage V_f to be applied to the synchronous machine block 2nd input (p.u).

3.1.3 Three phase dynamic load model

The dynamic load model implements a three-phase dynamic load with active power and reactive power controlled from an external input. The external control has two inputs which are used to control the active and reactive powers of the load from a vector of two signals [P, Q]. In the simulation three dynamic loads are assumed to consume active power [P] only (no reactive power load/demand) as shown in figure 28, 29 and 30. Afterwards the signal output (active power demand) from dynamic load is transmitted to local controller or coordination control centre (see figure 27).

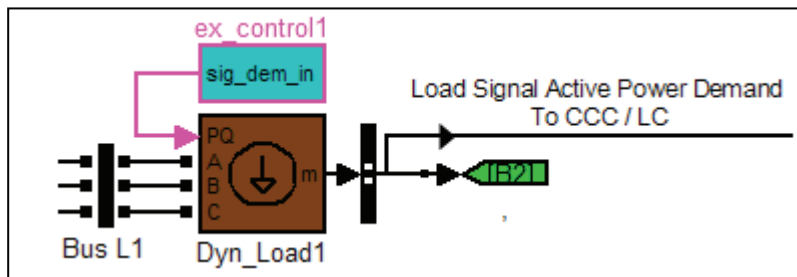


Figure 27. Dynamic load model

Figure 28 shows that active power demand of load 1 consumes circa 22 kW. In 20th second, the load ramps up to 31.9 kW then it moves with a steady constant demand. The load 2 is constant stable in 22 kW as shown in figure 29. And load 3 consumes active power demand 24 kW then in 80th second, it ramps down significantly to circa 13.1 kW.

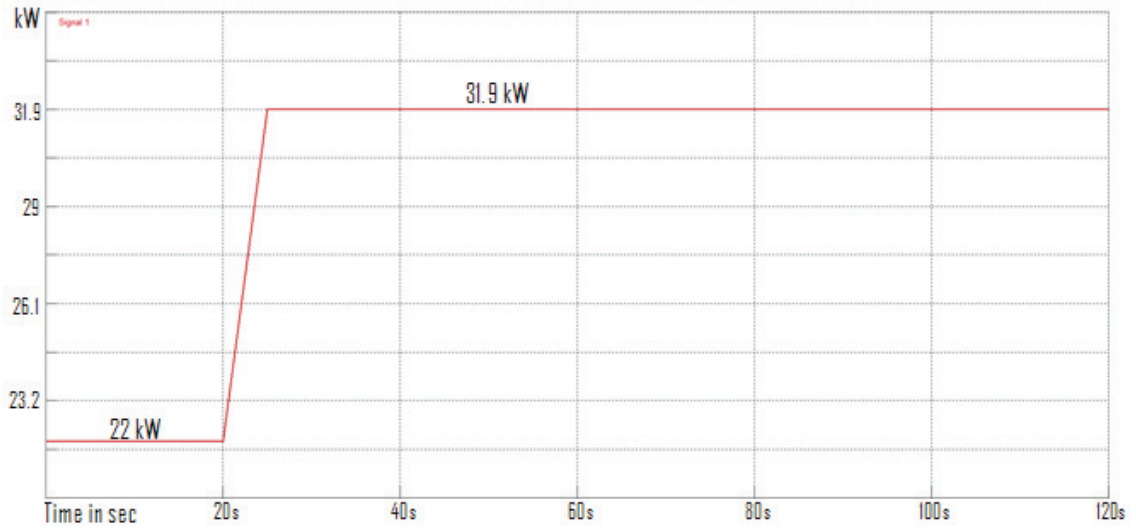


Figure 28. Profile of active power demand of load 1

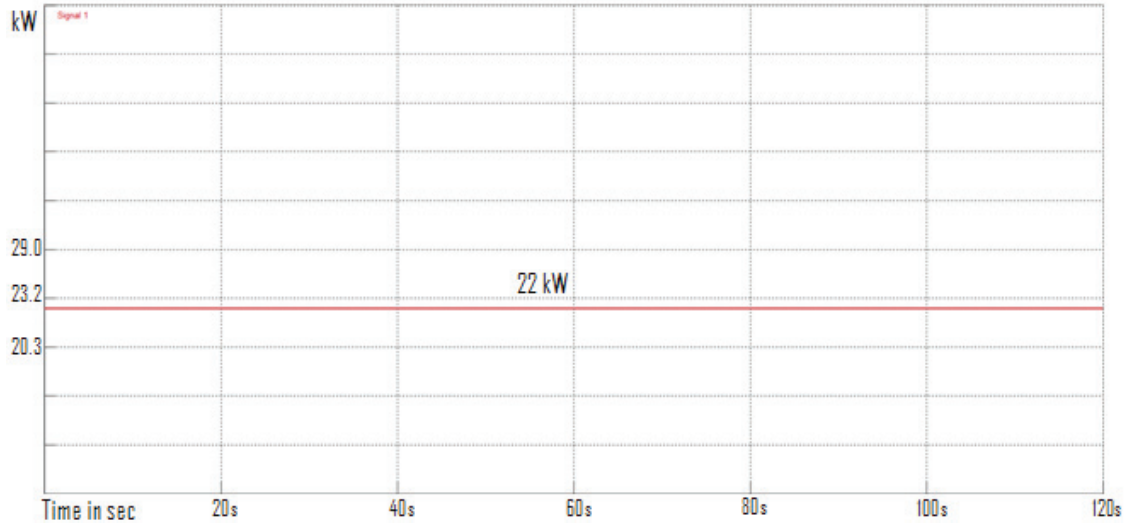


Figure 29. Profile of active power demand of load 2

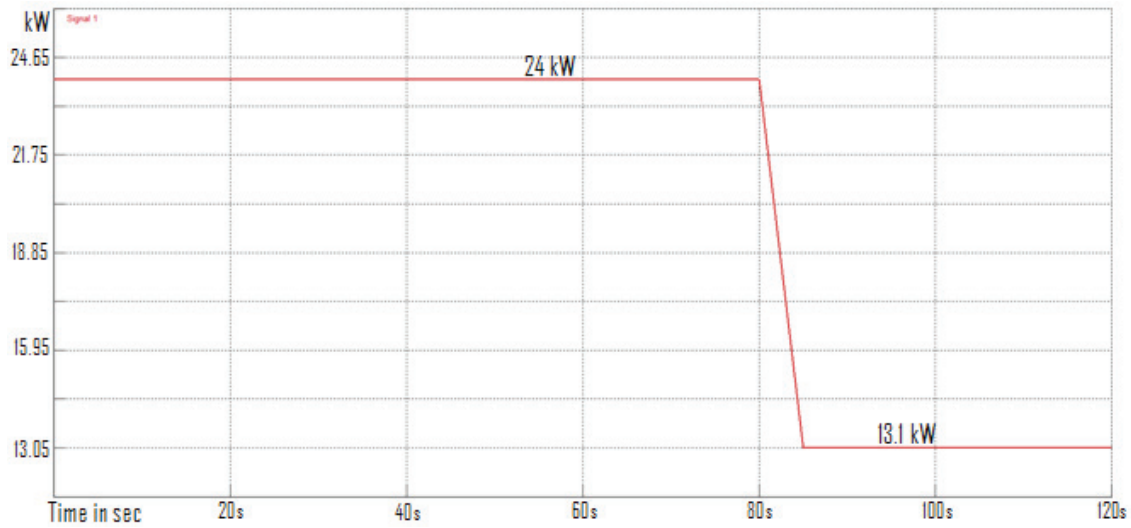


Figure 30. Profile of active power demand of load 3

3.1.4 Measurement unit (data acquisition)

The electrical parameter such as voltage, current, frequency, active and reactive power in instantaneous and rms value, of DG units, loads and lines are measured at data acquisition (green block). The three phase V-I measurement block is used to measure three-phase voltages and currents in a circuit (see figure 31).

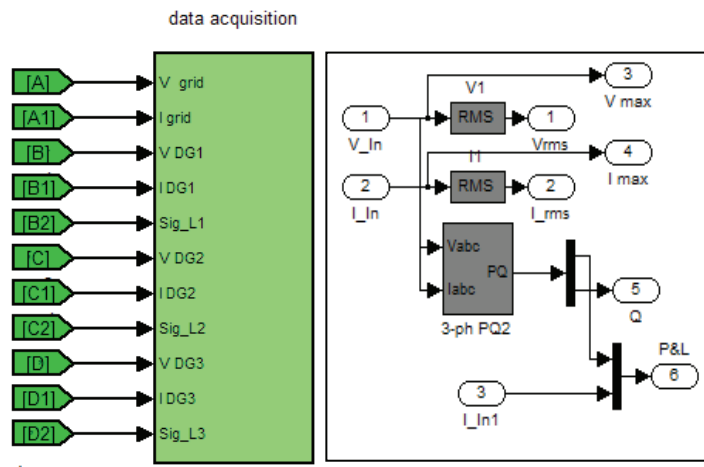


Figure 31. Data acquisition and measurement block

Below is the list summarized of the VPP system in simulation for the developed model of VPP.

Table 10. Component of VPP system in simulation

No	Component	Description
1	Main grid	20 kV, 50 Hz
2	Branch / line	Transmission at medium voltage 20 kV, L1 500 m and L2 5 km. Distribution grid 0.4 kV, L3 400 m and L4 100 m (low voltage)
3	Transformer	1 unit, 250 kVA, step down transformer 20 kV to 400 V, YgD11
4	Distributed generation and control	Consisting of three units synchronous machine @ 31.3 kVA, 50 Hz, 400 V, prime mover (hydraulic turbine governor) and excitation
5	Dynamic load	Assuming as active power demand
6	Fix load	Assuming as resistive load
7	Control and coordination centre/ local controller	<p>Consisted of three levels:</p> <p>-1st level is BAS (basic autocontrol system), the aim of this controller is controlling power output of DG units to follow the dynamics load.</p> <p>-2nd level is SAS (smart autocontrol system), the control centre is installed with logic algorithm to allow coordination of signal exchange. The aim of SAS is to coordinate dispatching power of three DG units during dynamics load. Thereby exporting and importing power from the main grid can be minimized.</p> <p>-3rd level is TEAS (tracking efficiency autocontrol system). The objective of TEAS is tracking optimum efficiency during dynamics load and minimizing export/import power.</p> <p>The discussion of BAS, SAS and TEAS is presented at chapter 5 and 6 in detail.</p>

Chapter 4

Virtual Power Plant under Autocontrol System

4.1 The concept of basic autocontrol system

In this chapter, two different kinds of direct control for distributed generation are proposed and developed. The first control level is basic autocontrol system (BAS); it is applied to control DG output according to its load signal in order to follow dynamic loads. The second control level is smart autocontrol system (SAS) which has a central controller to allow coordination and dispatching power of three DG units. The schemes of autocontrol system in simulation are:

- The DG unit is operating parallel to the main grid
- The power output of DG unit is controlled according to load signal (active power demand) from the local controller or central controller.
- The DG provides peaking or base load power to the load and the main grid provides supplemental/back up power.
- Fast communication infrastructure is provided between loads to CCC/LC and CCC/LC to DG units in order to guarantee the signal exchange.

The illustration of DG under basic autocontrol system is shown on figure 32.

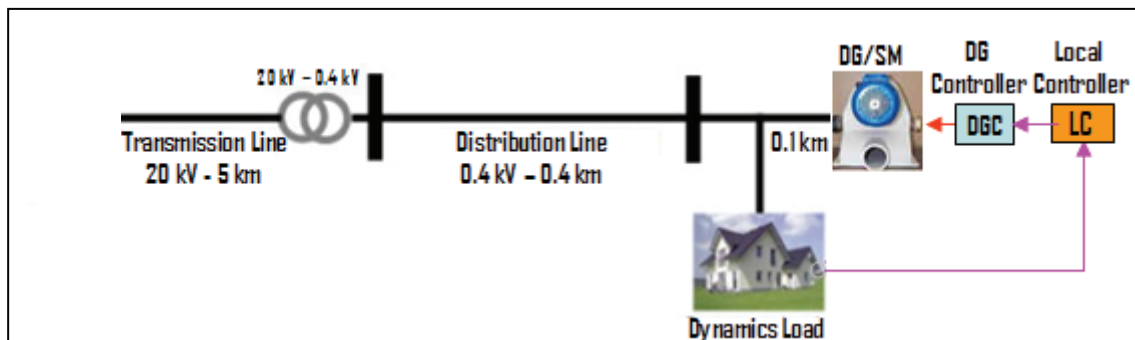


Figure 32. The illustration of Basic Autocontrol System (BAS)

The load signal (active power demand) is sent to LC. The local controller, particularly in BAS, is the interface which can receive and adjust load signal proportionally into speed reference input in the governor. Increasing the speed reference of a generator that is connected to a large power system will result in more power being produced by the unit. It shows that changing the active power output of DG is accomplished by a change in speed reference. The schematic diagram of basic autocontrol system is shown at figure 33 below.

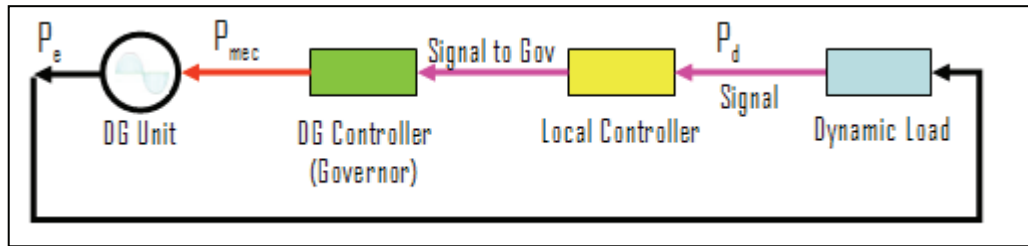


Figure 33. Schematic diagram of Basic Autocontrol System

P_d : signal of active power demand

P_{mec} : power mechanic

P_e : active power output from DG

Figure 37 describes the DG unit under basic autocontrol system in simulation.

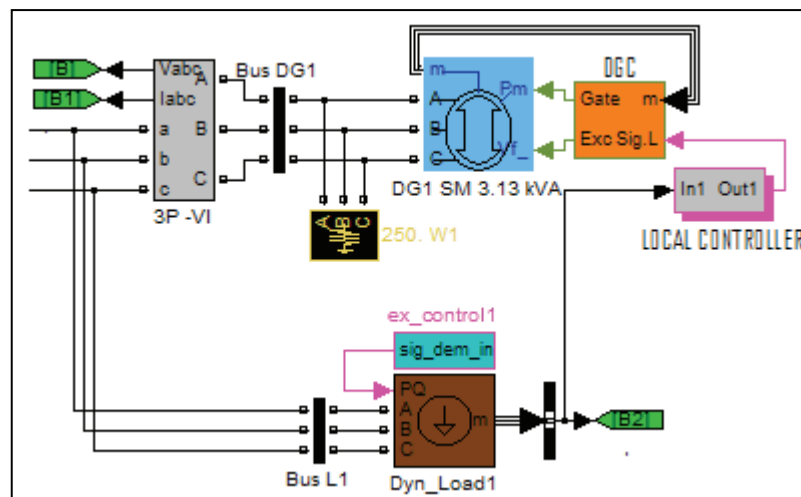


Figure 34. The BAS in Matlab Simulink environment

The block model of local controller is developed by using look up table model which is provided in Matlab Simulink. It is a mathematical function to compute an approximation to some function $y = f(x)$. The vectors of x and y are taken from result of speed reference ramp down test of the DG model. The vectors x are variation of speed reference in pu, and the vectors y are the active power also in pu. The interpolation-extrapolation method is applied in look up table. It performs linear interpolation and extrapolation of the inputs. If a value matches the block's input, the output is the corresponding element in the output vector. If no value matches the block's input, then the block performs linear interpolation between the two appropriate elements of the table to determine an output value. If the block input is less than the first or greater than

the last input vector element, then the block extrapolates using the first two or last two points [34].

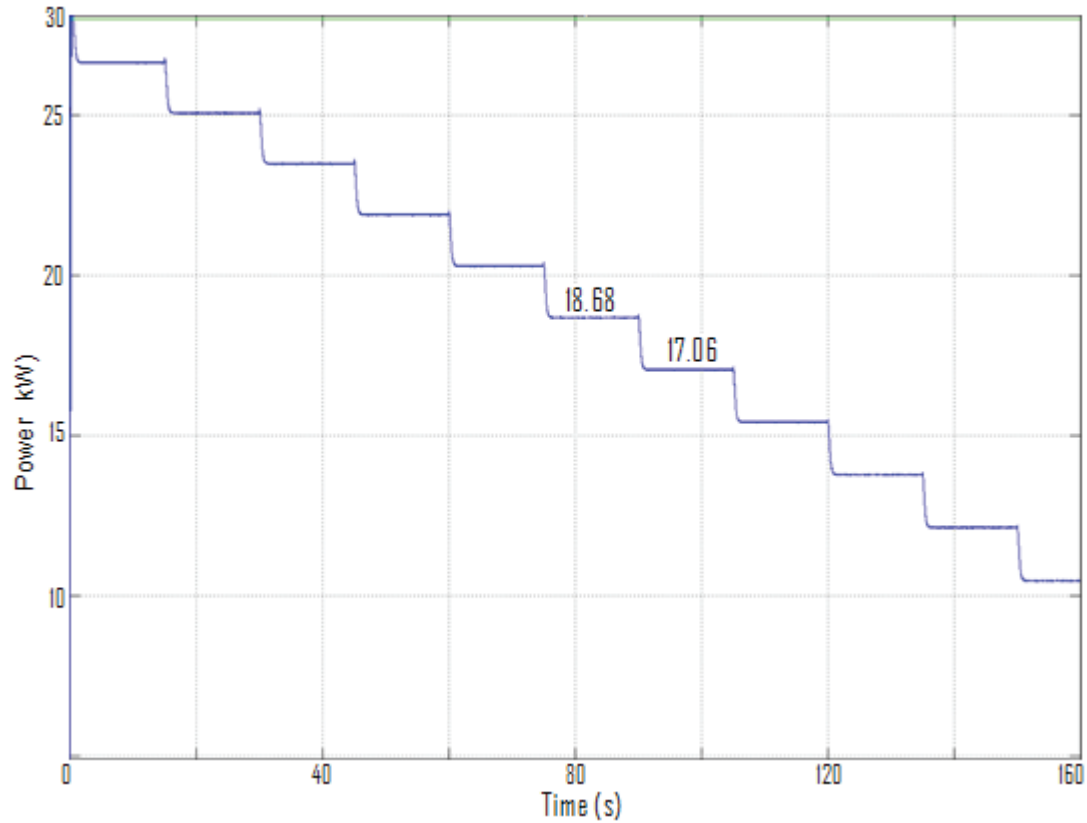


Figure 35. Ramp down test result

Figure 35 shows the active power output (vectors y) from a ramp down test by varying the speed reference (vectors x). The correlation between active power output from DG and variation of speed reference is shown in figure 36.

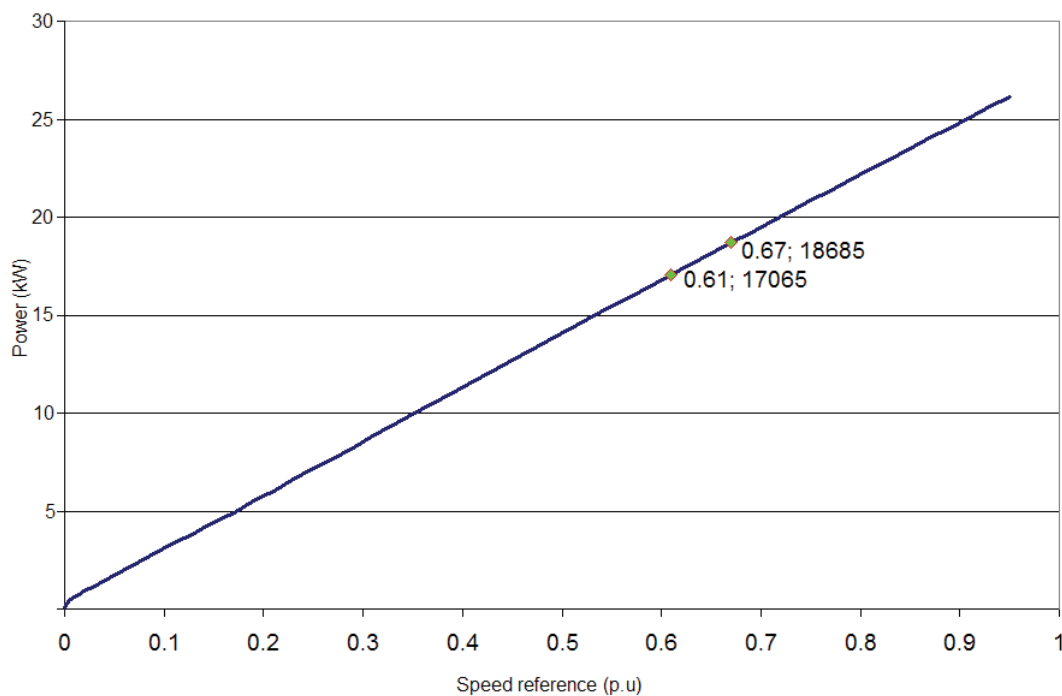


Figure 36. Active power vs Speed reference

As shown in figure 36, if the speed reference is slightly reduced from 0.67 pu to 0.61 pu, the active power output decreases from circa 18.7 kW to 17.0 kW. The correlation between gate opening and power output is presented at figure 37. If the gate is varies from 0.66 to 0.61 pu, the power output decreases also from circa 18.7 kW to 17.0 kW.

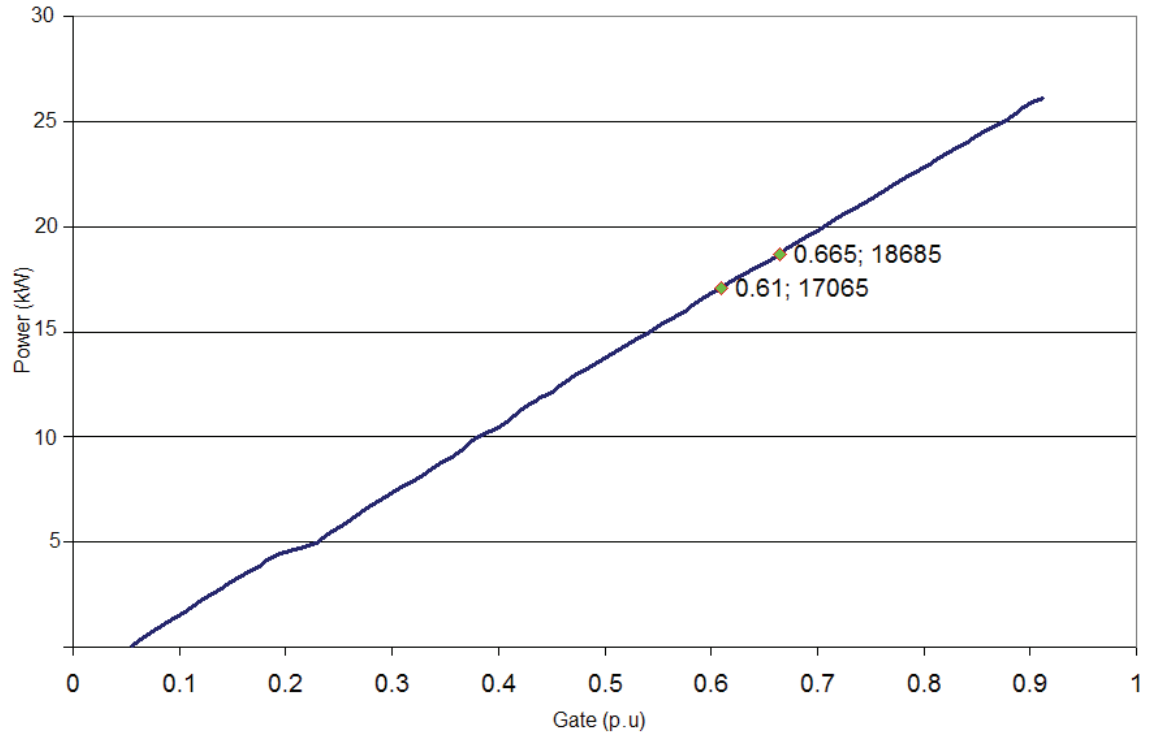


Figure 37. Active power vs gate characteristics

The detailed schematic basic autocontrol system is shown in figure 38.

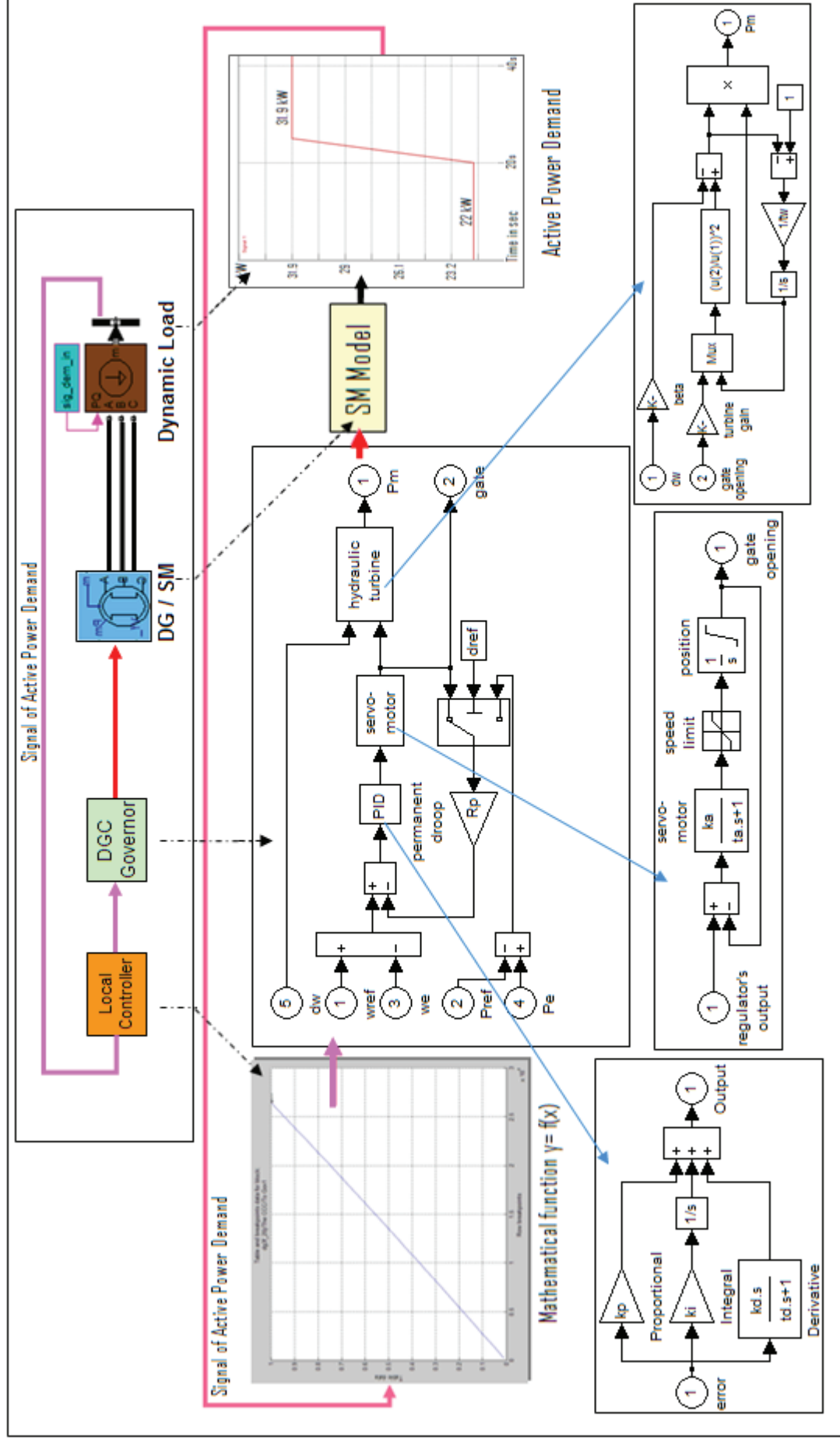


Figure 38. The schematic block of Basic Autocontrol System in detail

Figure 39 below presents the result of basic autocontrol system. The DG is running continuously in order to follow the dynamic load. Both load and DG power are a steady constant circa 29 kW for 30 seconds; then ramp down gradually to 20.3 kW and remained at this level for circa half minute, finally they ramp up to increase again to 29 kW.

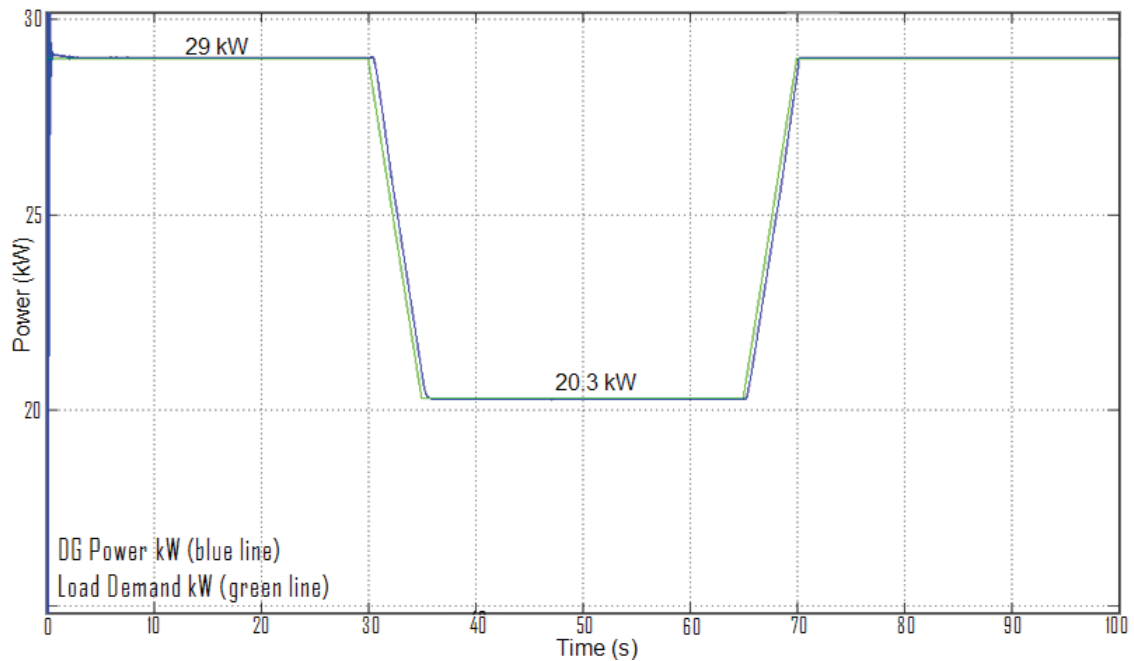


Figure 39. The active power output follows the dynamic load

During following dynamic load, the response of electromagnetic torque and load angle delta are measured also (see figure 40). When the DG produces active power circa 29 kW, both torque and load angle are measured at 0.99 pu, 42.4 pu respectively. When the active power decreases to 20.3 kW, the torque falls to 0.68 pu and load angle falls to 27.3 deg.

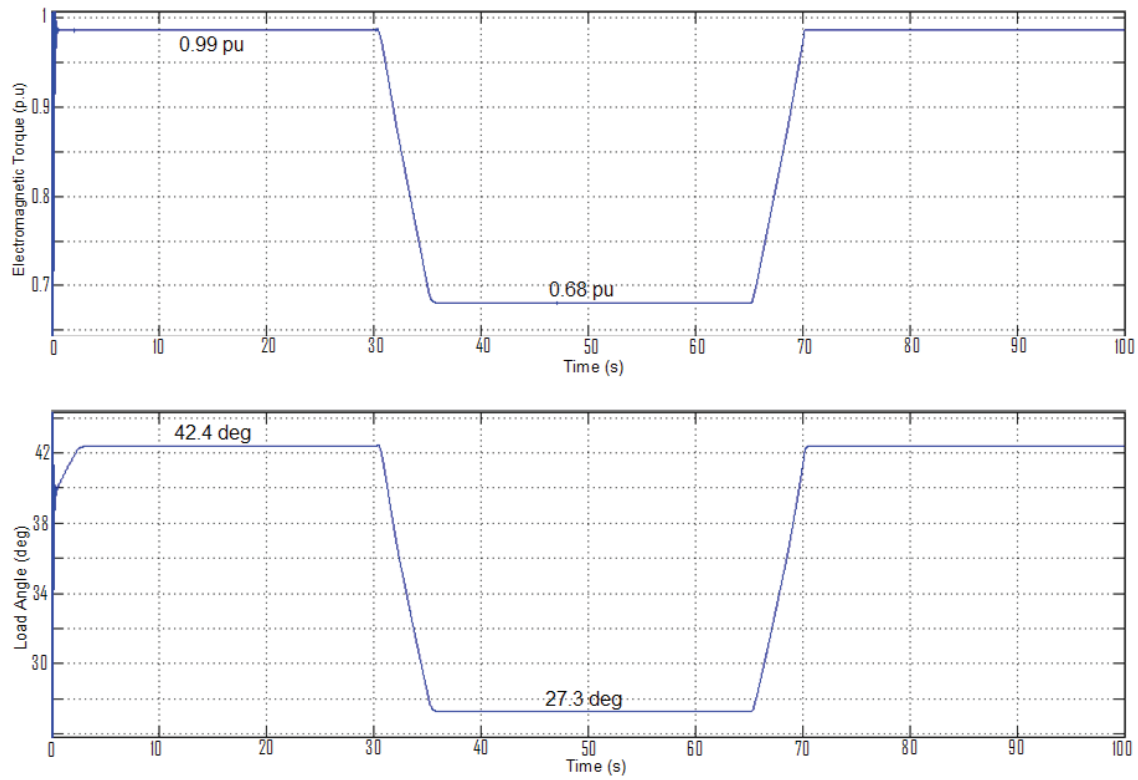


Figure 40. Electromagnetic torque and Load angle

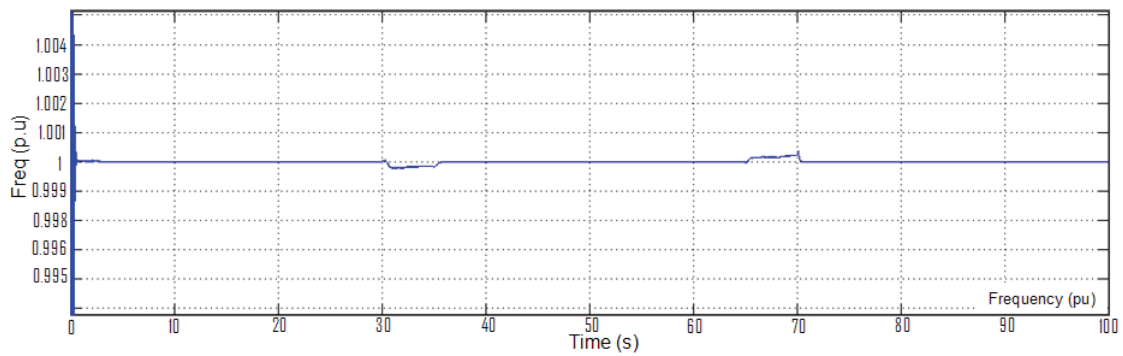


Figure 41. Frequency

As shown in figure 41 the frequency during dynamic load is constant at 50 Hz. These mechanical parameters as shown above indicate that the operation of DG unit under basic autocontrol system during dynamic load is running well.

4.2 Simulation scenarios

Several scenarios are simulated in simulation in order to compare the performance of three DG under BAS and three DG units which are operated at constant full power output.

1. Scenario A, three dynamic loads before DG installation.

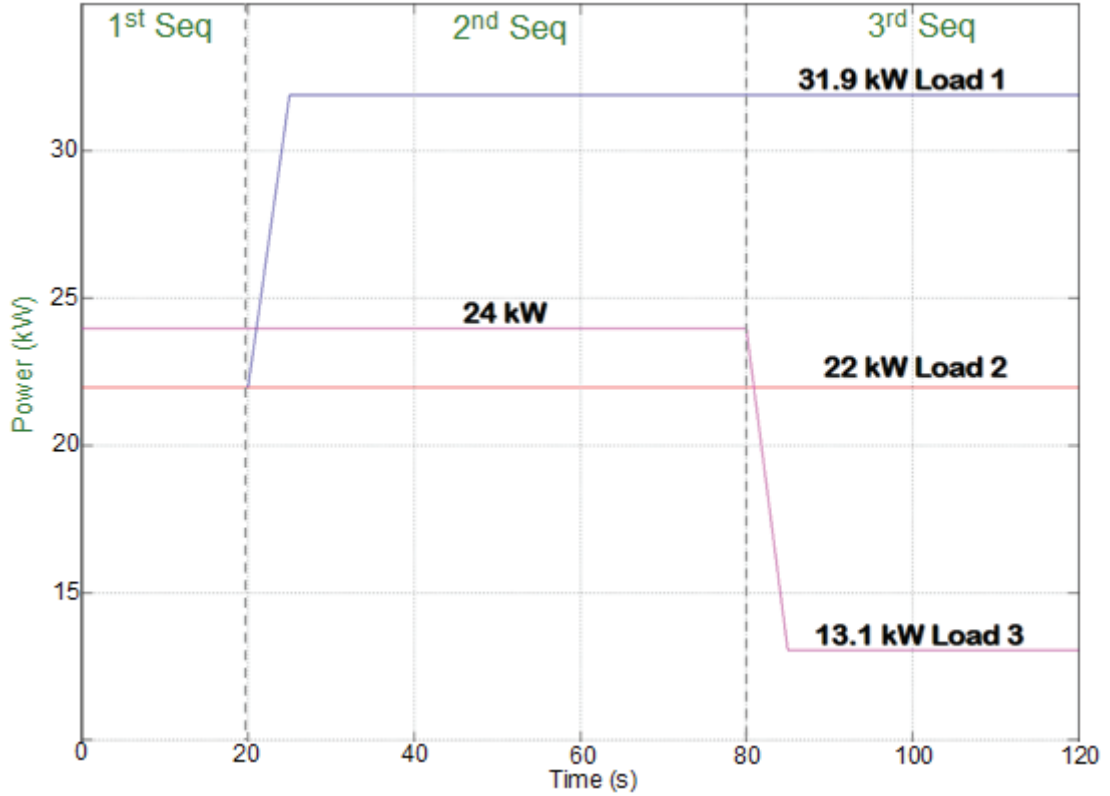


Figure 42. Profile of three dynamic loads

Figure 42 shows the dynamic profile of load 1, load 2 and load 3. The load 1 and load 2 hold steady at 22 kW then load 1 increases significantly to 31.9 kW in 20th second and load 2 is still stable at 22 kW. The load 3 is a steady constant at 24 kW, and then it falls significantly from 24 kW to 13.1 kW at 80th second.

The total demand of three loads is shown in figure 43, the peak load is circa 77.9 kW and the lowest load is around 67 kW. The blue line denotes import power from main grid to cover the total loads before DG installation.

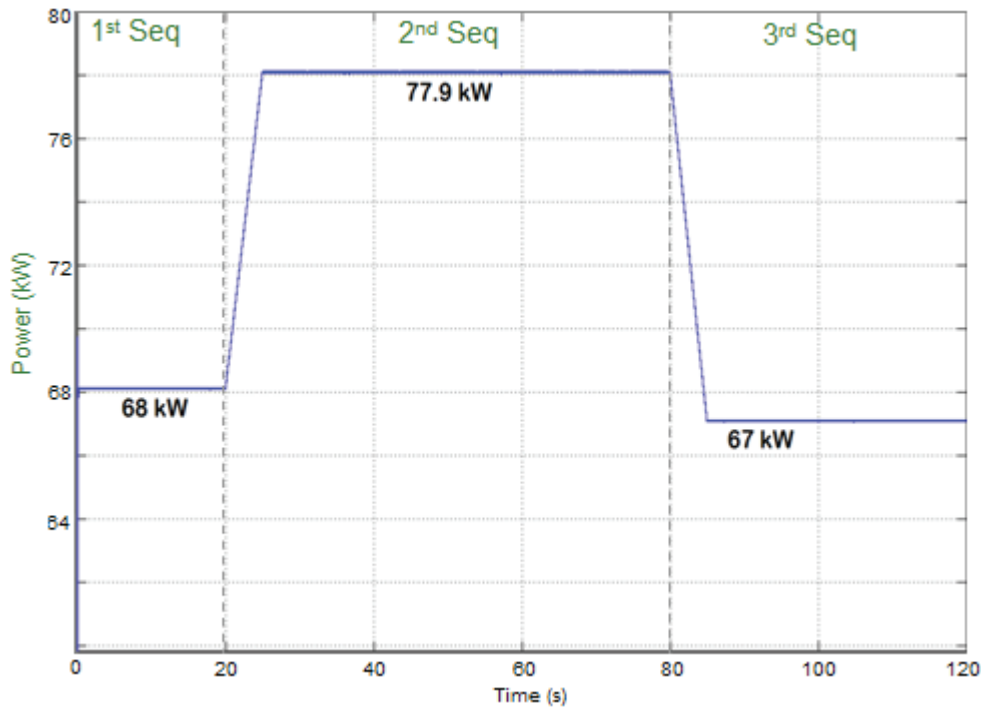


Figure 43. Grid power import to cover the total loads

2. Scenario B, three DG units running with constant full power output.

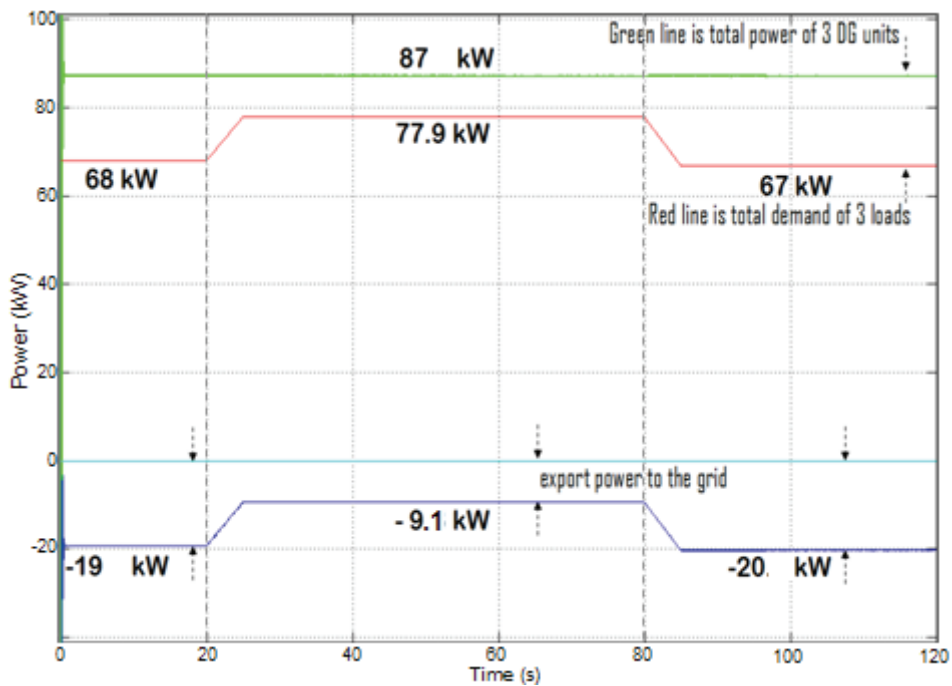


Figure 44. Total three loads demand vs Total power of three DG units with constant full power output

In this scenario, three DG units are connected to distribution line; therefore the loads have possibility to be supplied power from four sources: main grid, DG1, DG2 and DG3. As shown in figure 44, all DG units are running at constant full power operation

with total power output circa 87 kW, although the total loads are around 67 kW until 77.9 kW only. Consequently, the DG units export power to the grid in the range of 9.1 kW to circa 20 kW. The detail of the power sharing during scenario B is shown in figure 45 below.

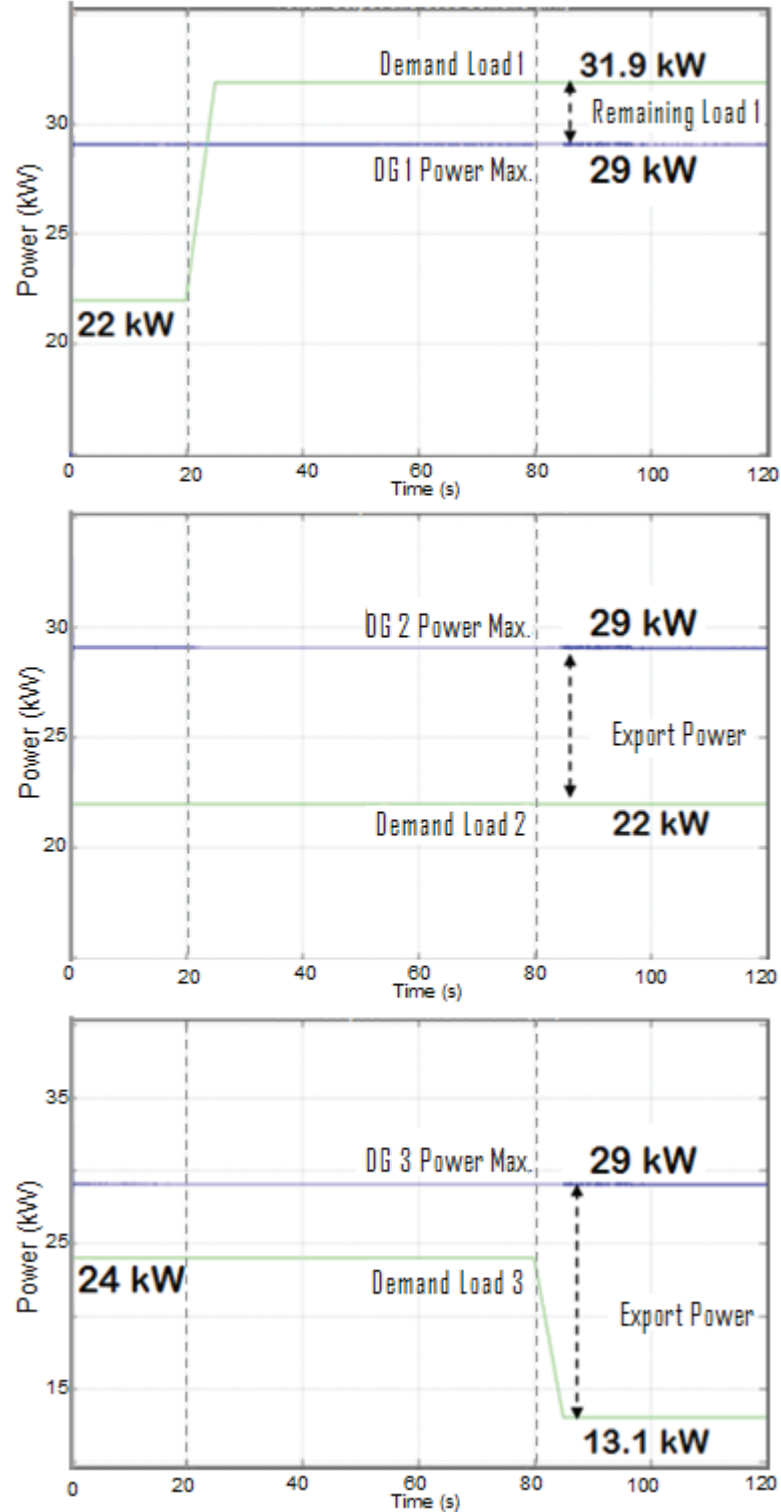


Figure 45. Power output and demand of three DG units
at constant full power output

That figure shows that the remaining load 1 is covered by DG 2 and DG 3, since total power output from DG 2 and DG 3 is higher than their total demand.

3. Scenario C, three DG units control under BAS

In scenario C three DG units are interconnected and installed near the load. Each DG unit has a local controller to control the power output according to the load signal, thereby enabling the DG unit to follow the local variation load until maximum capacity. As shown in figure 46, if load 1 is varies under the maximum capacity then the DG 1 fully cover the demand. If load 1 increases until 31.9 kW, DG 1 provides maximum power of 29 kW, and uncovered load is compensated by main grid of 2.9 kW.

At load 2, DG 2 produces power to cover the load 22 kW. When load 3 is decreasing from 24 kW to 13.1 kW, the power output of DG 3 is able to cover this load. However when the load is around 13.1 kW, DG 3 produces power only circa 12.8 kW. This mismatch between load 3 and DG 3 (circa 0.3 kW) is covered by main grid. Therefore the total power import is slightly rising from 2.9 kW to 3.2 kW. The profile of total load and total power output from three DG units under basic autocontrol system is shown in figure 47.

The BAS performance shows that this control system is successful in controlling DG output from the load signal. The drawback of the BAS is the lack of coordination and communication among the DG units. Consequently power import is still flowing to cover the remaining load. It shows that the objective to minimize import power is still not achieved using BAS.

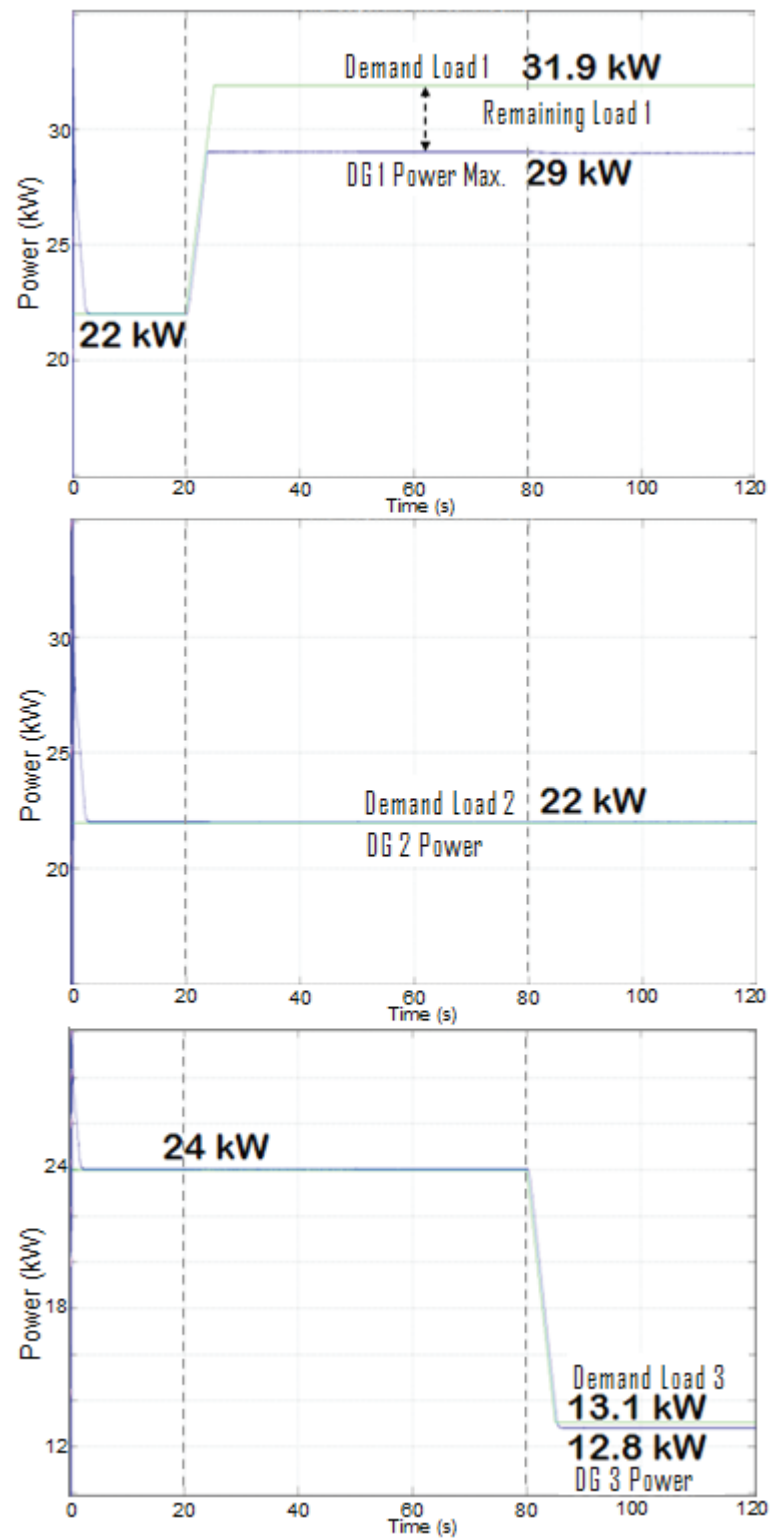


Figure 46. Power output and demand of three DG units under BAS

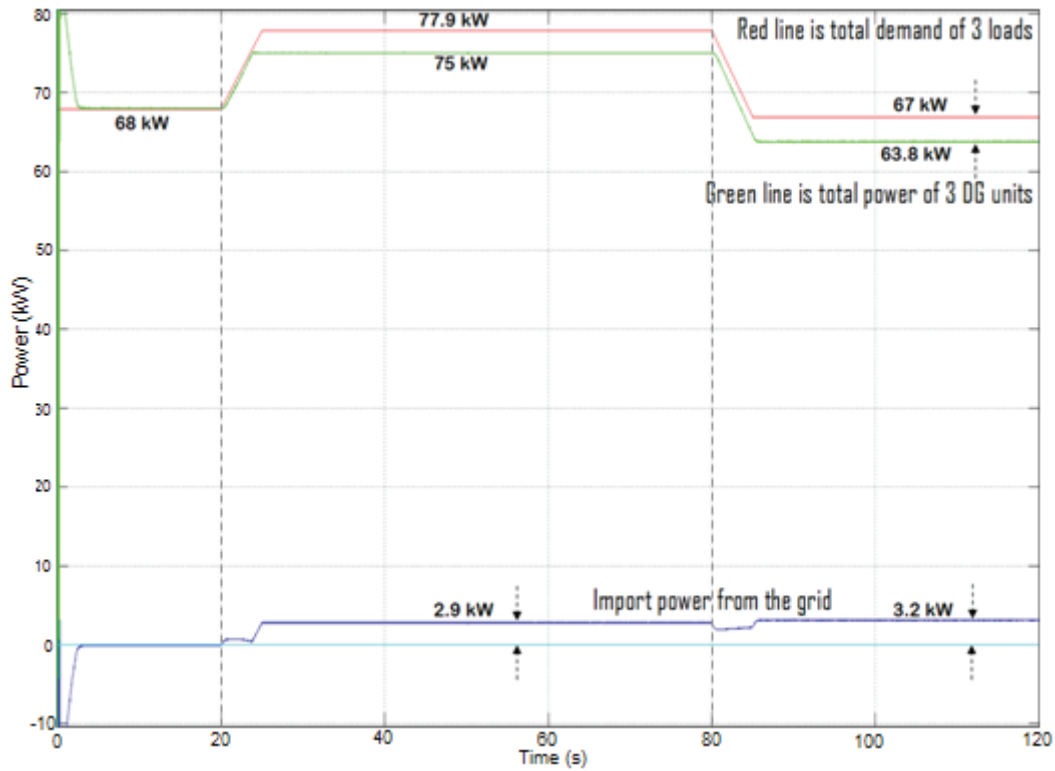


Figure 47. Total three loads demand and total power output of three DG units with BAS

4.3 The concept of Smart Autocontrol System (SAS)

After evaluation of the performance of BAS, an improvement should be done to minimize power import from main grid (circa 2.9 – 3.2 kW). The drawback of BAS is that DG units are running individually. The key solution to improve BAS is developing coordination and communication among DG units to allow information exchange. The information exchange among DG units is one of the promising ways to realize the coordinated operation of new distribution system [35]. Therefore the second control of DG units in this chapter is proposed, namely smart autocontrol system (SAS). This control system makes use of a control centre or control coordination centre (CCC) which is responsible with the DG units power dispatch.

In simulation three DG units are located near the load, and the distance of each load to the CCC is 100 meters only. This small geographical area is an important aspect that enables the establishment of fast communication infrastructure. Figure 48 shows a general overview of three DG units under smart autocontrol system and the detailed figure in appendix C.

The CCC as central controller is consisted of interface and logic algorithm which controls the information/signal exchange from the load signals. Thus the DG units are able to dispatch power to the loads by means of logic algorithm in the CCC. The

schematic diagram of logic algorithm in CCC is shown in figure 49 (the detail logic algorithm of SAS is in appendix D).

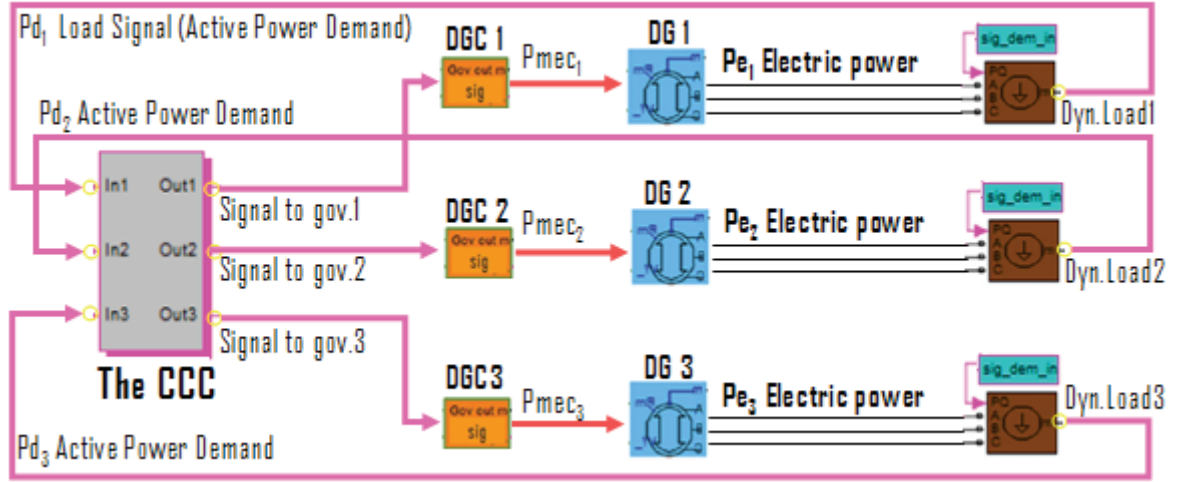


Figure 48. Smart Autocontrol System (SAS)

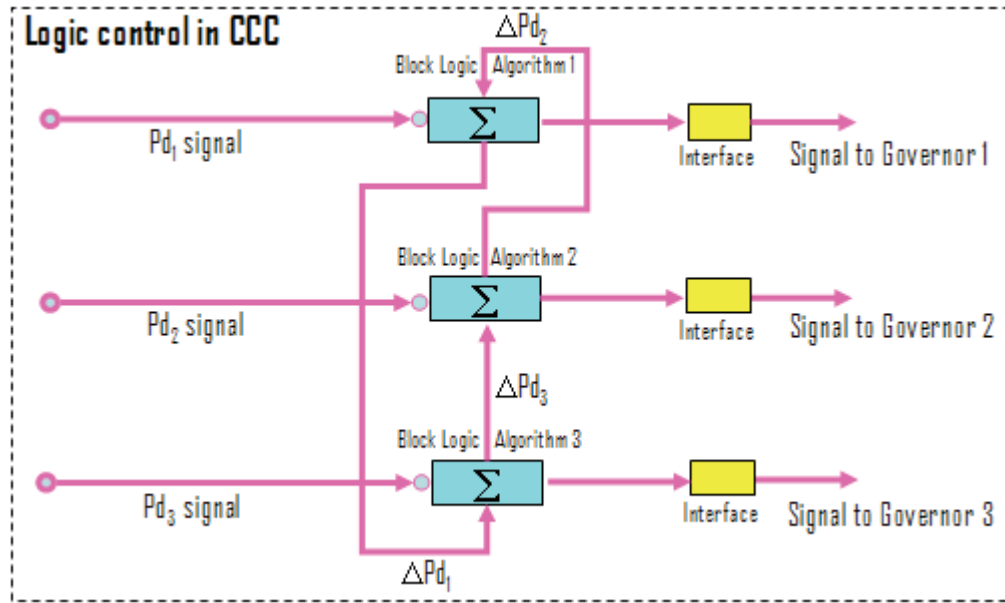


Figure 49. Simplicity logic algorithm in CCC

Where:

$P_{d(1,2,3)}$: signal of active power demand from load 1, 2 or 3

$\Delta P_{d(1,2,3)}$: signal of remaining active power demand from load 1, 2 or 3

$P_{e(1,2,3)}$: signal of active power output from DG 1, 2 or 3

The procedure in smart autocontrol system is each DG unit feeds the allocated local load until the maximum capacity (29 kW). When the load exceeds the DG limit, then

the next DG unit will try to cover the remaining part. When the remaining load can not be covered by coordination of three DG units, then power is imported from the main grid. The DG priority to cover remaining load is listed at table 11 below.

Table 11. The DG priority to cover remaining loads

Demand Priority	Remaining load 1	Remaining load 2	Remaining load 3
1 st priority	DG3	DG1	DG2
2 nd priority	DG2	DG3	DG1
3 rd priority	Grid	Grid	Grid

4.4 The analysis of dispatching DG power under SAS

The load profile is divided into three sequences as shown in figure 50, 51 and 52 to make easier the analysis.

4.4.1 Dispatching power in 1st sequence

In first sequence, load 1 and load 2 consume power circa 22 kW, and load 3 around 24 kW. During this condition, each load is fully covered by its DG unit.

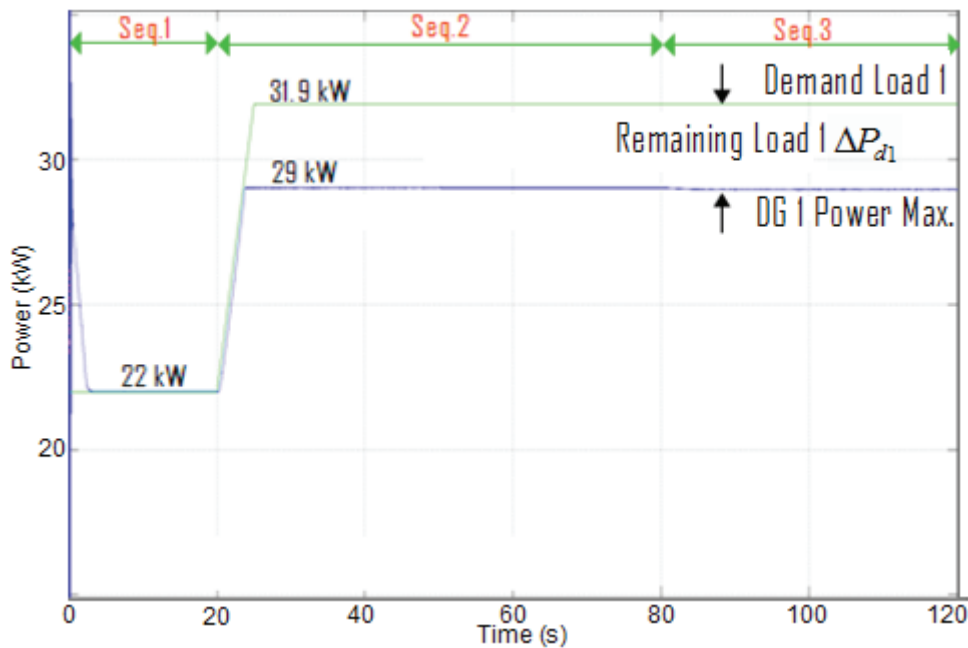


Figure 50. Power output and demand of DG 1 under SAS

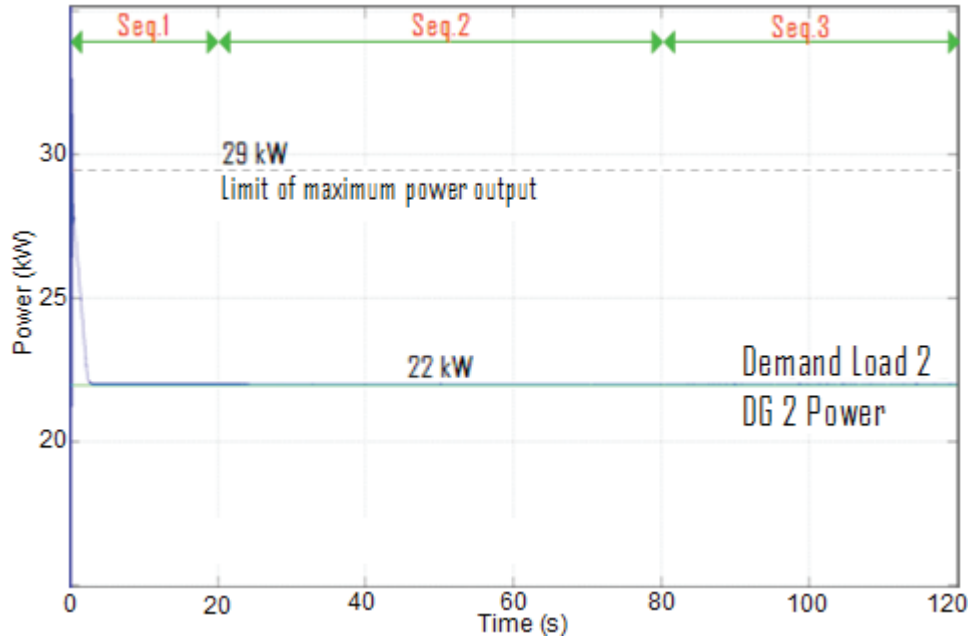


Figure 51. Power output and demand of DG 2 units under SAS

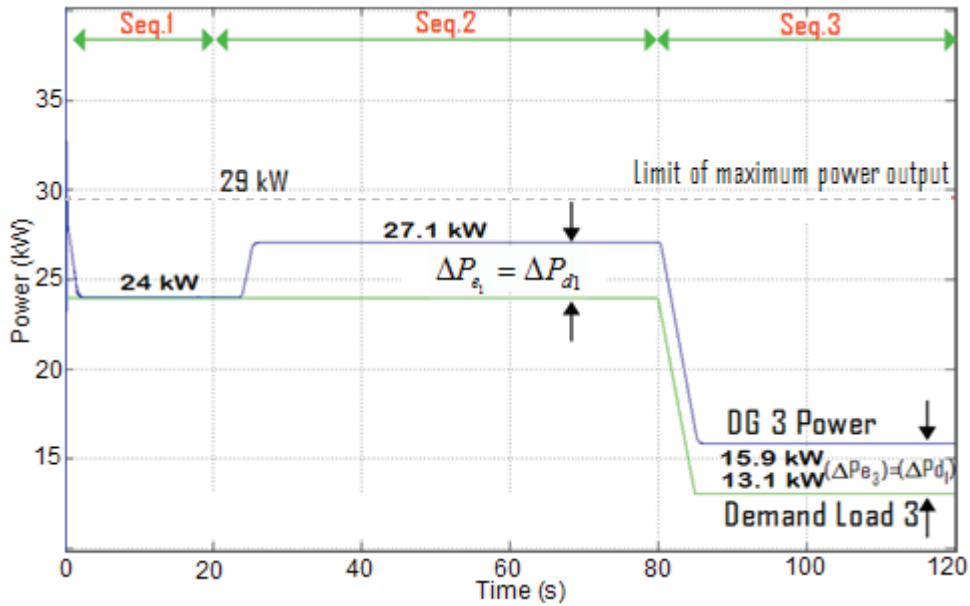


Figure 52. Power output and demand of DG 3 under SAS

The schematic diagrams of active power dispatch of each DG unit are shown in figures 53 and 54. The diagram describes the power production of three DG units in order to supply the demand. During the operation, each load transmits the load signals (green dash line) to the CCC, and then the DG units produce power according to signals from CCC (magenta dash line).

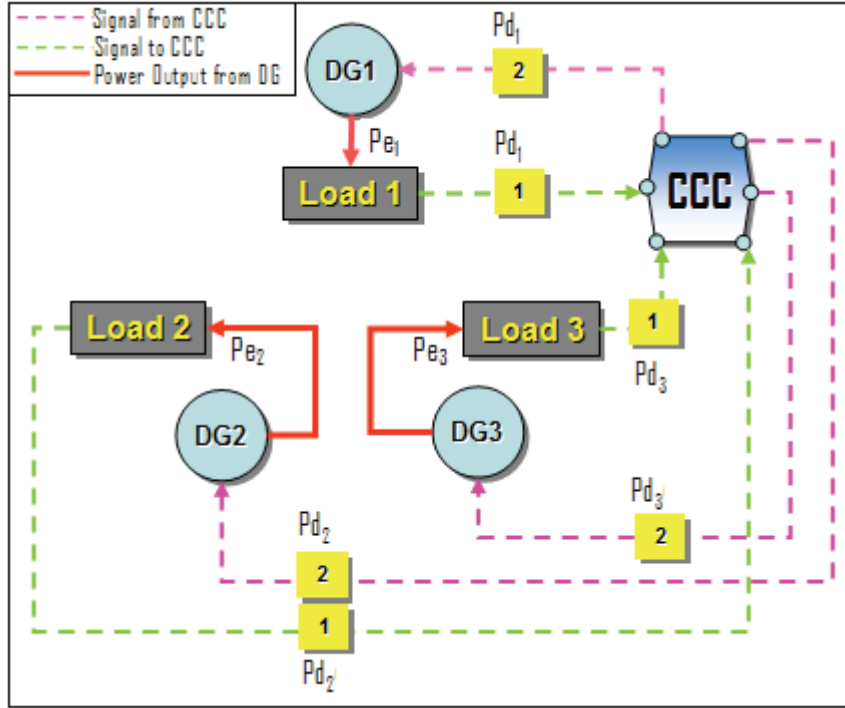


Figure 53. Dispatching power of three DG units in 1st sequence

The equations describing the correlations of active power demand of each load and active power production from three DG units in 1st sequence can be written down as:

$$P_{d_1} = P_{e_1}$$

$$P_{d_2} = P_{e_2}$$

$$P_{d_3} = P_{e_3}$$

4.4.2 Dispatching power in 2nd sequence

As shown in figure 52 loads 2 and 3 in second sequence are still lower a maximum capacity of DG. On the other hand load 1 is increasing over the maximum capacity of DG 1. In this condition, according to DG priority as shown in table 11 previously, the CCC transmits the remaining load signal to DG 3. If the power of DG 3 is still below its maximum capacity, then DG 3 will increase its power output in response the CCC signal. If the compensation from DG 3 is not sufficient to cover the remaining load 1, thereafter the signal is transmitted to DG 2. Finally if power from DG 2 is not sufficient, then power flows from the grid to supply/cover the remaining load.

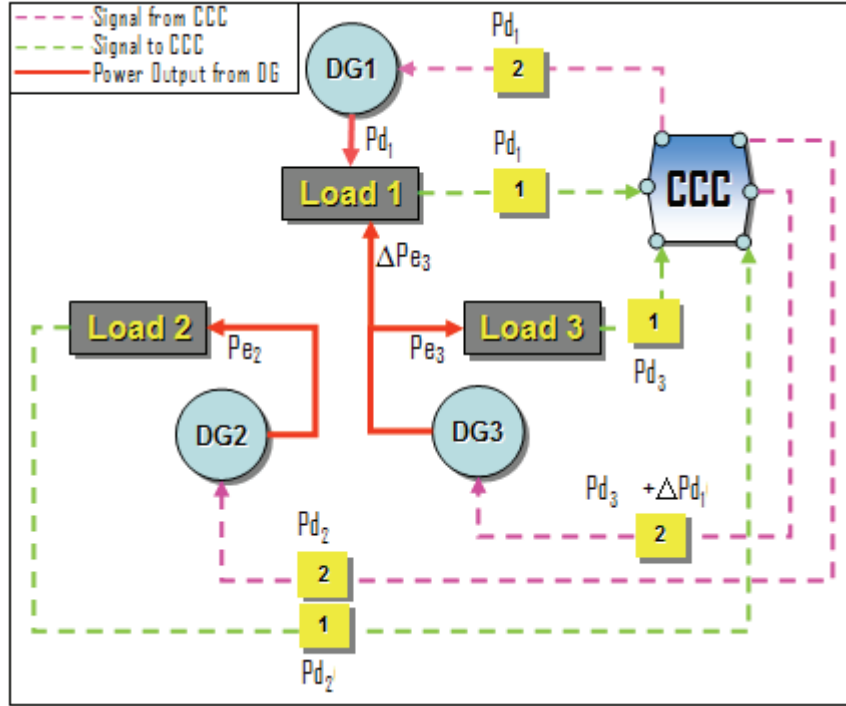


Figure 54. Dispatching of power of three DG units in 2nd and 3rd sequences

However the remaining load 1 can be compensated by DG 3 and load 2 is fully covered by DG 2. The schematic diagram as shown above can be represented by following mathematical equation:

$$P_{d1} = P_{e1} + \Delta P_{d1}$$

$$\Delta P_{d1} = \Delta P_{e3}$$

$$P_{d2} = P_{e2}$$

$$P_{d3} = P_{e3} - \Delta P_{d1}$$

Where:

$\Delta P_{e(1,2,3)}$ is active power compensation from DG 1, 2, or 3

4.3.3 Dispatching of power in 3rd sequence

In third sequence, load 1 and load 2 are still stable at 31.9 kW and 22 kW, respectively. On the other hand as shown in figure 52, load 3 is decreasing significantly from 24 kW to 13.1 kW. During this condition, DG 2 is still adequate to supply power to load 2 and DG 3 is still covering power to load 3 and load 1. Therefore the correlation between active power demand of each load and active power production of each DG are similar with case in 2nd sequence.

The total loads and total power of VPP under SAS can be seen in figure 55, the green line is total power production of three DG units and the red line is total demand of three

loads. In first and third sequence when the total demands are circa 68 kW and 67 kW, the VPP is able to produce power proportionally. And when the total demand reaches 77.9 kW, the VPP injects active power slightly higher until 78.1 kW. Therefore the main grid receives active power from VPP circa 0.2 kW.

However the dispatching of power and coordination among DG units during dynamics load is running satisfactorily.

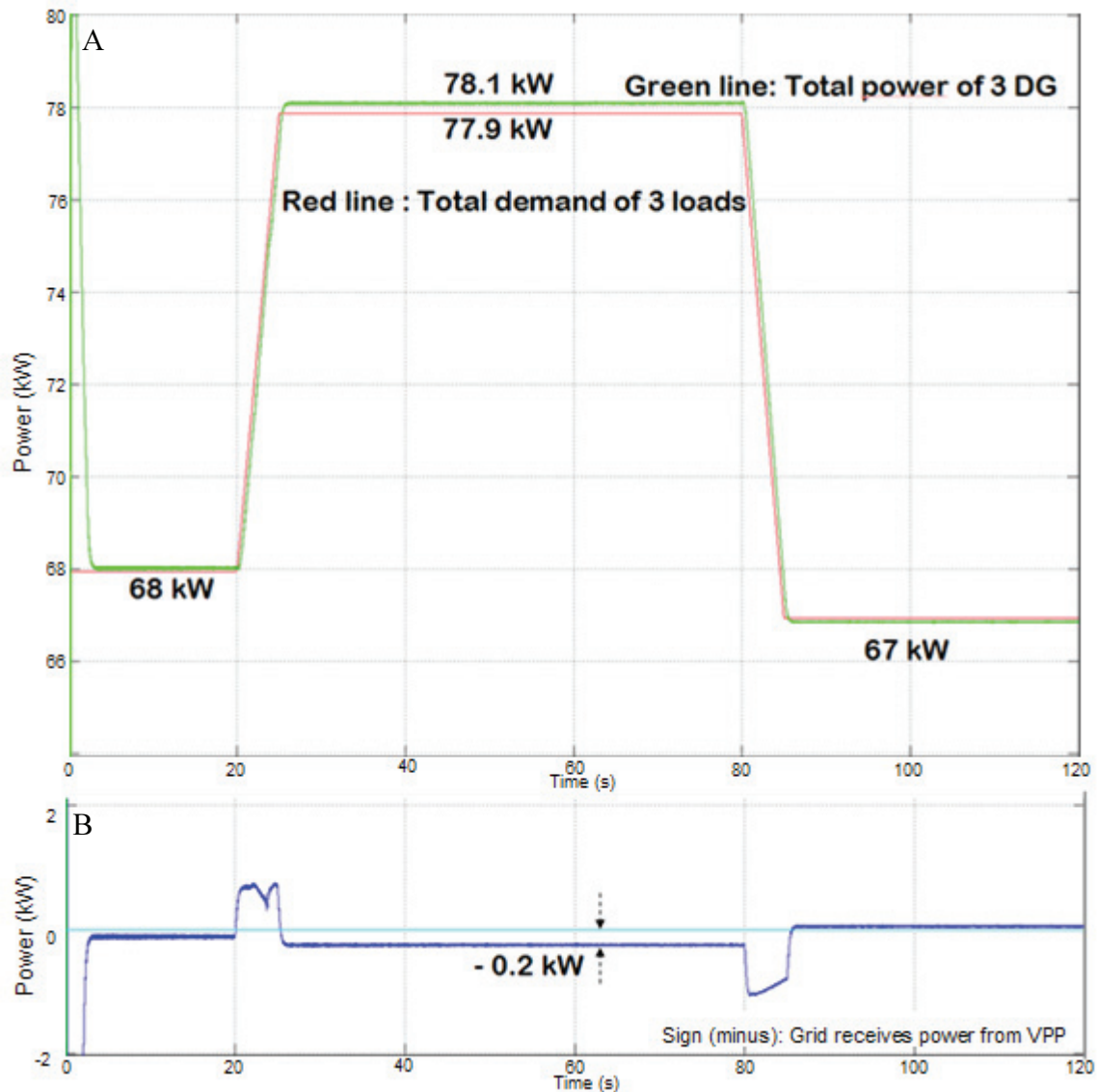


Figure 55.A. Total loads demand and total power of VPP under SAS, B. Power metering (from main grid side)

Some achievements of smart autocontrol system are:

- a. Control coordination centre is able to coordinate the loads demand and control dispatching of power of DG units in order to minimize export/import of power. Comparing with BAS performance as shown in figure 47, the power import from the main grid can be preventable under SAS. Although during high power demand scenario, the export power from VPP to the main grid is still flowing circa 0.2 kW.
- b. The minimizing of export and import power impact to reduce power flow through the transformer. Thereby the age of transformer could be longer.
- c. The DG units under SAS can compensate the remaining load as fast as possible rather the main grid by means of coordination and information exchange in CCC.
- d. The concept of SAS is possible to be applied to control more than three DG units, however at least two requirements should be prepared:
 - a. Expanding logic algorithm at the CCC.
 - b. Providing new communication line from CCC to new DG unit.

Chapter 5

Tracking Optimum Efficiency of VPP

5.1. Efficiency Curve of distributed generation unit

This chapter presents the development of efficiency tracking control of VPP depending on the DG efficiency curve. The objective is to achieve optimum efficiency of VPP and improve reliability of VPP in terms of minimization of export/import of power during dynamic loads. In order to accomplish this objective, the DG efficiency curve is used as an important parameter for developing logic algorithm at each local controller. During the simulation, the efficiency of three DG units is assumed similar as shown in figure 56 and the load profiles of three DG units are also like those in the previous scenarios.

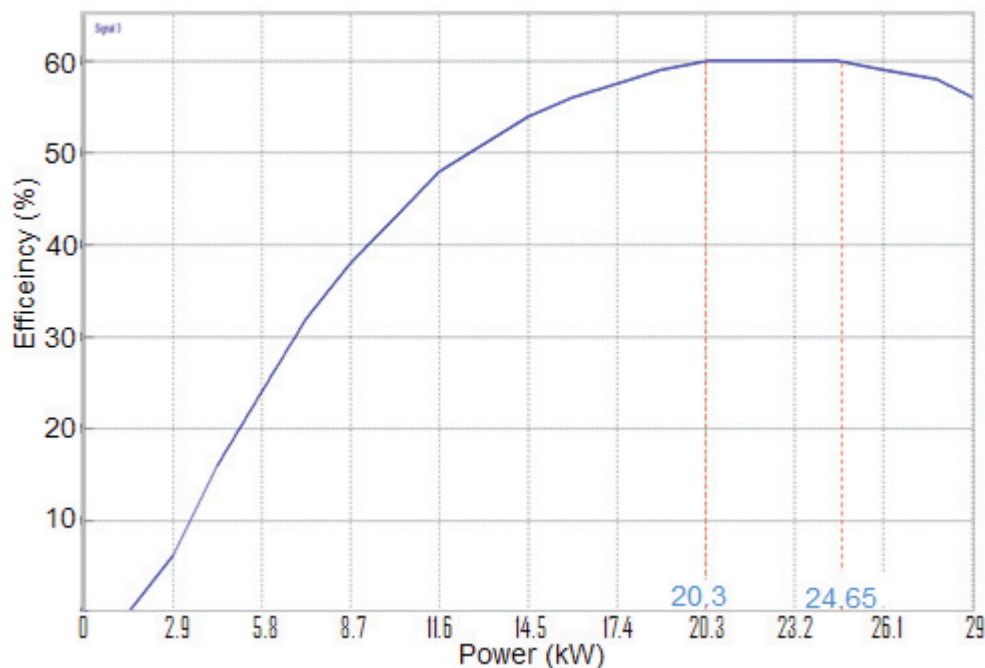


Figure 56. Efficiency curve of the DG

This figure shows that the maximum efficiency of DG (60%) is achieved when active power output of DG units is in the range of 20.3 kW - 24.65 kW. If the DG unit operates out of this power range, the efficiency decreases. Table 12 presents the correlation between power output and efficiency.

Table 12. Power output and DG efficiency

No	Power (%)	Power (kW)	Eff. (η) %	No	Power (%)	Power (kW)	Eff. (η) %
1	5	1.45	0	11	55	15.95	56
2	10	2.9	6.2	12	60	17.4	57.5
3	15	4.35	16	13	65	18.85	59
4	20	5.8	24	14	70	20.3	60
5	25	7.25	32	15	75	21.75	60
6	30	8.7	38	16	80	23.2	60
7	35	10.15	43	17	85	24.65	60
8	40	11.6	48	18	90	26.1	59
9	45	13.05	51	19	95	27.55	58
10	50	14.5	54	20	100	29	56

In contrast with previous simulation, the topology of VPP is changed into decentralised system which consists of three DG units and three loads (see appendix E). The schematic diagram of decentralised VPP in the simulation is shown in figure 57.

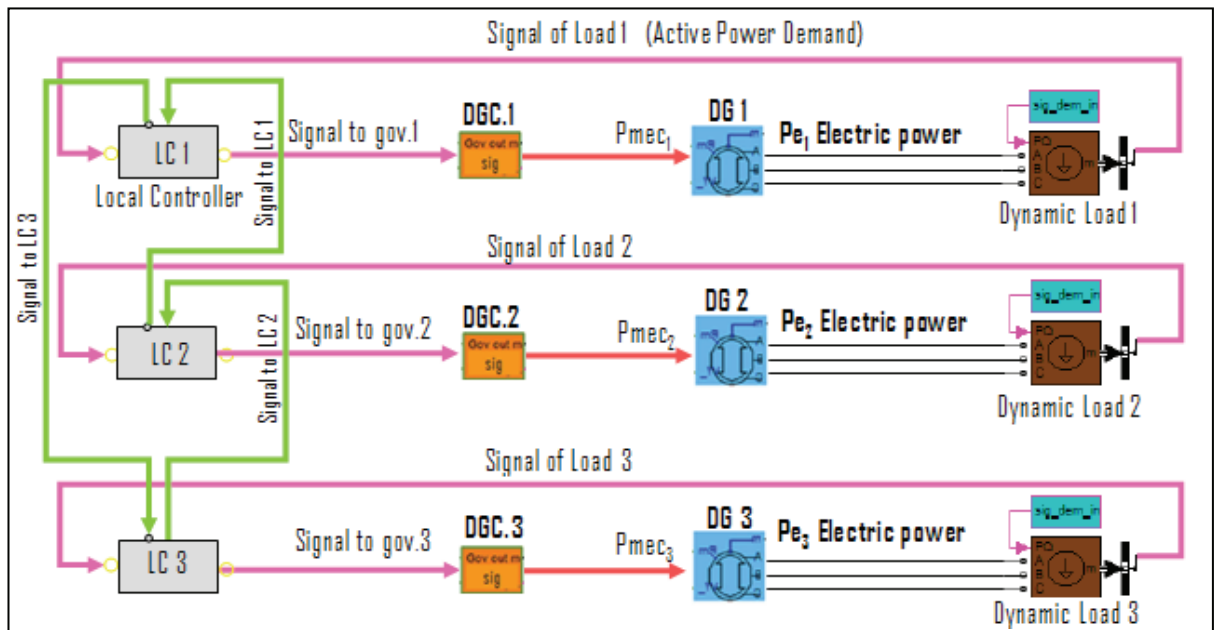


Figure 57. The schematic diagram of decentralised Virtual Power Plant

The figure shows that each load sends signal (active power demand) to its local controller and these controllers are connected to each other forming a cycle or a ring (shown in green line) and communicate to allow information/signals exchange. Afterwards the signal is transmitted to DGC/governor, thus the DG output is controlled to feed the dynamic loads. In all-optical networks, the ring topology is a popular configuration.

Some top reasons that make the ring topology a favoured one are its simplicity, scalability and survivability in the presence of link failures [36].

In this simulation, the main scenario is if the load varies then the DG power output will change in order to follow the load, consequently the DG efficiency changes also (except when the load varies from 20.3 kW to 24.65 kW - the efficiency is constant). If the varying load impacts to the efficiency of the DG then the total efficiency of VPP is affected. Due to this condition, each local controller will run iteration process and exchange the signals following the ring topology as shown in figure 57. The signal from local controller (LC) 1 is transmitted to LC 3, signal of LC 3 is sent to LC 2, and signal from LC 2 is transferred to LC 1. Therefore by tracking new optimum efficiency of VPP and minimization of power export/import can be achieved.

The performance of this control called Tracking Efficiency Autocontrol System (TEAS) is demonstrated through a simulation scenario with three DG units under varying loads conditions.

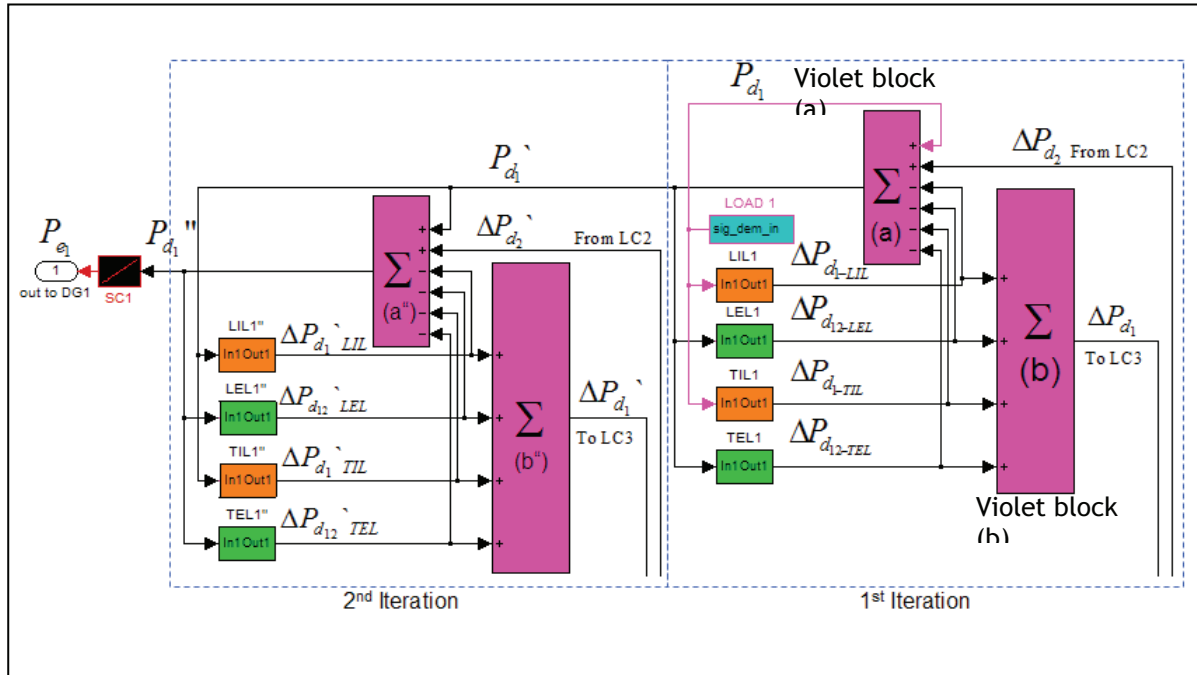


Figure 58. TEAS logic algorithm at local controller 1

5.2. Developing logic algorithms

The procedure of logic algorithm of TEAS is mentioned generally in previous pages. The detailed explanation of this logic algorithm at local controller of DG 1 is shown figure 58. Here two steps iteration are performed in order to track optimum efficiency and minimizing power export/import. The blue block receives signal from load 1. Then the signal is transmitted to three blocks: two orange blocks and a violet block (a). In the orange blocks -LIL- (Low Internal Limiter) block and TIL (Top Internal Limit) blocks, the power limit of maximum DG efficiency is set at 20.3 kW to 24.65 kW. Then the signal of load 1 is detected and determined whether it is over or lower than the limit. The output signal from these blocks is transmitted to violet blocks (a) and violet block (b).

In the violet blocks (a), the output signal from LIL or TIL block and signal from load 1 is processed with external signal from local controller (LC) 2. Afterwards the signal is transmitted to 2nd iteration process and two green blocks (LEL – Low External Limiter and TEL – Top External Limiter). At LEL and TEL blocks, the signal from violet block (a) is detected whether is over or lower than the range of maximum efficiency limit. Then the 1st output from these blocks is transmitted to violet blocks (a) again to be processed with new signal from load 1 and new signal from LC 2. The 2nd output is transmitted to the violet block (b). Here, four signals from LIL, TIL, LEL and TEL blocks are processed; afterwards the signal is transmitted to LC 3 for the next algorithm process. The procedure of logic algorithm at LC 2 and LC 3 is similar as described above. However the output signal from violet block (b) at LC 2 and LC 3 is transmitted to violet block (a) at LC 1 and LC 2 respectively. The detailed diagram of TEAS algorithm and the flow chart is in appendix F.

5.2.1 The formulation of power output of DG1 according to the logic algorithm

Notation:

- $P_{e_{1,2,3}}$ = signal of active power output of DG 1, 2 or 3
- $P_{d_{1,2,3}}$ = signal of active power demand from load 1, 2 or 3
- $P_{d_{1,2,3}}'$ = signal of active power output of load 1, 2 or 3 after 1st iteration
- $\Delta P_{d_{2,3,1}}$ = signal of remaining active power demand from load 2, 3 or 1 after 1st iteration
- $\Delta P_{d_{1-LIL}}$ = output signal from *lowest* internal limiter (1st iteration)

ΔP_{d_1-TIL} = output signal from *top* internal limiter (1st iteration)

$\Delta P_{d_{12}-LEL}$ = output signal from *lowest* external limiter (1st iteration)

$\Delta P_{d_{12}-TEL}$ = output signal from *top* external limiter (1st iteration)

$\Delta P_{d_{2,3,1}}$ = signal of remaining active power demand from load 2, 3 or 1 after 2nd iteration

$P_{d_1}'_{LIL}$ = output signal from *lowest* internal limiter (2nd iteration)

$P_{d_1}'_{TIL}$ = output signal from *top* internal limiter (2nd iteration)

$P_{d_{12}}'_{LEL}$ = output signal from *lowest* external limiter (2nd iteration)

$P_{d_{12}}'_{TEL}$ = output signal from *top external* limiter (2nd iteration)

P_{d_1}'' = output signal of active power demand after 2nd iteration

The power output of DG 1 after 2nd iteration can be obtained as

$$P_{e_1} = P_{d_1}''$$

Where

$$\begin{aligned} P_{d_1}' &= P_{d_1} - \Delta P_{d_1-LIL} - \Delta P_{d_{12}-LEL} - \Delta P_{d_1-TIL} - \Delta P_{d_{12}-TEL} + \Delta P_{d_2} \\ P_{d_1}'' &= P_{d_1}' - \Delta P_{d_1}'_{LIL} - \Delta P_{d_{12}}'_{LEL} - \Delta P_{d_1}'_{TIL} - \Delta P_{d_{12}}'_{TEL} + \Delta P_{d_2}' \end{aligned}$$

Then

$$P_{e_1} = P_{d_1} - \Delta P_{d_1-LIL} - \Delta P_{d_{12}-LEL} - \Delta P_{d_1-TIL} - \Delta P_{d_{12}-TEL} + \Delta P_{d_2} - \Delta P_{d_1}'_{LIL} - \Delta P_{d_{12}}'_{LEL} - \Delta P_{d_1}'_{TIL} - \Delta P_{d_{12}}'_{TEL} + \Delta P_{d_2}' \quad (1)$$

The equation of active power output of DG 1 can be specified into four conditions:

Condition A: if demand of load 1 is at $20.3 \text{ kW} \leq P_{d_1} \leq 24.65 \text{ kW}$ and no signal from LC 2 is

$$P_{e_1} = P_{d_1}$$

Condition B: if demand of load 1 is at $20.3 \text{ kW} \leq P_{d_1} \leq 24.65 \text{ kW}$ and receiving signal from LC 2 is

$$\begin{aligned} P_{e_1} &= P_{d_1} + \Delta P_{d_2} \\ P_{e_1} &= P_{d_1} - \Delta P_{d_{12}-LEL} - \Delta P_{d_{12}-TEL} + \Delta P_{d_2} - \Delta P_{d_1}'_{LIL} - \Delta P_{d_{12}}'_{LEL} - \Delta P_{d_1}'_{TIL} - \Delta P_{d_{12}}'_{TEL} + \Delta P_{d_2}' \end{aligned}$$

Condition C: if demand of load 1 is less than 20.3 kW and receiving signal from LC 2 is formulated as

$$P_{e_1} = P_{d_1} + \Delta P_{d_2}$$

$$P_{e_1} = P_{d_1} - \Delta P_{d_{1-LIL}} - \Delta P_{d_{12-LEL}} - \Delta P_{d_{12-TEL}} + \Delta P_{d_2} - \Delta P_{d_1-LIL} - \Delta P_{d_{12-LEL}} - \Delta P_{d_1-TIL} - \Delta P_{d_{12-TEL}} + \Delta P_{d_2}$$

Condition D: if the demand of load 1 is more than 24.65 kW and receiving signal from LC 2 can be expressed as:

$$P_{e_1} = P_{d_1} + \Delta P_{d_2}$$

$$P_{e_1} = P_{d_1} - \Delta P_{d_{1-TIL}} - \Delta P_{d_{12-LEL}} - \Delta P_{d_{12-TEL}} + \Delta P_{d_2} - \Delta P_{d_1-LIL} - \Delta P_{d_{12-LEL}} - \Delta P_{d_1-TIL} - \Delta P_{d_{12-TEL}} + \Delta P_{d_2}$$

5.2.2 The formulation of power output of DG2 according to the logic algorithm

$$P_{e_2} = P_{d_2} - \Delta P_{d_{2-LIL}} - \Delta P_{d_{23-LEL}} - \Delta P_{d_{2-TIL}} - \Delta P_{d_{23-TEL}} + \Delta P_{d_3} - \Delta P_{d_2-LIL} - \Delta P_{d_{23-LEL}} - \Delta P_{d_2-TIL} - \Delta P_{d_{23-TEL}} + \Delta P_{d_3} \quad (2)$$

Condition A: if demand of load 2 is at $20.3 \text{ kW} \leq P_{d_2} \leq 24.65 \text{ kW}$ and no signal from LC 3 is

$$P_{e_2} = P_{d_2}$$

Condition B: if demand of load 2 is at $20.3 \text{ kW} \leq P_{d_2} \leq 24.65 \text{ kW}$ and receiving signal from LC 3 is

$$P_{e_2} = P_{d_2} + \Delta P_{d_3}$$

$$P_{e_2} = P_{d_2} - \Delta P_{d_{23-LEL}} - \Delta P_{d_{23-TEL}} + \Delta P_{d_3} - \Delta P_{d_2-LIL} - \Delta P_{d_{23-LEL}} - \Delta P_{d_2-TIL} - \Delta P_{d_{23-TEL}} + \Delta P_{d_3}$$

Condition C: if demand of load 2 is less than 20.3 kW and receiving signal from LC 3 is formulated as

$$P_{e_2} = P_{d_2} + \Delta P_{d_3}$$

$$P_{e_2} = P_{d_2} - \Delta P_{d_{2-LIL}} - \Delta P_{d_{23-LEL}} - \Delta P_{d_{23-TEL}} + \Delta P_{d_3} - \Delta P_{d_2-LIL} - \Delta P_{d_{23-LEL}} - \Delta P_{d_2-TIL} - \Delta P_{d_{23-TEL}} + \Delta P_{d_3}$$

Condition D: if the demand of load 2 is more than 24.65 kW and receiving signal from LC 3 can be expressed as:

$$P_{e_2} = P_{d_2} + \Delta P_{d_3}$$

$$P_{e_2} = P_{d_2} - \Delta P_{d_2-TIL} - \Delta P_{d_{23}-LEL} - \Delta P_{d_{23}-TEL} + \Delta P_{d_3} - \Delta P_{d_2} \cdot_{LIL} - \Delta P_{d_{23}} \cdot_{LEL} - \Delta P_{d_2} \cdot_{TIL} - \Delta P_{d_{23}} \cdot_{TEL} + \Delta P_{d_3} \cdot$$

5.2.3 The formulation of power output of DG3 according to the logic algorithm

$$P_{e_3} = P_{d_3} - \Delta P_{d_3-LIL} - \Delta P_{d_{31}-LEL} - \Delta P_{d_{31}-TIL} - \Delta P_{d_{31}-TEL} + \Delta P_{d_1} - \Delta P_{d_3} \cdot_{LIL} - \Delta P_{d_{31}} \cdot_{LEL} - \Delta P_{d_3} \cdot_{TIL} - \Delta P_{d_{31}} \cdot_{TEL} + \Delta P_{d_1} \cdot \quad (3)$$

Condition A: if demand of load 3 is at $20.3 \text{ kW} \leq P_{d_3} \leq 24.65 \text{ kW}$ and no signal from LC 1 is

$$P_{e_3} = P_{d_3}$$

Condition B: if demand of load 3 is at $20.3 \text{ kW} \leq P_{d_3} \leq 24.65 \text{ kW}$ and receiving signal from LC 1 is

$$P_{e_3} = P_{d_3} + \Delta P_{d_1}$$

$$P_{e_3} = P_{d_3} - \Delta P_{d_{31}-LEL} - \Delta P_{d_{31}-TEL} + \Delta P_{d_1} - \Delta P_{d_3} \cdot_{LIL} - \Delta P_{d_{31}} \cdot_{LEL} - \Delta P_{d_3} \cdot_{TIL} - \Delta P_{d_{31}} \cdot_{TEL} + \Delta P_{d_1} \cdot$$

Condition C: if demand of load 3 is less than 20.3 kW and receiving signal from LC 1 is formulated as

$$P_{e_3} = P_{d_3} + \Delta P_{d_1}$$

$$P_{e_3} = P_{d_3} - \Delta P_{d_3-LIL} - \Delta P_{d_{31}-LEL} - \Delta P_{d_{31}-TEL} + \Delta P_{d_1} - \Delta P_{d_3} \cdot_{LIL} - \Delta P_{d_{31}} \cdot_{LEL} - \Delta P_{d_3} \cdot_{TIL} - \Delta P_{d_{31}} \cdot_{TEL} + \Delta P_{d_1} \cdot$$

Condition D: if the demand of load 3 is more than 24.65 kW and receiving signal from LC 1 can be expressed as:

$$P_{e_3} = P_{d_3} + \Delta P_{d_1}$$

$$P_{e_3} = P_{d_3} - \Delta P_{d_3-TIL} - \Delta P_{d_{31}-LEL} - \Delta P_{d_{31}-TEL} + \Delta P_{d_1} - \Delta P_{d_3} \cdot_{LIL} - \Delta P_{d_{31}} \cdot_{LEL} - \Delta P_{d_2} \cdot_{TIL} - \Delta P_{d_{31}} \cdot_{TEL} + \Delta P_{d_1} \cdot$$

5.3 The analysis of tracking efficiency and dispatching power according to TEAS algorithm

The analysis of tracking efficiency and dispatching power of VPP under TEAS is divided into three sequences as shown in figure 62, 63 and 64 for the dispatching power according to TEAS algorithm to be seen clearly.

5.3.1 Tracking efficiency and dispatching power in first sequence.

During first sequence the load 1 and load 2 are consuming power circa 22 kW and load 3 around 24 kW . Under these loads, all DGs run at the maximum efficiency (60 %) as

shown in figure 62, 63 and 64. The schematic diagram of dispatching active power according to signal from each local controller is shown in figure 59.

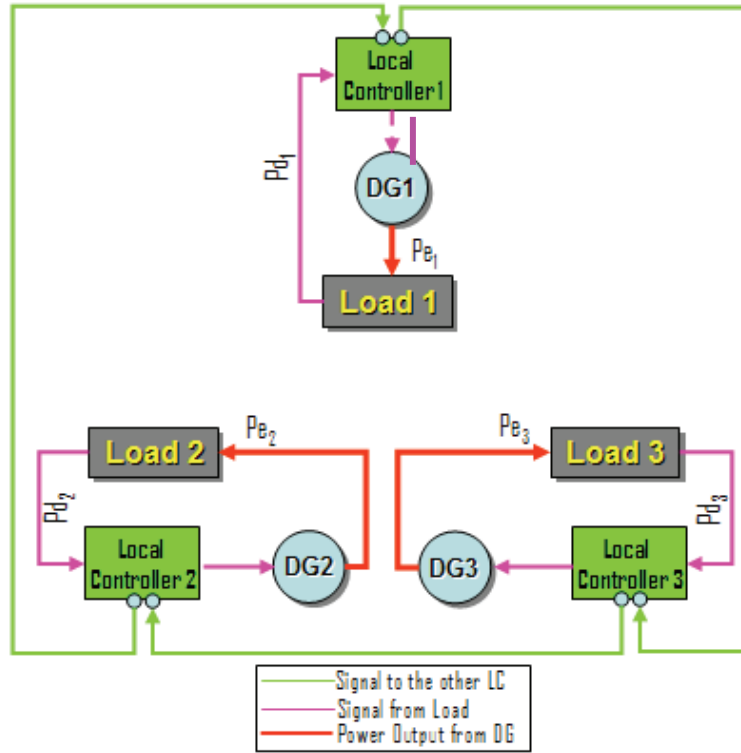


Figure 59. Power dispatching of three DG units under TEAS in 1st sequence

The correlation between active power production (P_e) and power demand (P_d) of each DG during 1st sequence can be expressed as

$$P_{e_1} = P_{d_1}$$

$$P_{e_2} = P_{d_2}$$

$$P_{e_3} = P_{d_3}$$

5.3.2 Tracking efficiency and dispatching power in 2nd sequence

The load 1 in 2nd sequence is increasing circa 45% from 22 kW to 31.9 kW, and then the efficiency of virtual power plant decreases significantly. Therefore the iteration algorithm of each local controller and information exchange among LC are running simultaneously to track new optimum efficiency of the three DG units. Afterwards as shown in figure 62, 63 and 64, the DG 1 produces power from 22 kW to 25.9 kW, then its efficiency slightly goes down from 60 % to 59.2 %. The DG 2 increases its power from 22 kW to 26.8 kW, then the efficiency moves down from 60 % to 58.5 %. And power output of DG 3 slightly

risks from 24 kW to 25.4 kW; it brings the efficiency slightly down to 59.5 % from 60 %. However the remaining load 1 can be covered by DG 2 and DG 3 thus the import of power from main grid is preventable. Moreover the DG units can run at their optimum efficiency. The schematic diagram of power dispatching is shown in figure 60 below.

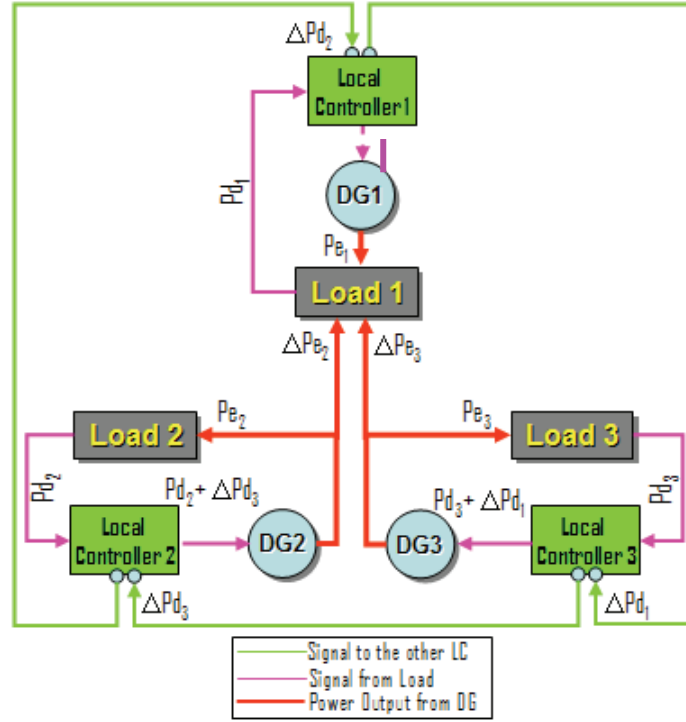


Figure 60. Power dispatching of three DG units under TEAS in 2nd sequence

The active power production of DG 1 and load 1 during 2nd sequence can be written down as

$$P_{d_1} = P_{e_1} + \Delta P_{d_1}$$

$$\Delta P_{d_1} = \Delta P_{e_2} + \Delta P_{e_3}$$

$$P_{d_1} = P_{e_1} + \Delta P_{e_2} + \Delta P_{e_3}$$

$$P_{e_1} = P_{d_1} - \Delta P_{d_1-TIL} - \Delta P_{d_12-TEL} + \Delta P_{d_2} - \Delta P_{d_1-LIL} - \Delta P_{d_12-LEL} - \Delta P_{d_1-TIL} - \Delta P_{d_12-TEL} + \Delta P_{d_2}$$

Where

ΔP_{e_2} is compensation power from DG2

ΔP_{e_3} is compensation power from DG3

The increase of active power output from DG 2 to compensate load 1 can be expressed as

$$P_{e_2} = P_{d_2} + \Delta P_{e_2}$$

$$P_{e_2} = P_{d_2} - \Delta P_{d_{23-TEL}} + \Delta P_{d_3} - \Delta P_{d_2}^{`_{LIL}} - \Delta P_{d_{23}}^{`_{LEL}} - \Delta P_{d_2}^{`_{TIL}} - \Delta P_{d_{23}}^{`_{TEL}} + \Delta P_{d_3}^{`}$$

And active power production of DG 3 is

$$P_{e_3} = P_{d_3} + \Delta P_{e_3}$$

$$P_{e_3} = P_{d_3} - \Delta P_{d_{31-TEL}} + \Delta P_{d_1} - \Delta P_{d_3}^{`_{LIL}} - \Delta P_{d_{31}}^{`_{LEL}} - \Delta P_{d_3}^{`_{TIL}} - \Delta P_{d_{31}}^{`_{TEL}} + \Delta P_{d_1}^{`}$$

5.3.3 Tracking efficiency and dispatching power in 3rd sequence

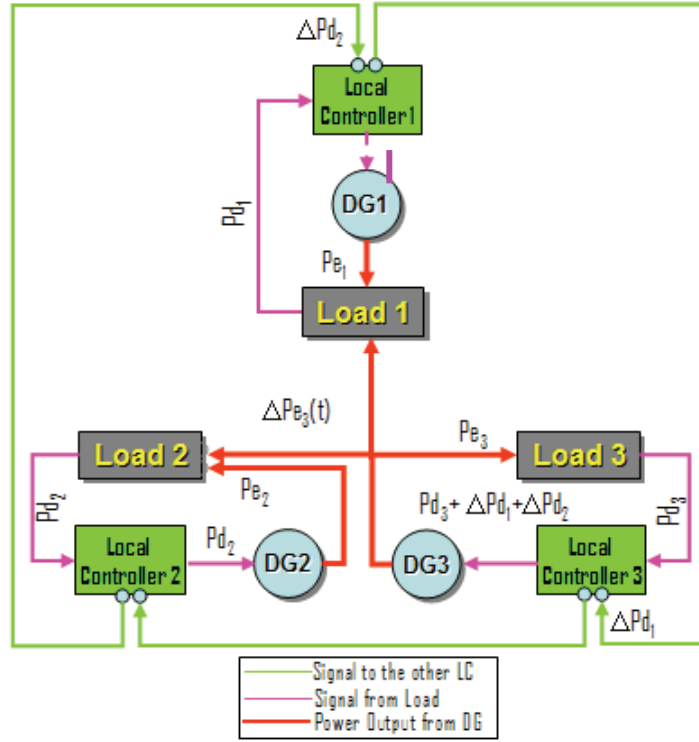


Figure 61. Power dispatching of three DG units under TEAS in 3rd sequence

In third sequence, load 3 decreases drastically from 24 kW to 13.1 kW and impact significantly on the total efficiency of the VPP. Therefore the iteration and coordination of each local controller is running again to track new optimum efficiency of VPP. Afterwards DG 1 decreases its power from circa 25.9 kW to 20.5, and then the efficiency increases from 59.2 % to 60 %. The power output of DG 2 is reduced also from 26.8 kW to 21.7 kW and its efficiency moves up from 58.5% to 60 %. As shown in figure 64, the power output of DG 3 is slightly decreased from 25.4 to 24.8 kW, then the efficiency rises from 59.5% to circa 60%.

The demand of load 1 and 2 in 3rd sequence as shown in figure 61 can be formulated as

$$P_{d1} = P_{e1} + \Delta P_{d1}$$

$$P_{d2} = P_{e2} + \Delta P_{d2}$$

The active power production of DG 1 and DG 2 in 2nd sequence is expressed as

$$P_{e1} = P_{d1} - \Delta P_{d1-TIL} - \Delta P_{d12-TEL} + \Delta P_{d2} - \Delta P_{d1-LIL} - \Delta P_{d12-LEL} - \Delta P_{d1-TIL} - \Delta P_{d12-TEL} + \Delta P_{d2}$$

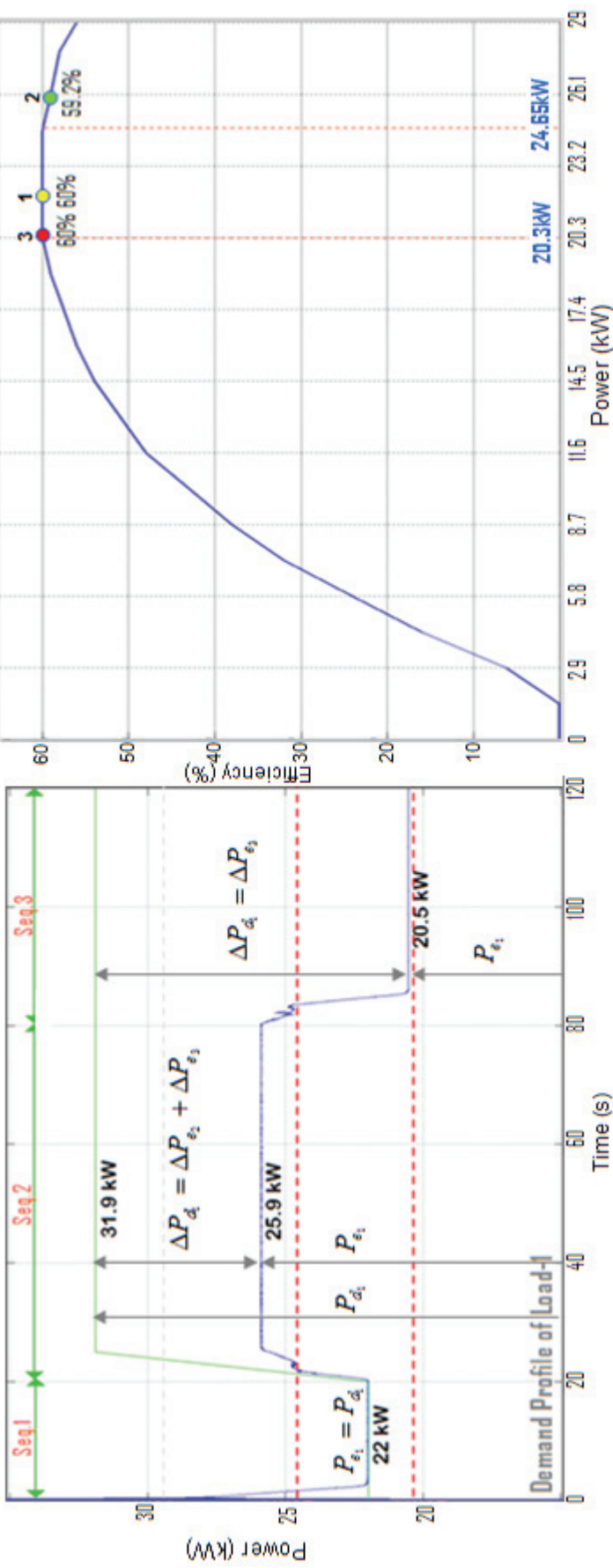
$$P_{e2} = P_{d2} - \Delta P_{d23-TEL} + \Delta P_{d3} - \Delta P_{d2-LIL} - \Delta P_{d23-LEL} - \Delta P_{d2-TIL} - \Delta P_{d23-TEL} + \Delta P_{d3}$$

The active power production of DG 3 during 3rd sequence is written as

$$P_{e_3} = P_{d_3} + \Delta P_{e_3}$$

$$\Delta P_{e_3} = \Delta P_{d_1} + \Delta P_{d_2}$$

$$P_{e_3} = P_{d_3} - \Delta P_{d_3-LLL} - \Delta P_{d_{31-TEL}} + \Delta P_{d_1} - \Delta P_{d_3_LLL} - \Delta P_{d_{31_LEL}} - \Delta P_{d_3_TIL} - \Delta P_{d_{31_TEL}} + \Delta P_{d_1}$$



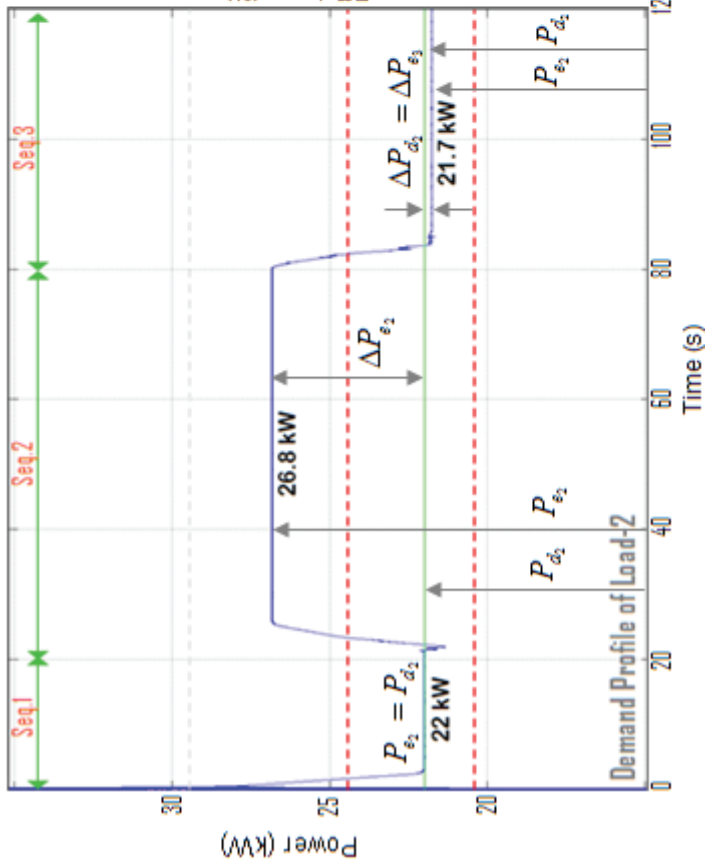
(a). Power sharing load 1

(b) Tracking efficiency at load 1

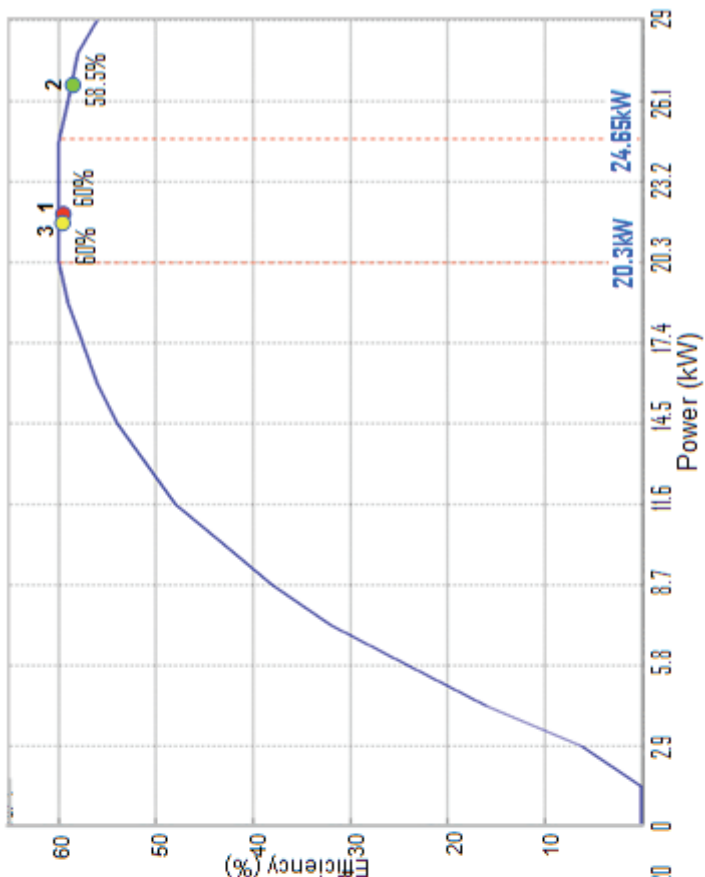
Legends :

- Limit of Maximum Efficiency of DG in (%)
- Power Output of DG 1 in kW in figure 62 (a) or Efficiency in figure 62 (b)
- Demand of Load 1 in kW
- Efficiency of DG at 1st sequence
- Efficiency of DG at 2nd sequence
- Efficiency of DG at 3rd sequence

Figure 62. Power sharing and tracking of efficiency at load 1



(a). Power sharing load 2

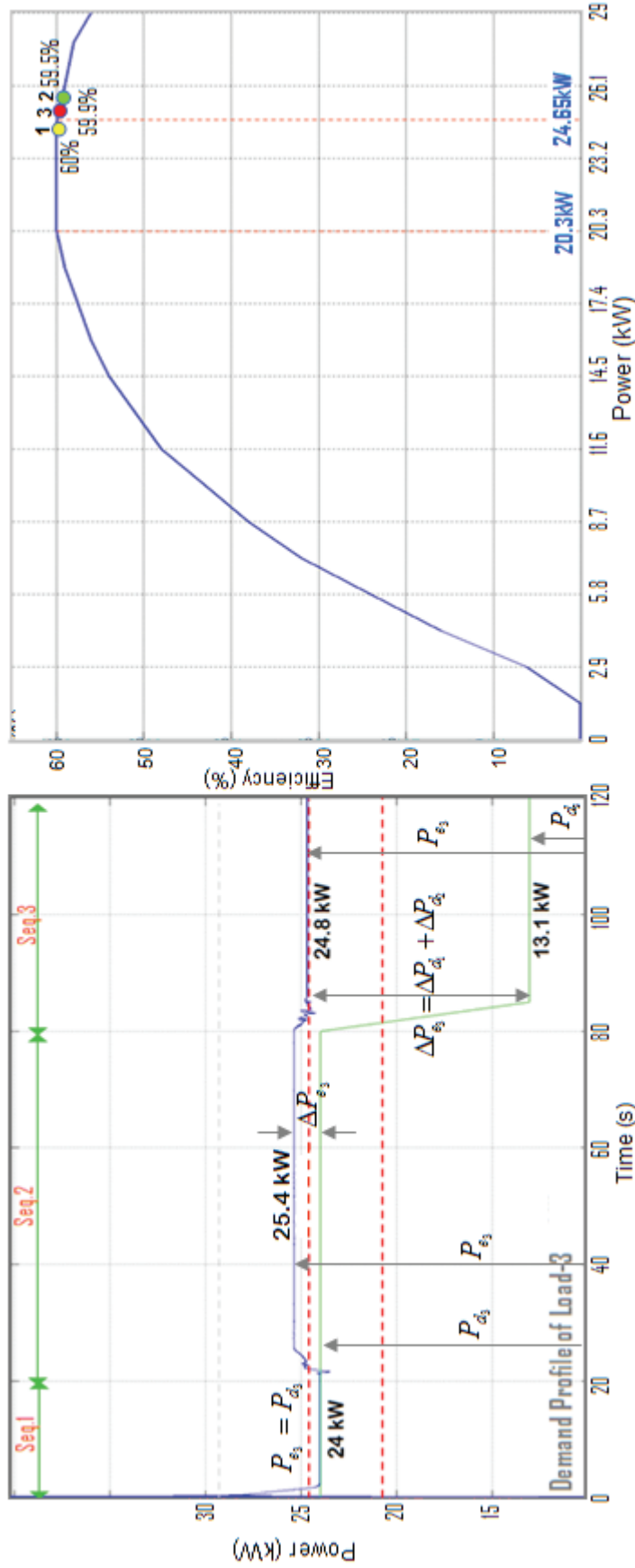


(b) Tracking efficiency at load 2

Legends:

- Limit of Maximum Efficiency of DG in (%)
- Power Output of DG 1 in kW in figure 63 (a) or Efficiency in figure 63 (b)
- Demand of Load 1 in kW
- Efficiency of DG at 1st sequence
- Efficiency of DG at 2nd sequence
- Efficiency of DG at 3rd sequence

Figure 63 Power sharing and tracking of efficiency at load 2



(a). Power sharing load 3

(b) Tracking efficiency at load 3

Legends:

- Limit of Maximum Efficiency of DG in (%)
- Power Output of DG 1 in kW in figure 64 (a) or Efficiency in figure 64 (b)
- Demand of Load 1 in kW
- Efficiency of DG at 1st sequence
- Efficiency of DG at 2nd sequence
- Efficiency of DG at 3rd sequence

Figure 64. Power sharing and tracking of efficiency at load 3

The total power (green line) of three DG units can follow three dynamic loads (red line) by means of coordination and iteration process of three local controllers (see figure 65A). The metering of power at interconnection point shows that import/export power achieved is near 0 kW, particularly when the load is circa 67-68 kW. However when the total load is circa 77.9 kW, the total power of three DG units are slightly higher circa 78.1 kW, then the VPP export power of 0.2 kW into the grid.

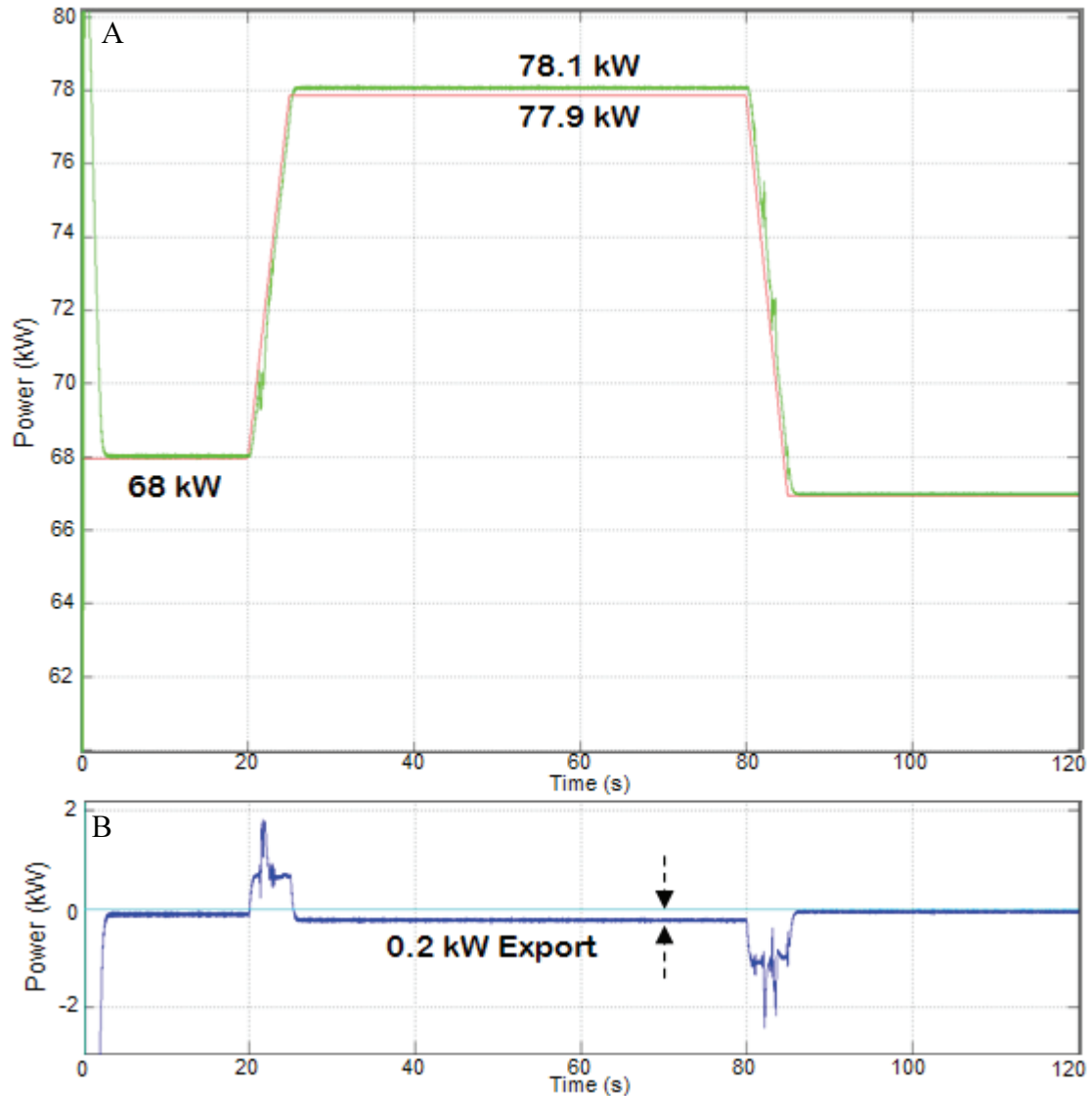


Figure 65.A. Total load demand and total power of VPP under TEAS, B. Power metering (from main grid side)

In the following paragraphs the performance of TEAS is compared with previous controls (BAS and SAS).

5.4 Comparison result of BAS, SAS and TEAS according to the efficiency curve

5.4.1. Comparison at load 1

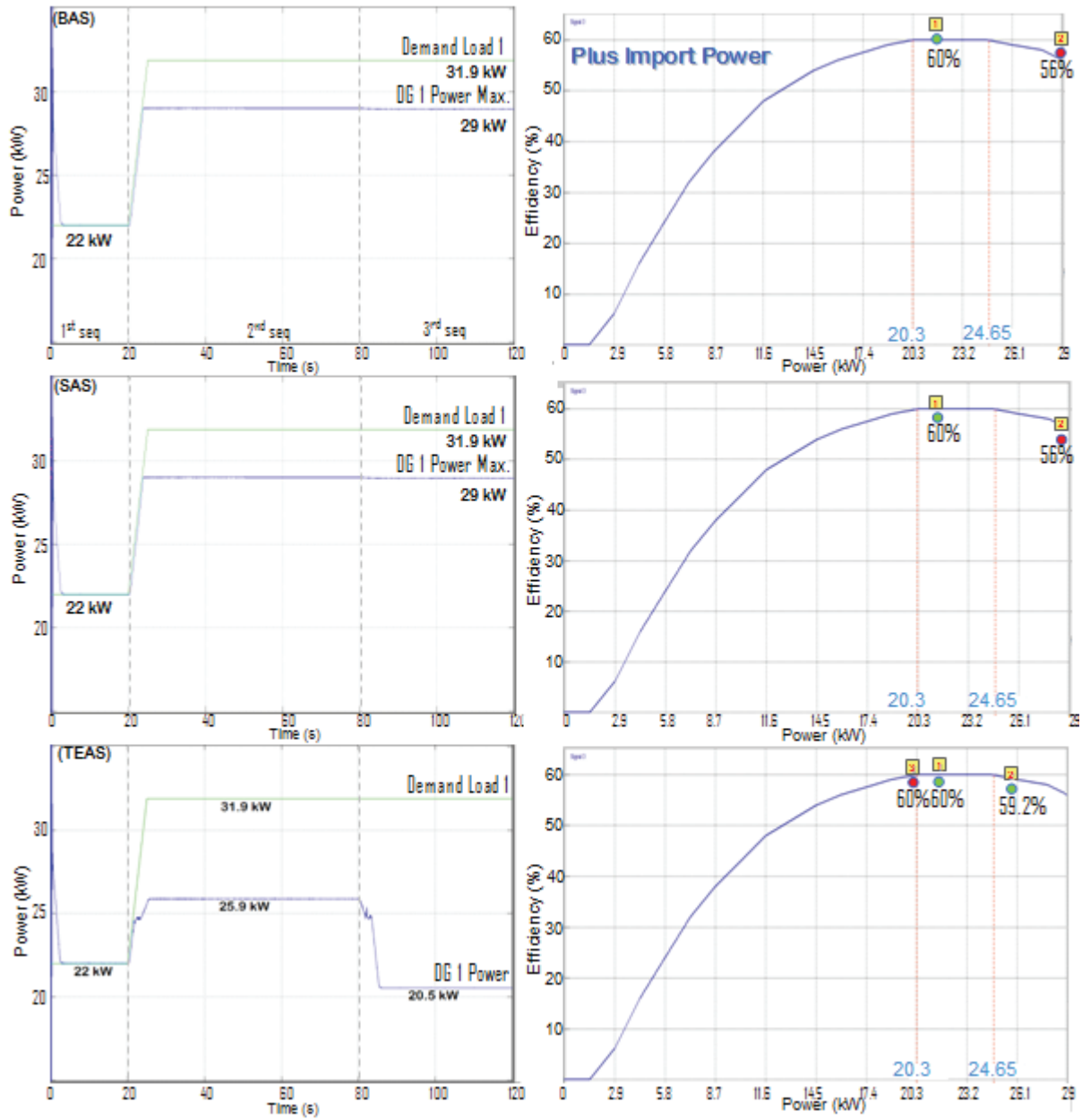


Figure 66. Comparison of efficiency at load 1

In figures 66, 67 and 68, the comparison of efficiency in BAS, SAS and TEAS is presented. The comparison is done for similar load profiles and DG efficiency curve. In the 1st sequence, the DG 1 which is operated under BAS, SAS and TEAS runs well at maximum efficiency 60 %. In 2nd sequence when load 1 is increasing to around 31.9 kW, the DG efficiency under BAS decreases to 56% (29 kW) and the remaining load of 2.9 kW is supplied from the main grid.

The efficiency of DG 1 under SAS is also falling to 56 %, but the power import can be avoided by DG 2 compensation of 3 kW. Under TEAS, the efficiency of DG 1 decreases slightly to 59 % or 25.9 kW power output and thus DG 2 and DG 3 are increasing their power to compensate load 1 (see figure 67). In the 3rd sequence the power output of DG 1 is decreasing to 20.5 kW and the efficiency is increasing to 60 %.

5.4.2. Comparison at load 2

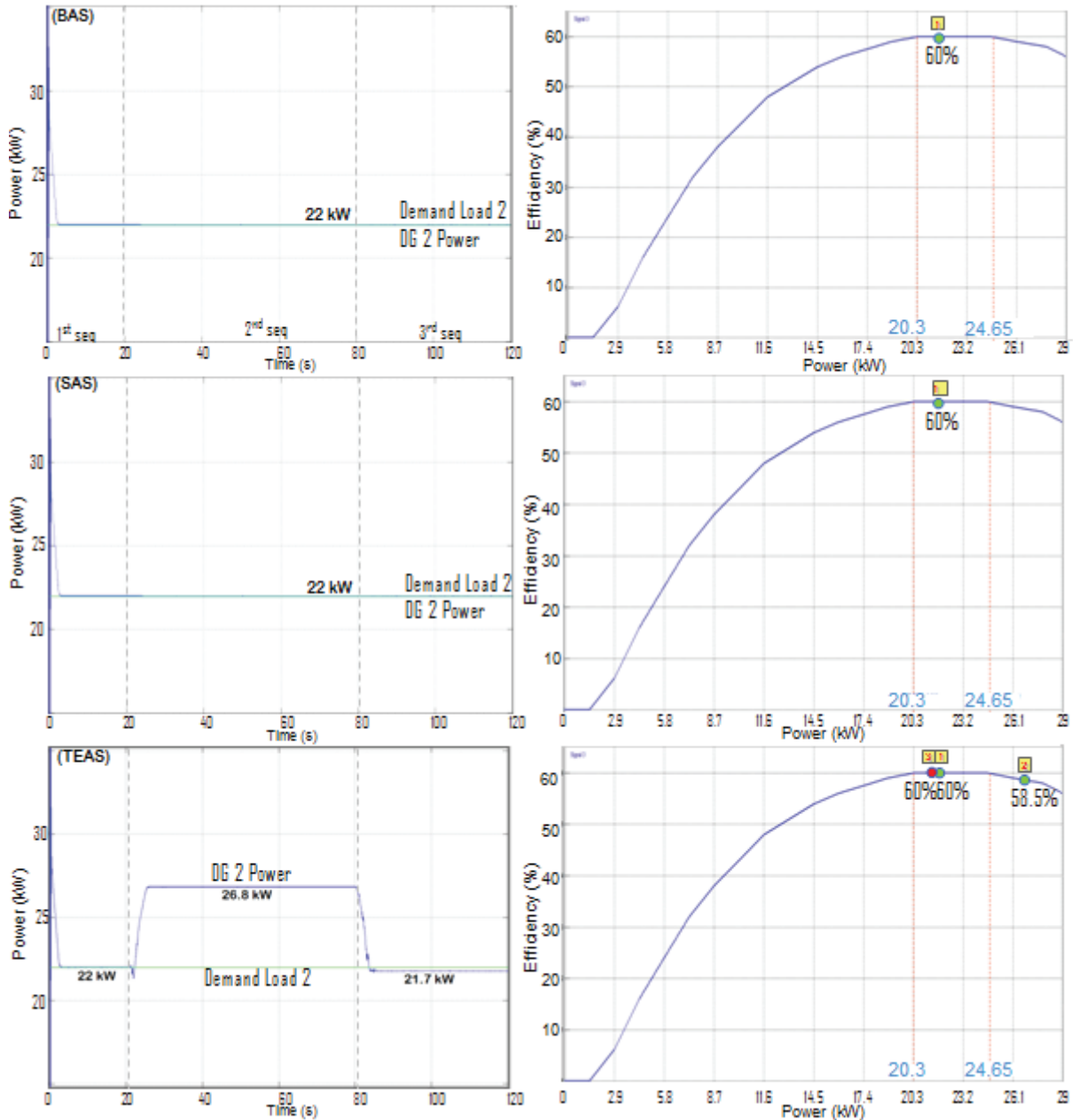


Figure 67. Comparison of efficiency at load 2

Due to the constant load at 22 kW, the efficiency of DG 2 under BAS and SAS is operating stably at maximum efficiency 60%. Under TEAS, the efficiency of DG 2 in

1st sequence is 60% and produce power circa 22 kW, then slightly goes down to 58.5% due to the increasing of power to compensate load 1 circa 4.8 kW. In 3rd sequence, the efficiency is increasing until 60 % due to the decreasing of power output to 21.7 kW.

5.4.3. Comparison at load 3

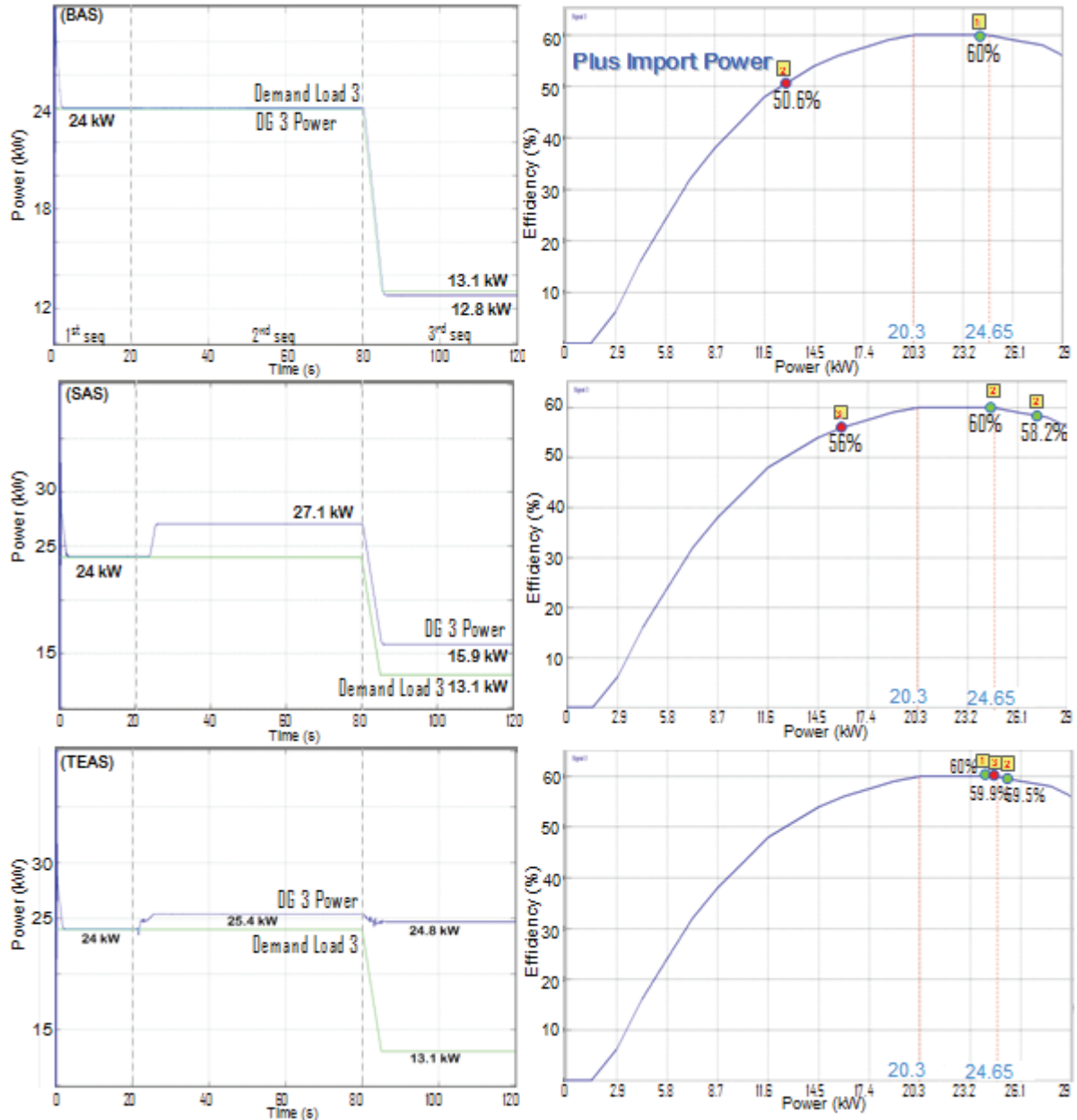


Figure 68. Comparison of efficiency at load 3

In load 3, the efficiency of DG 3 under BAS in 1st sequence and 2nd sequence is at maximum (60%). However when the load is falling down to circa 12.8 kW, the efficiency of DG 3 also drops significantly to 50.6%. The efficiency of DG 3 under SAS in 1st sequence is 60% and when the DG 3 is increasing the power to compensate load 1,

then the efficiency is decreasing to 58.2%. In 3rd sequence the output of DG 3 is reducing in order to follow the load into 15.9 kW and the efficiency is dropping to 56%. Under TEAS, the efficiency of DG 3 in 1st sequence is 60% with 24 kW power output, then slightly down to 59.5 % in 2nd sequence due to the increase of power to compensate load 1. Finally in 3rd sequence, the efficiency of DG 3 is rising up again to 59.9 % with power output circa 24.8 kW.

The simulation results show that during dynamic loads, the logic algorithm of TEAS is able to track the optimum efficiency of three DG units. The detailed comparison of efficiency among BAS, SAS and TEAS is listed at table 13 below.

Table 13. Detail DG comparison efficiency under BAS, SAS and TEAS in each sequence

DG	Logic control	Efficiency of VPP at different load conditions		
		in 1 st sequence (%)	in 2 nd sequence (%)	in 3 rd sequence (%)
DG 1	BAS	60	56	56
	SAS	60	56	56
	TEAS	60	59.2	60
DG 2	BAS	60	60	60
	SAS	60	60	60
	TEAS	60	58.6	60
DG 3	BAS	60	60	50.6
	SAS	60	58.2	56
	TEAS	60	59.5	59.9

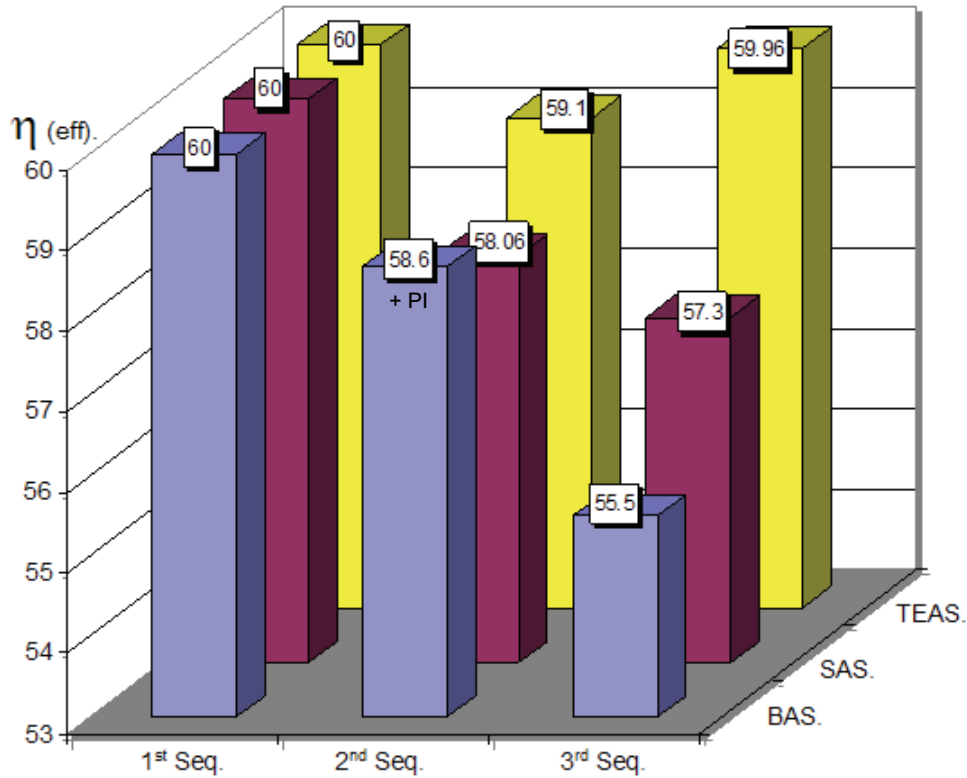


Figure 69. Summary of efficiency comparison under BAS, SAS and TEAS

This figure shows that in 1st sequence, the total efficiency of three DG units under BAS and VPP under SAS and TEAS is at 60 %. In 2nd sequence where the total loads are high, the total efficiency of three DG units under BAS is slightly down to 58.6% plus import power from the grid. The efficiency of VPP under SAS is decreasing to 58.06 % (without import power) and the total efficiency under TEAS is higher circa 59.1 %. In 3rd sequence, the efficiency of the three DG units under BAS is dropping significantly to 55.5%, VPP under SAS is around 57.3% and VPP under TEAS can reach 59.96% \approx 60% efficiency. This result clearly shows that the logic control algorithm of TEAS is able to achieve optimum efficiency of VPP satisfactorily.

5.5. General equation of Tracking Efficiency Autocontrol System

The detailed derivation of the equation of TEAS was already shown previously. In order to formulate general equation of active power output signal under TEAS, the schematic diagram in figure 57 and 58 are simplified into figure 70.

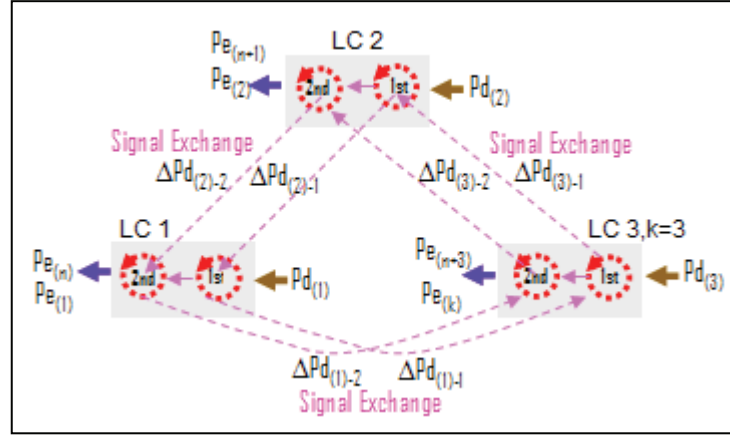


Figure 70. Principle of signal exchange under TEAS algorithm for three local controllers

According to the signal exchange mechanism as shown above, the general equation of active power output signal at each DG unit can be written as:

$$P_{e(n)} = P_{d(n)} + \sum_{m=1}^i \left[\Delta P_{d(n+1)} \right]_{(m)} + \sum_{m=1}^i (-1) \cdot \left[\Delta P_{d(n)} \right]_{(m)} \quad (4)$$

Where:

P_e is signal of active power output

P_d is signal of active power demand

ΔP_d is signal of remaining active power demand

$n = 1 \rightarrow k$, the DG unit. The (k) is the last DG on the ring topology.

$m = 1 \rightarrow i$, the loops in local controller.

If $n = k$, then

$$\left[\Delta P_{d(n+1)} \right]_{(m)} = \left[\Delta P_{d(k+1)} \right]_{(m)} = \left[\Delta P_{d(1)} \right]_{(m)}$$

By using general equation (4), the TEAS algorithm can be applied for application of Virtual Power Plant which is consisted of more than three DG units. The relation between equation (4) and (1) is shown in appendix J.

Moreover, the TEAS algorithm is able to be applied for Virtual Power Plant which is consisted of non similar DG efficiency curves. It is accomplished by changing the settings of DG power operation parameter at LIL, LEL, TIL and TEL blocks of each local controller. The detailed description is shown in appendix K, L and M.

5.6 Conclusions

The table 14 in the next page shows the summary of comparison result of different types of DG controls concerning total efficiency and metering power flow at grid interconnection.

Table 14. The summary of comparison result of different types DG control

Type of control	Total Loads			Total Power Production of 3 DG Units			Metering on Grid Connection			Total Efficiency of 3 DG Units		
	1 st seq.	2 nd seq.	3 rd seq.	1 st seq.	2 nd seq.	3 rd seq.	1 st seq.	2 nd seq.	3 rd seq.	1 st seq.	2 nd seq.	3 rd seq.
1.Full P.O	68 kW	77.9kW	67 kW	87 kW	87 kW	87 kW	-19 kW	-9.1 kW	-20 kW	56 %	56 %	56 %
2.BAS	68 kW	77.9kW	67 kW	68 kW	75 kW	63.8 kW	0 kW	2.9 kW	3.2 kW	60 %	58.6 %	55.5 %
3.SAS	68 kW	77.9kW	67 kW	68 kW	78.1 kW	67 kW	0 kW	-0.2 kW	0 kW	60 %	58.06 %	57.3 %
4.TEAS	68 kW	77.9kW	67 kW	68 kW	78.1 kW	67 kW	0 kW	-0.2 kW	0 kW	60 %	59.1 %	59.96 \approx 60 %

- Three DG units under full power output (Full P.O) during dynamics load are exporting power to the grid circa 9 kW (in 2nd sequence) and circa 19- 20 kW (in 1st and 3rd sequences). The efficiency of each DG is a stable constant at 56 %. According to the objectives, the performance of DG units under full power output is not satisfactorily to be applied.
- The total power of DG units under BAS actually can cover the total loads; But due to individual operation of DG units without any communication and coordination, the import power from the main grid is needed particularly in 2nd and 3rd sequences. The DG efficiency under BAS in 1st sequence is 60%, and slightly drops to 58.6% in 2nd sequence. Finally the efficiency decreases again to 55.5% at 3rd sequence.
- By developing logic algorithm supported with communications which allow information exchange among the DG units, the SAS can improve BAS performance. The metering on the grid connection shows that the power flow can be minimized to zero (in 1st and 3rd sequences) and slightly export power circa 0.2 kW to the grid (in 2nd sequence).
- At TEAS the logic control algorithm had been improved to track optimum efficiency of the VPP, thus the efficiency is increased significantly particularly in 2nd and 3rd sequences to 59.1% and 60% respectively. Moreover the power export/import of near zero kW is achieved and thus due to these performances, the TEAS is the ultimate solution for Virtual Power Plant.

Chapter 6

VPP Contribution to Voltage Regulation

6.1 Introduction

As known from the static analysis the voltage in a system is strongly influenced by the reactive power flow. Consequently the voltage can be controlled to desired values, by control of the reactive power. Increased production of reactive power gives higher voltage nearby the production source, while an increased consumption of reactive power gives lower voltage. Some components and devices can be used to regulate the reactive power in a power system. While the active power is entirely produced in the generators of the system, there are several sources of reactive power.

Important producers of reactive power are:

- Overexcited synchronous machines
- Capacitor banks
- The capacitance of overhead lines and cables

Important consumers of reactive power are:

- Inductive static loads
- Under-excited synchronous machines
- Induction motors
- Shunt reactors
- The inductance of overhead lines and cables
- Transformer inductances
- Line commutated static converters

The following factors influence primarily the voltages in a power system:

- Terminal voltages of synchronous machines
- Impedances of lines
- Transmitted reactive power
- Turns ratio of transformers

For some of these the reactive power is easy to control, while for others it is practically impossible. The reactive power of the synchronous machines is easily controlled by means of the excitation [35].

6.2 The simulation and scenarios

This chapter shows the investigation of voltage and reactive power behaviour between VPP and main grid during dynamic load. The focus is to know the VPP contribution of voltage regulation. In order to achieve this objective, various scenarios are applied.

During simulation, the distribution networks models (main grid/line parameters, distributed generation and dynamic loads model) are similar with previous chapters. The DG units are also controlled to follow the dynamic loads. The difference is only at the load profile; as shown in figure 71 and 72, load 1 and load 3 are constant at full power consumption (29 kW). On the other hand, load 2 has dynamic profile, at first sequence load 2 is running constant at 29 kW, but at the second sequence the load is decreasing to 20.3 kW. And at third sequence, the load is rising back to full power consumption 29 kW.

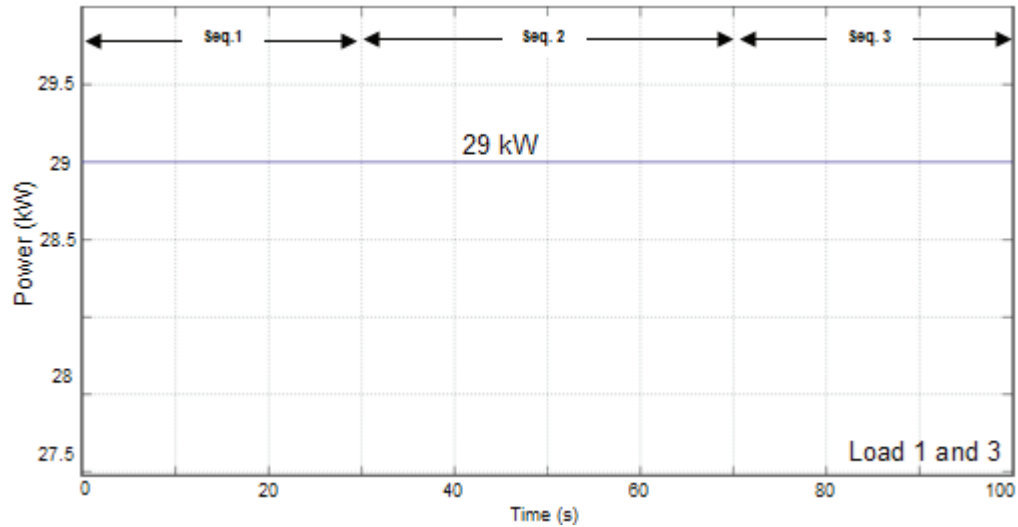


Figure 71. Profile of load 1 and load 3

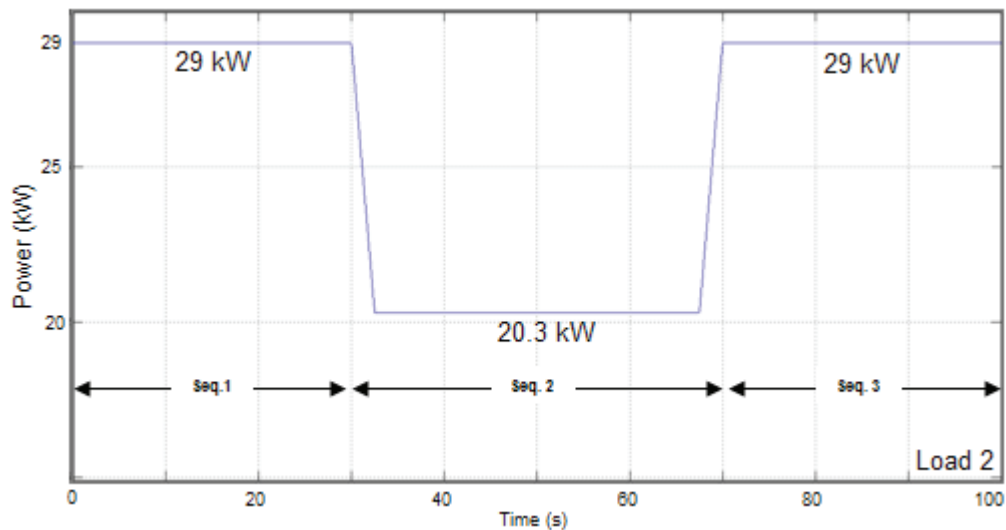


Figure 72. Profile of load 2

6.2.1. Simulation of one DG unit parallel to main grid.

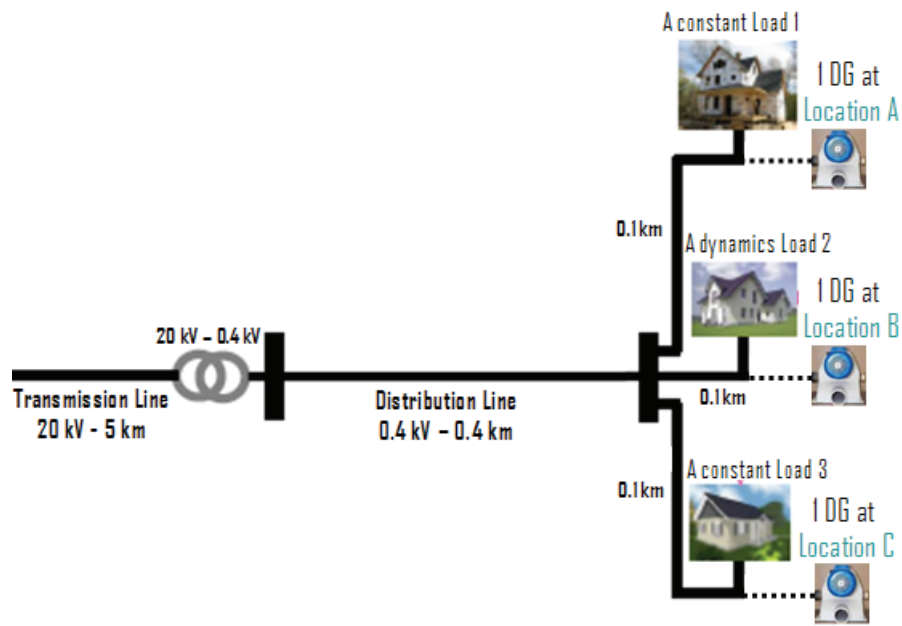


Figure 73. Installation of one DG unit at variation location

As shown in figure 73, there are three possibilities to place one DG unit at the main grid e.g. at location A, B and C in order to cover load 1, load 2 and load 3 respectively. The first scenario is placing one DG unit at location A to supply power for load 1, and the other loads are supplied power from the main grid. The second scenario, one DG unit is placing at location B, then the DG follows the dynamic load as describe in figure 72. Whereas load 1 and load 3 are supplied power from the main grid. In the last scenario, one DG unit is placed at location C, and the main grid supplies power to the load 1 and load 2. The voltage profiles during these scenarios are shown in figure 74, 75 and 76.

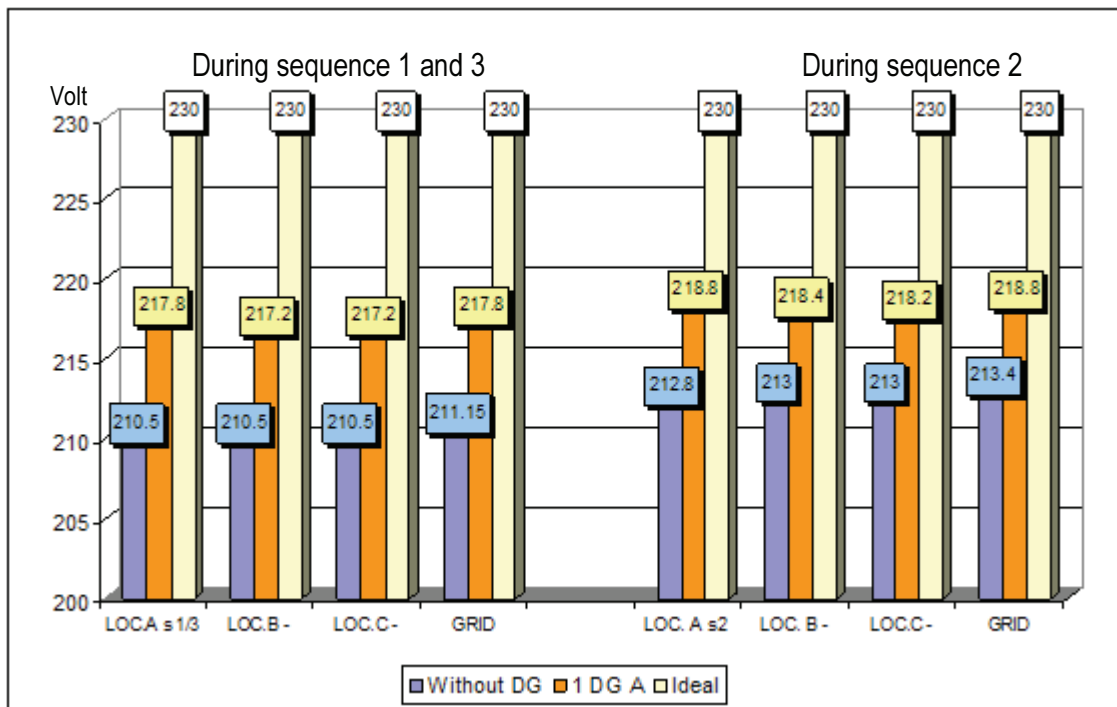


Figure 74. Voltage profile after installation one DG unit at location A

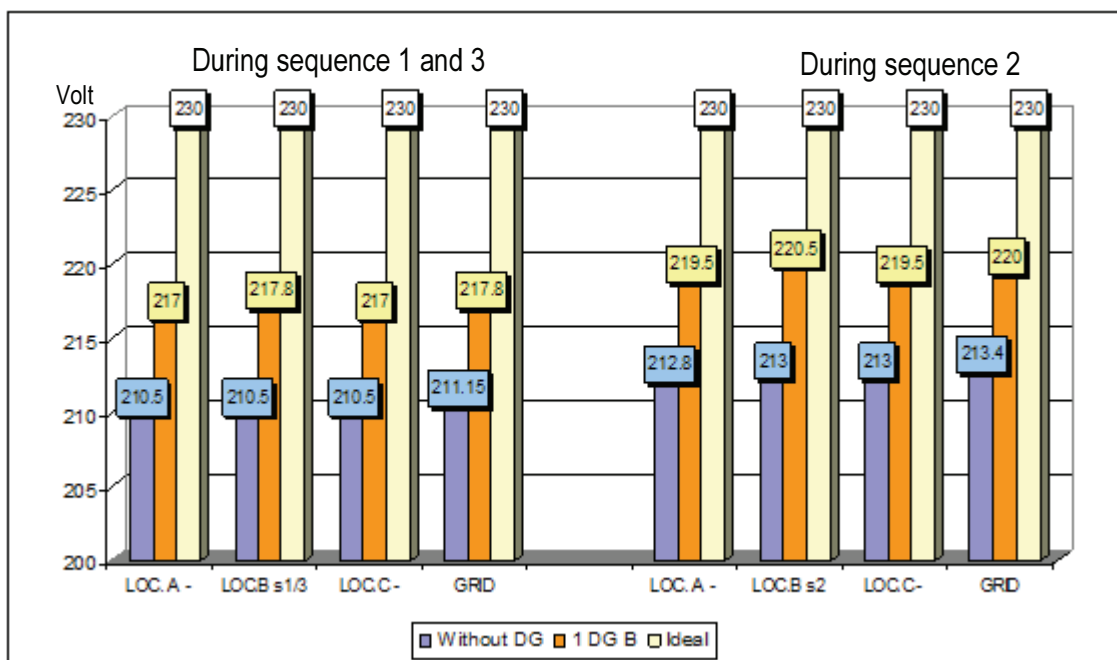


Figure 75. Voltage profile after installation one DG unit at location B

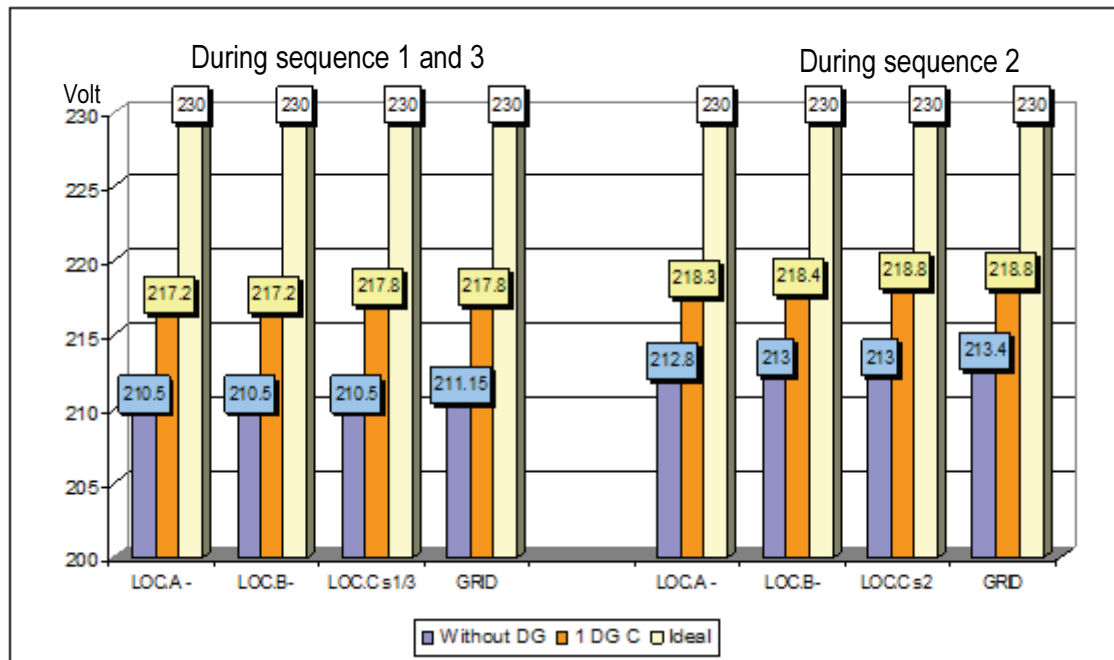


Figure 76. Voltage profile after installation of one DG unit at location C

The graphs show that before installing one DG unit, the voltage profile in load 1 particularly during 1st and 3rd sequences is around 210 – 211 V. When the load is decreasing circa 30 % the voltage is increasing slightly circa 213 volt. Generally, installation of one DG at each location can improve the voltage profile circa 5.5-7 volt. These voltage profiles are affected by reactive power produced or consumed by DG. When the DG is placed at location A or location C, then the DG unit produces low reactive power circa 0.25 kVAr during peak demand (see figure 77). When load 2 is decreasing and the other loads are still constant at full demand, then the DG reacts by absorbing reactive power circa 1.5 kVAr from the grid. Afterwards the voltage profile is kept around 218-220 volt. It shows that the DG (synchronous machine) can be made to generate or absorb reactive power depending upon the excitation applied. The output of synchronous machines continuously varies over the operating range and automatic voltage regulators can be used to control the output so as to maintain a constant system voltage.

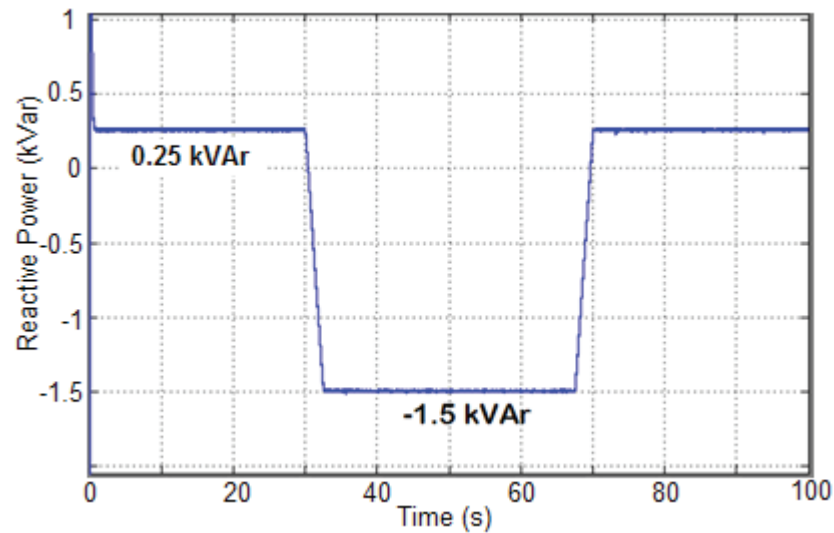


Figure 77. Reactive power from DG unit at location A or C

When the DG is placed at location B, and all load is steady at full demand, the DG produces reactive power of around 0.25 kVar. And when the load 2 decreases from 29 kW to 20 kW, the DG injects more reactive power from 0.25 kVar to 5.4 kVar (see figure 78), then the voltage is stable at around 219-220 volt.

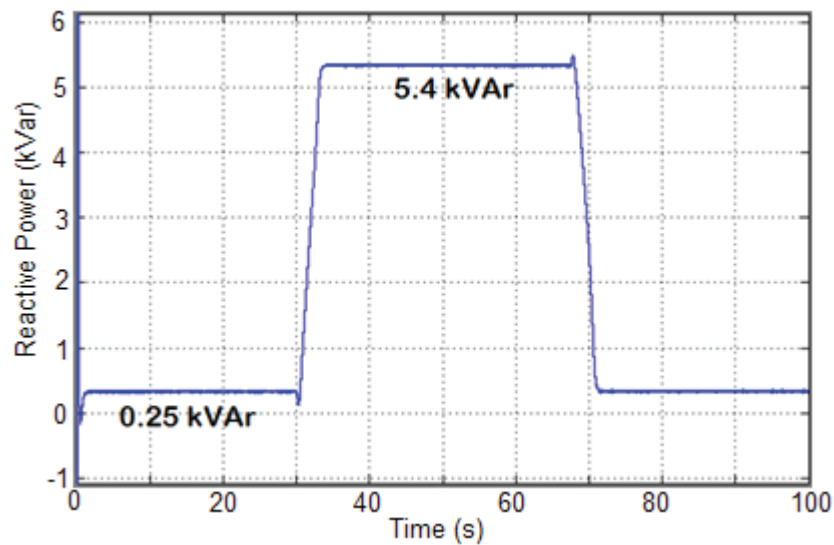


Figure 78. Reactive power from DG unit at location B

6.2.2 Simulation two DG units parallel with main grid

There are three combination possibilities to place two DG units on the grid as shown in figure 79.

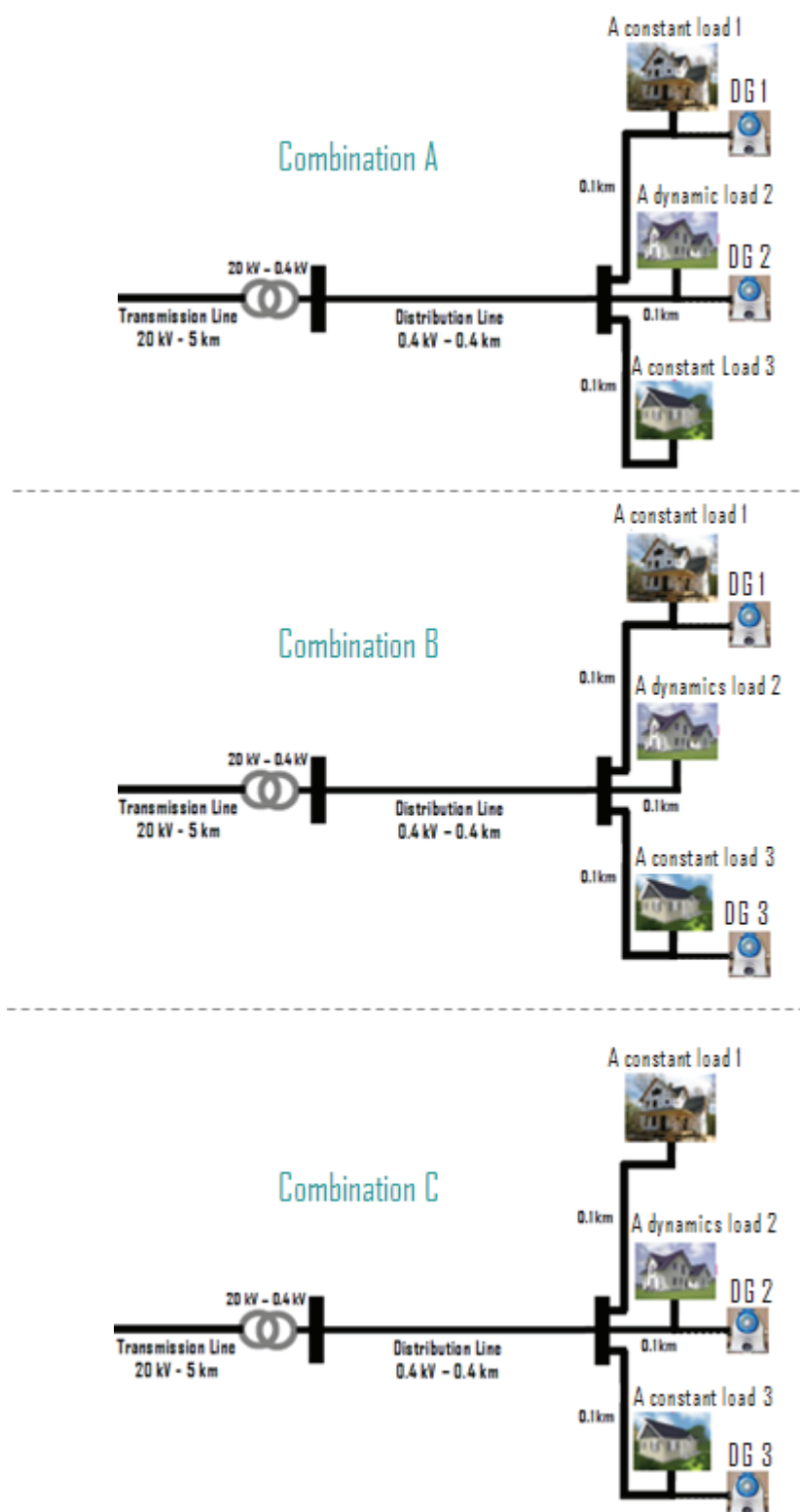


Figure 79. Location of two DG units with three variation combination

The results of installing two DG units are shown below.

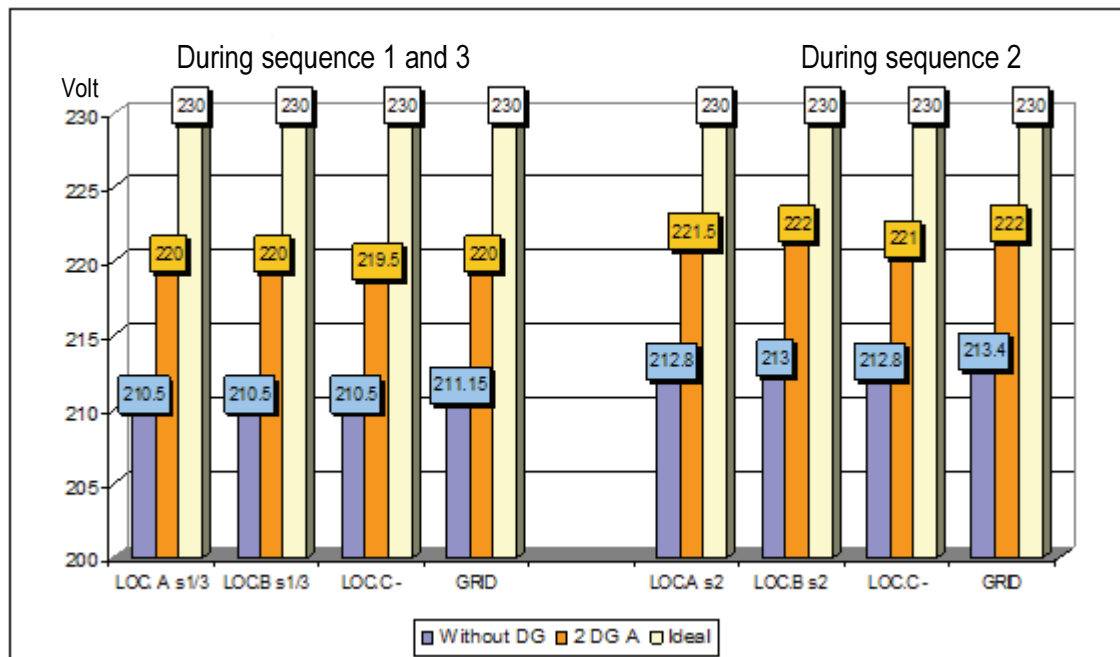


Figure 80. Voltage profile after installation of two DG unit (combination A)

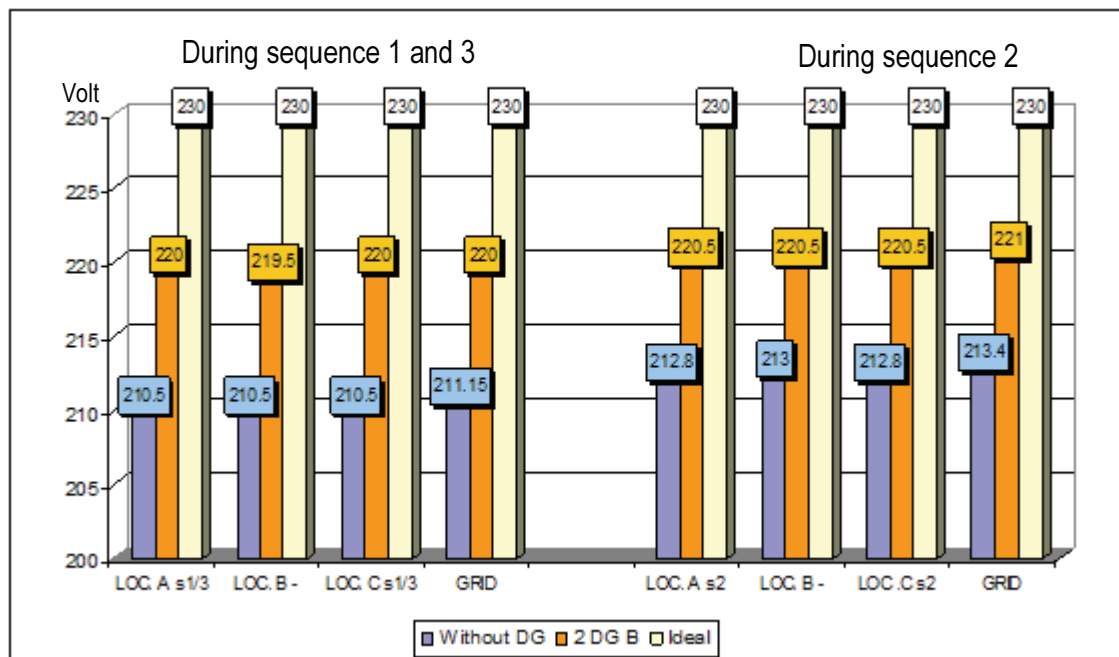


Figure 81. Voltage profile after installation of two DG unit (combination B)

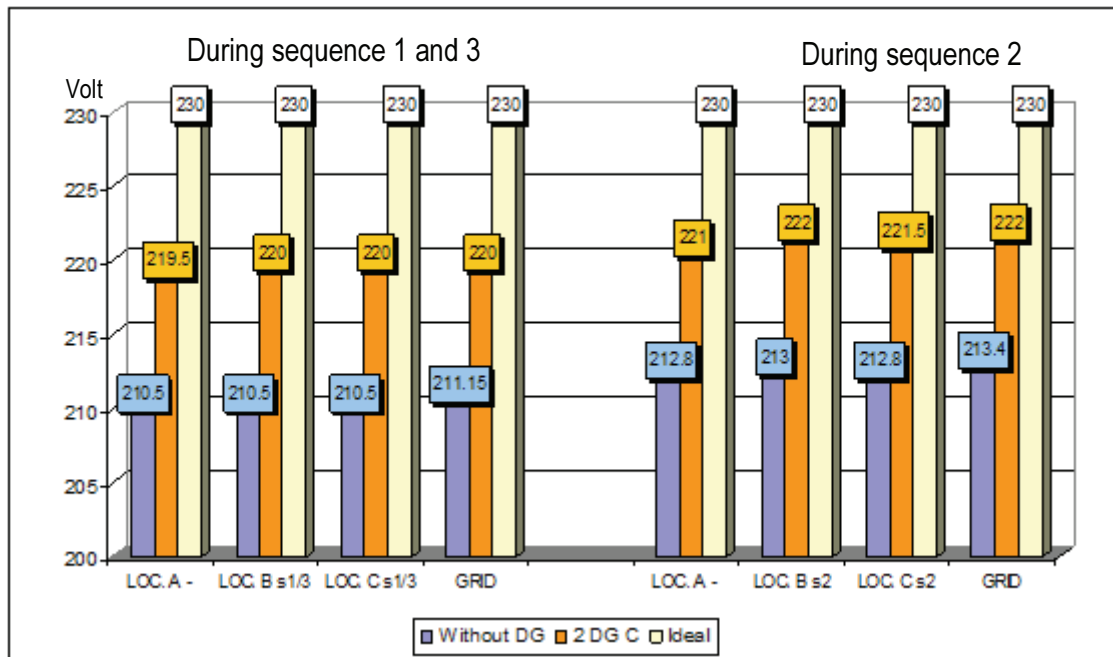


Figure 82. Voltage profile after installation of two DG unit (combination C)

Figures 83,84 and 85 show that the installation of two DG units improves the voltage profile from 210.5 (without DG) to circa 220 – 222 volt. The increasing voltage is around 9-10 volt from the condition without DG, and only circa 2 volt slightly higher than installation of one DG unit. During simulation of two DG units, the value of gain regulator at excitation system is similar to previous simulation (1 DG unit).

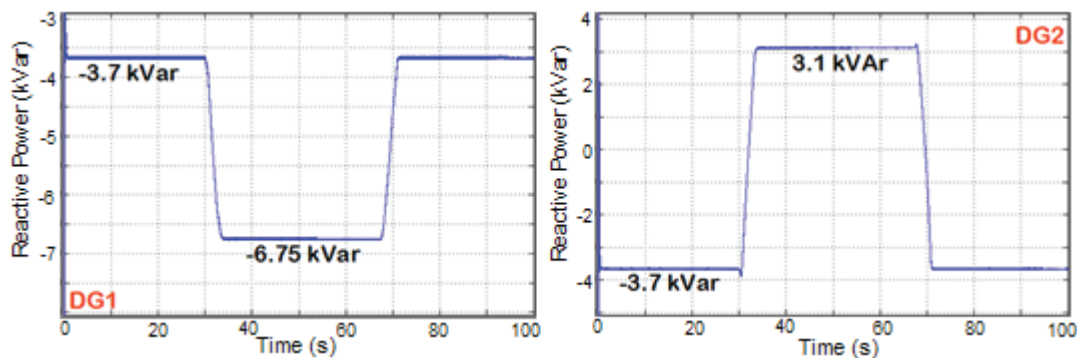


Figure 83. Reactive power behaviour of DG 1 and DG 2 (combination A)

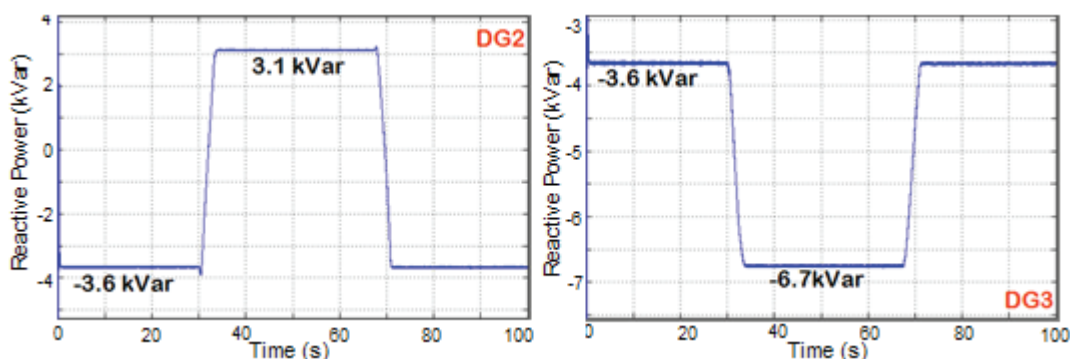


Figure 84. Reactive power behaviour of DG 2 and DG 3 (combination C)

At combinations A and C, when all load is running stable at 29 kW, then all DG units absorb reactive power from the grid circa 3.6 kVar - 3.7 kVar. And when load 2 is decreasing, DG 2 produces reactive power until circa 3.1 kVar. On the other hand, DG 1 or DG more absorbs more reactive power from 3.7 kVar to around 6.7 kVar. Therefore reactive power from the grid is coming to feed DG 1 and DG 3. Afterwards the voltage is kept stable at 220-221 volt.

At combination B (DG1 and DG 3), when the loads are stable constant at full demand, then DG1 and DG3 absorb reactive power 3.6 kVar from the grid to keep the voltage. And when load 2 is decreasing, DG 1 and DG 3 absorb more reactive power from the grid to circa 4.7 kVar to keep the voltage around 220 volt (see figure 85).

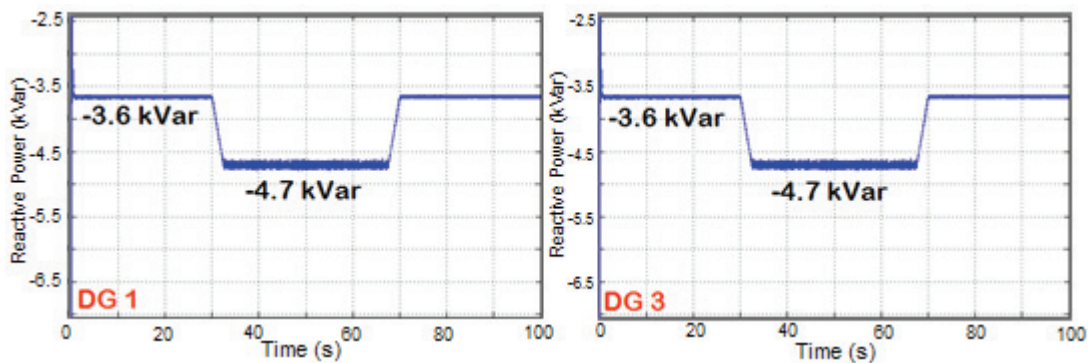


Figure 85. Reactive power behaviour of DG 1 and DG 3 (combination B)

6.2.3 Simulation of three DG units parallel to main grid

Three DG units under autocontrol system are connected to the grid with variation of gain regulator at excitation system (see figure 86). The behaviour of the reactive power and the voltage profile are presented in figure 87.

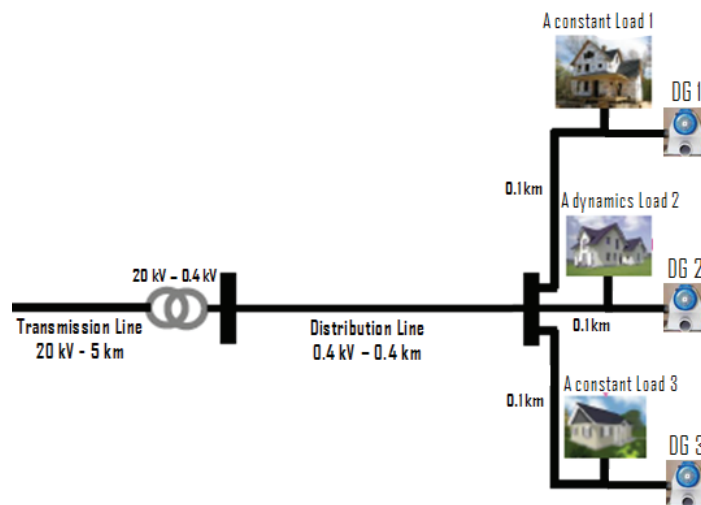


Figure 86. Three DG units parallel with main grid

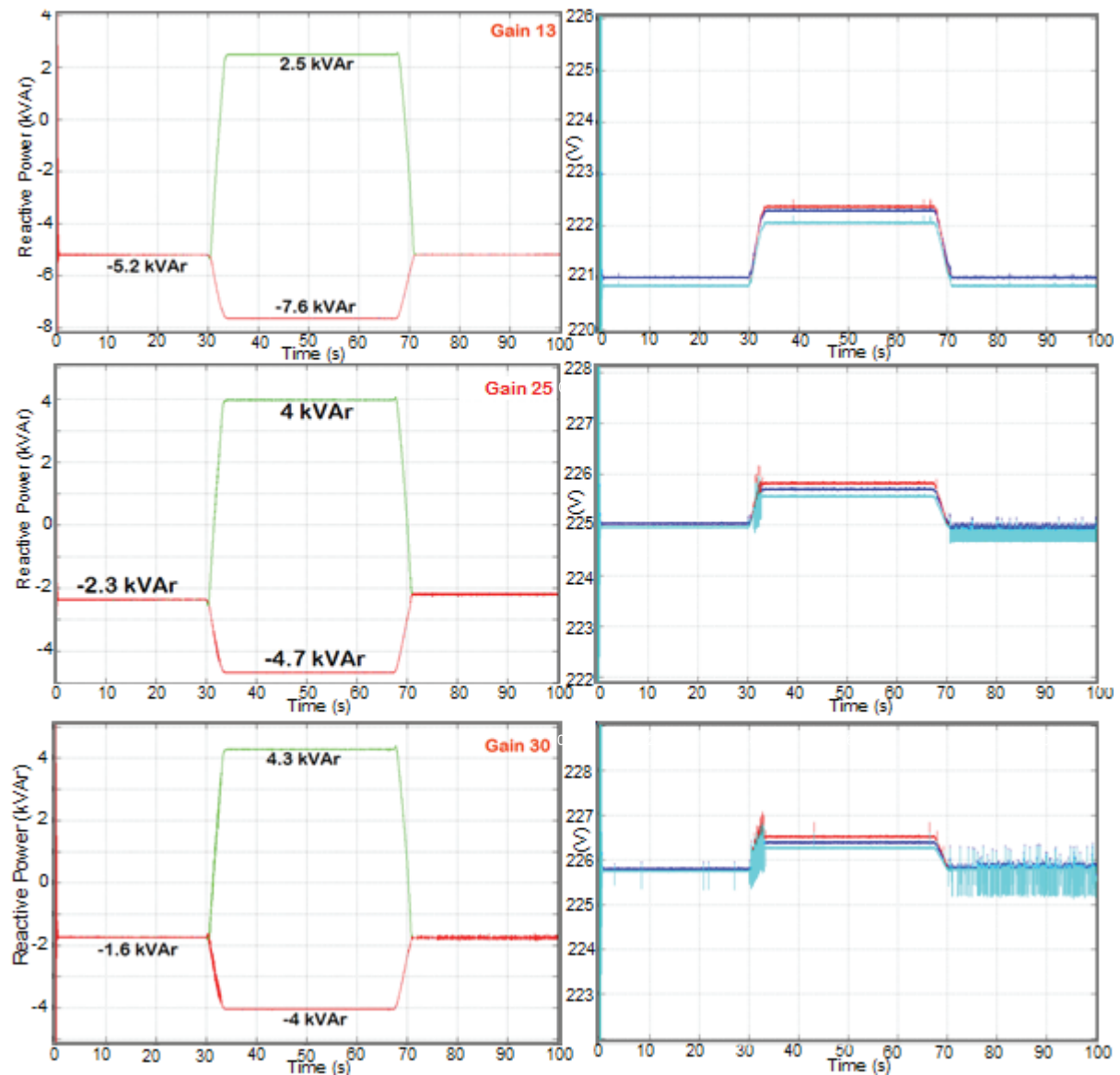


Figure 87. Reactive power behaviour and voltage profile of three DG units with gain variation

The figure shows that at gain 13 during 1st and 3rd sequence, each DG unit absorbs reactive power circa - 5.2 kVar. And when load 2 ramps down circa 30 % (at 2nd sequence), the reactive power of DG 2 (green line) rises from - 5.2 kVar to 2.5 kVar. On the other hand, DG 1 and DG 3 are absorbing reactive power from the grid until - 7.6 kVar (red lines). Then the voltage profile remains stable at around 221- 222 volts (see figure 88).

Adjusting gain regulator from 13 to 20 of each DG decreases the absorption of reactive power from the grid. The total reactive power of three DG units at 1st and 2nd sequence is circa - 3.2 kVar. And when load 2 is decreasing, total absorption of reactive power is circa - 5.5 kVar (smaller than at gain 13). On the other hand, DG 2 produces more

reactive power until circa 3.5 kVar (slightly higher than at gain 13). The voltage profile is also increasing slightly from 221-222 volt to 224 – 225 V.

At gain 25, the absorption of reactive power at DG 1 and DG 3 during 1st and 3rd sequence is circa minus 2.3 kVar (smaller than at gain 20). And in 2nd sequence, the absorption of reactive power at DG 1 and DG 3 is around - 4.7 kVar. In contrary DG 2 produce reactive power slightly higher than at gain 20. Then the system voltage achieve circa 225-226 volts. It shows that adjusting gain regulator on the DG enables to control the reactive power behaviour; furthermore it influences voltage profile on the system.

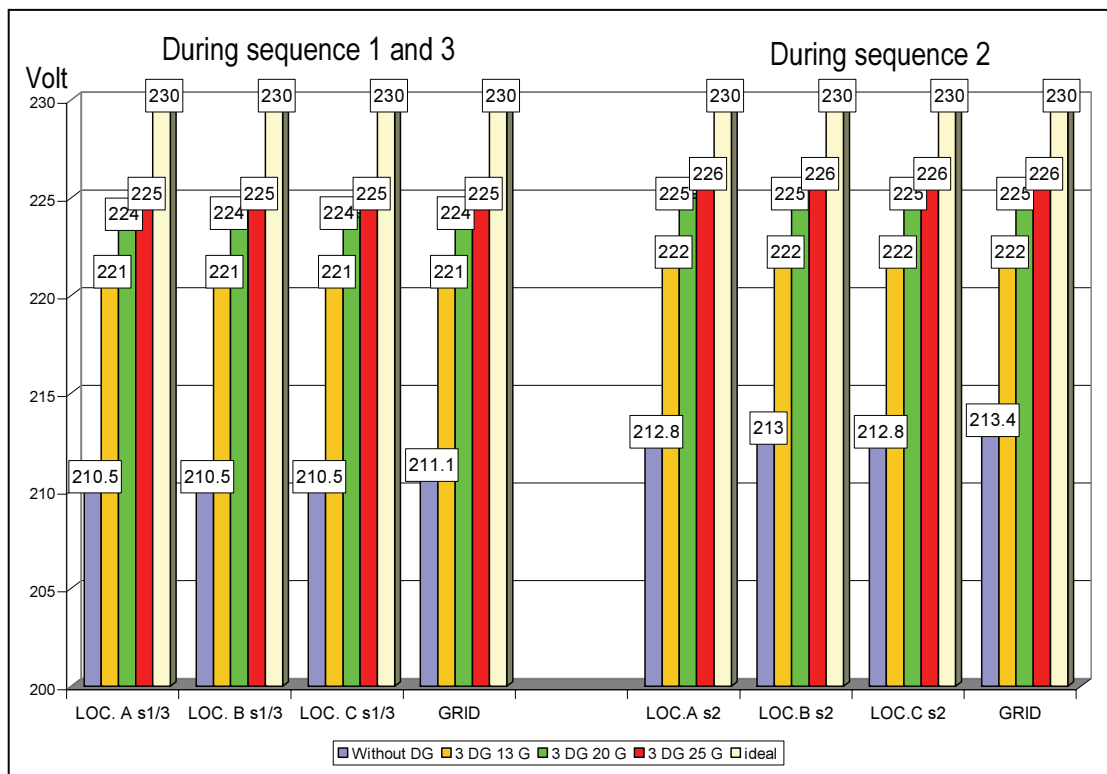


Figure 88. Voltage profile of three DG units with gain excitation variation

The correlation between DG installation and voltage profile is shown in figure 89. The voltage profile before installing DG units is around 210 volt (lower than minimum Australian standard (-6%) but still within in European standard (-10%). The voltage profile rises by the increase of DG installation on the main grid.

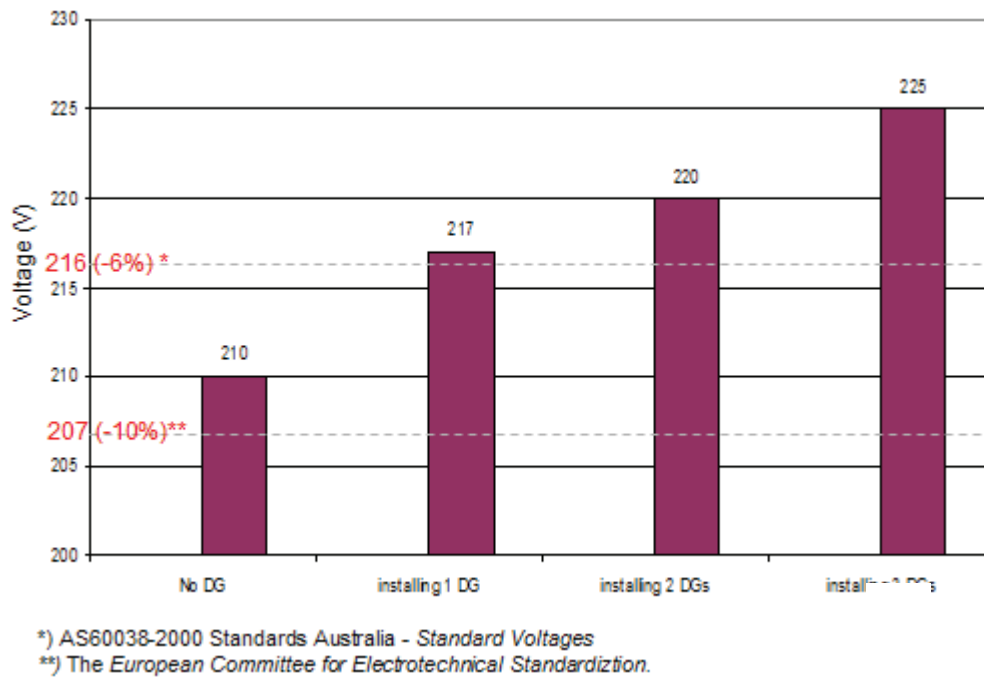


Figure 89. The correlation between DG units installation and increasing voltage profile

6.2.4 The voltage profile of three DG units under BAS, SAS and TEAS.

This sub chapter presents the continuing comparison of three DG units under BAS, SAS and TEAS in terms of voltage profile. Before installing Virtual Power Plant near the loads, the voltage profile is around 212 to 215 volt (see figure 90). The colours lines are representation of voltage profile at three loads and the bus.

The simulation result in figure 91 shows that in 1st sequence, the voltage of each feeder under BAS, SAS and TEAS is stable at 226 volts. In 2nd sequence, the voltage is decreasing to around 225 volt. Due to this result, the virtual power plant which is consisted of three DG units improves the voltage profile significantly.

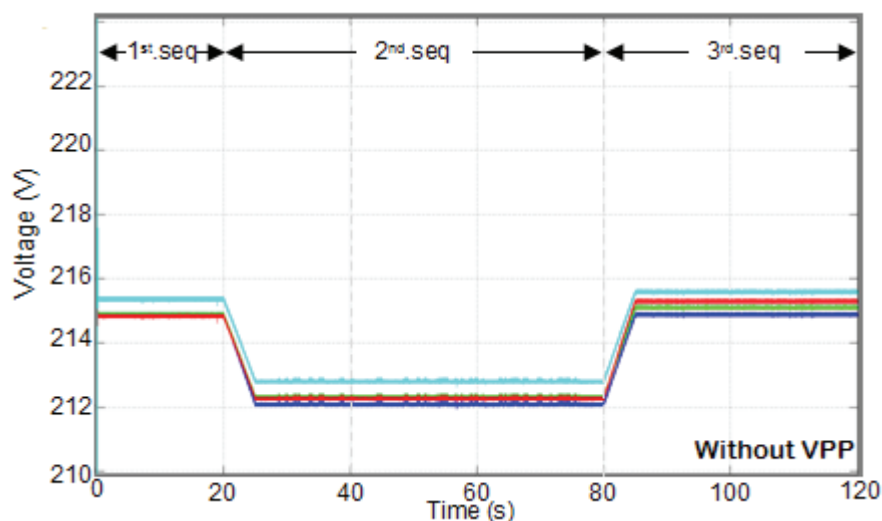


Figure 90. Voltage profile without Virtual Power Plant

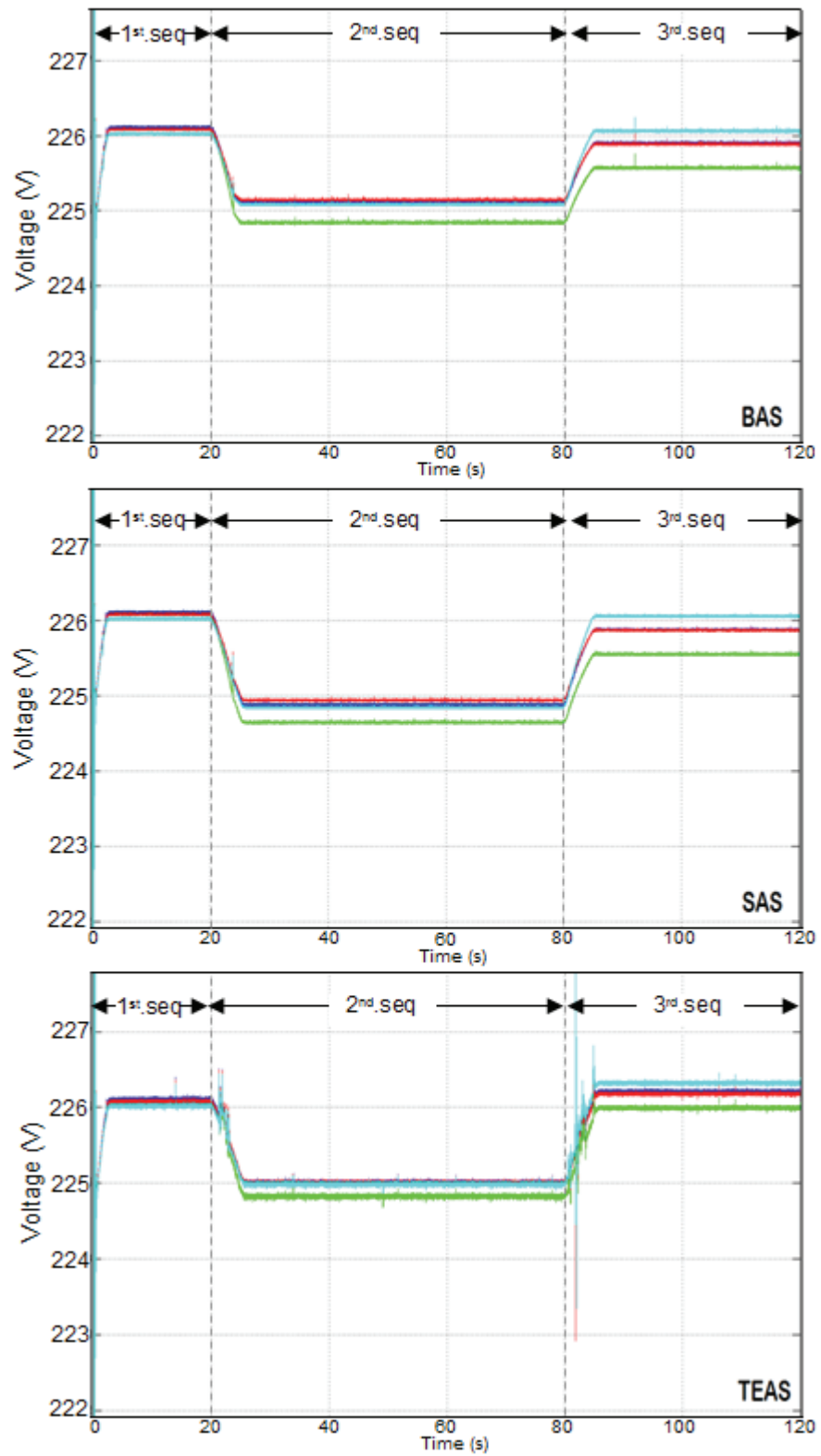


Figure 91. Comparison voltage profile under BAS, SAS and TEAS

6.3 Conclusion

- Placing one, two and three DG units near the load can improve voltage profile by 6-7 volt, 9-10 volt and 11-14 volt respectively. In this case, the variations /combinations of placing DG units do not impact to the increasing voltage profile.
- The controlling of gain regulator on the DG excitation affects the reactive power behaviour, furthermore it affecting the voltage profile. The increase in the quantity of DG installed into the distribution grid should be followed by adjusting excitation gain in order to achieve desired voltage profile.
- The voltage profile under BAS, SAS and TEAS during dynamic load is relatively stable at a range of 225 V – 226 V.

Chapter 7 Conclusion

7.1 Conclusion

The dissertation presented the concept for controllability of Virtual Power Plant focusing on the development of aggregation control of three DG units in order to achieve optimum efficiency of virtual power plant and minimize power export/import during dynamic load conditions. Starting with proposing definition and types of virtual power plant, the dissertation goes on to present the simulation results of various DG controls.

The first control system which has been applied in the simulation is called basic autocontrol system (BAS). This system is applied to control DG output according to load signal, thereby enabling the DG to follow dynamic loads. The drawback of this system is the absence of coordination among DG units, therefore as shown in simulation results and power is still imported from the main grid to compensate the remaining load. In order to improve the BAS performance, the smart autocontrol system (SAS) is developed. In contrast to the previous control system, this system has a control coordination centre (CCC) which is responsible for controlling a number of DG units. The coordination control of DG units and loads is realized by means of information exchange and logic algorithm. By using similar scenario, the SAS performance clearly shows that power import can be prevented and the load is fully covered by adequate coordination of the DG units. It further indicates that SAS can increase the reliability of VPP. However the efficiency issue is not considered in the two previous controls, therefore the TEAS (tracking efficiency autocontrol system) was developed. Principally this system is similar to SAS in terms of utilization of information exchange. In simulation, the VPP under TEAS is operated in decentralised control architecture where the local controllers are connected to each other forming a ring topology through communication line. The key role of this system is the logic algorithm which is able to track optimum total efficiency of VPP and still keeping export/import power minimized even during dynamic loads conditions.

The last simulation result shows that the VPP contributes to increase the voltage particularly to locations near the DG. Controlling gain regulator on the DG excitation affects the reactive power behaviour, and thus influencing the voltage profile.

7.2 Relevant contribution and future works

The most relevant contribution of this work is:

- Various DG controls have been proposed and applied in simulation showing particularly that the logic control algorithm of TEAS is able to achieve optimum efficiency and keep minimizing export and import power during dynamic loads. This logic algorithm can be applied to control more than three DG units. Moreover it can be used to achieve optimum total efficiency of VPP even if the DG units have different efficiency curves.

The suggestions for further research are:

- The autocontrol system should be tested by experiments. The local controller should be developed to process the load signals which will be transmitted to the DG controller. A fast communication infrastructure will be required.
- Another topic for further research is to investigate the performance of autocontrol system during transition mode from grid connected to isolated operation.

List of References

- [1] John Christensen, Fatima Denton, Amit Garg, Sami Kamel, Romeo Pacudan: The Role of Renewable Energy in a Carbon-Constrained World, A Paper Prepared for REN21, UNEP Risoe Centre Eric Usher, UNEP Energy Pre-Publication Draft December 2005.
- [2] Markus Bayegan: ABB's vision of the future electricity, Carnegie Mellon Electricity Industry Center March 20, 2002.
- [3] <http://www.planktos.com/educational/carbon.htm>.
- [4] Mohammad Shahidehpour, Yaoyu Wang: Communication and Control in Electric Power System Applications of Parallel and Distributed Processing, John Wiley & Sons Inc. Juli 2003.
- [5] CIGRE Working group WG 37-23: Impact of increasing contribution of dispersed generation on the power system, September 1998.
- [6] M.Vignolo and R.Zeballos: Transmission networks or distributed Generation?. In First International Symposium on Distributed Generation, Stockholm: Royal Institute of Technology, 2001.
- [7] H.L Willis.: Analytical Methods and Rules of Thumb for modelling DG – Distributed Generation Interaction, Proceeding of the 2000 IEEE Power Engineering Society Summer Meeting 2000, Vol. 3, pp.1643 – 1644, July 2000.
- [8] Judith B.Cardell and M.Ilic: Integrating Small Scale Distributed Generation into a Deregulated Market: Control Strategies and Price Feedback – Massachusetts Institute of Technology -PhD Thesis, pp 19 September 1997.
- [9] H.Lee Willis and Walter G.Stott: Distributed Power Generation Planning and Evaluation, New York, 2000.
- [10] Robert C. Sonderegger: Distributed Generation Architecture and Control ,<http://www.rand.org/scitech/stpi/Evision/Supplement/sonderegger.pdf>
- [11] Donald Von Dollen: Consortium for Electric Infrastructure to Support a Digital Society (CEIDS) Distributed Energy Resources Integration Element Program Plan, March 6, 2002.
- [12] Göran Andersson: Virtual Power Plants: Fiction or Reality? Lessons Learned and Challenges Ahead, ETH Zürich.
- [13] http://www.energyquest.ca.gov/time_machine/1870ce-1880ce.html
- [14] http://en.wikipedia.org/wiki/Electric_power_transmission

- [15] Markus Bayegan: A Vision of the Future Grid, IEEE Power Engineering Review, pp 10-11 December 2001.
- [16] EU Project: Virtual Fuel Cell Power Plant, pp 1-3, March 2003.
- [17] Erik Hennig: Die Idee des virtuellen Kraftwerks, EUS GmbH, Seminar Virtuelle Kraftwerke technische Voraussetzungen und Chancen, Unna, pp 2-3, March 2004
- [18] Fritz Santjer, Dr. Klaus Teichmann, Werner Steinert, Universität Siegen Grundlagen und Konzept eines Virtual Power Plant in Deutschland Basics and conception of a Virtual-Power plant in Germany.
http://www.dewi.de/dewi_neu/deutsch/themen/magazin/20/06.pdf
- [19] Gaudenz Koeppel: Distributed Generation Literature Review and Outline of the Swiss Situation. Internal report, pp 12-13, November 2003.
- [20] <http://www.gasunie.nl/downloads/jv/2003/docs/Flyer%20Virtual%20Power%20Plant.pdf>
- [21] Hans B.Puettgen, Paul R.Macgregor, Frank C. Lambert: Distributed Generation Semantic Hype or the Dawn of a New Era, IEEE Power and Energy Magazine, pp 24-25, January 2003.
- [22] Wuppertal Institut für Klima Umwelt Energie: Die technische Entwicklung auf den Strom und Gasmaerkten, April 2002.
- [23] Göran Ericsson: Classification of Power System Communications Needs and Requirements: Experiences From Case Studies at Swedish National Grid, IEEE Transactions Power Delivery, No.2, Vol. 17, April 2002.
- [24] A. Rufer: Solution for Storage of electrical Energy, Laboratoire d'électronique industrielle LEI EPFL, Ecole Polytechnique Fédérale de Lausanne, Switzerland, pp 1-4, 2003.
- [25] <http://ired.iset.uni-kassel.de/investire/index.html>
- [26] Göran Ericsson: Classification of Power System Communications Needs and Requirements: Experiences From Case Studies at Swedish National Grid, IEEE Transactions Power Delivery, No.2, Vol. 17. April 2002.
- [27] Donald J.Marihart: Communication Technology Guidelines for EMC/SCADA System, IEEE Transaction Power Delivery, No.2, Vol.16. April 2001.
- [28] An Arthur D. Little: Distributed Generation: System Interfaces, White Paper from http://www.encorp.com/dwnld/pdf/whitepaper/wp_AD_L_2.pdf.
- [29] Smith, Jeff and D.Tom Rizey: Power quality and the control of DG on distribution System, Electrotek Concept, Inc Knoxville – OAK Ridge National Laboratory, TN USA.

- [30] Ergebnisse der Arbeitsgruppe Energiemanagement und Betriebsführungsstrategien -praesentation_2006_0046.pdf, <http://neuk.iset.uni-kassel.de>
- [31] IEEE Working Group on Prime Mover and Energy Supply Models for System Dynamic Performance Studies: Hydraulic Turbine and Turbine Control Models for Dynamic Studies, IEEE Transactions on Power Systems, Vol. 7, No. 1, pp. 167-179. February, 1992.
- [32] Hoa D.Vu and J.E Agee: WECC Tutorial on Speed Governor, February 1998 WECC name revised 2002.
- [33] Recommended Practice for Excitation System Models for Power System Stability Studies, IEEE Standard 421.5-1992, August, 1992.
- [34]http://www.mathworks.com/access/helpdesk_r13/help/toolbox/simulink/ug/working_with_blocks15.html
- [35] K.Okuyama, T.Kato, K.Wu, Y. Yokomizu, T.Okamoto & Y Suzuoki: Improvement of Reliability of Power Distribution System by Information Exchange Between Dispersed Generators, IEEE PES Winter Power Meeting 2001.
- [36] R.Sai Anand: Algorithms for Call Control in Ring Based Networks, Dissertation. Swiss Federal Institute of Technology Zurich, 2004.
- [37] Goran Andersson: Modelling and Analysis of Electric Power Systems, Lecture 227-0526-00, ITET- Power Systems Laboratory ETH Zürich March 2006.

Appendix A. Calculation of R-L-C

All branches in simulation are represented by three phase parallel RLC branch. The length of overhead lines (L1) is 500 m, thus the R-L-C value can be obtained:

$$R = 0.156 \text{ ohm/km} \times 0.5 \text{ km} = 0.078 \text{ ohm}$$

$$X = \omega.L = 2.\pi.f.L \quad (5)$$

$$L = \frac{X}{2.\pi.f} = \frac{0.1226}{(2)(3.14)(50)} = 3.90e-4 \text{ H/km} ; 3.90e-4 \text{ H/km} \times 0.5 \text{ km} = 1.95e-4 \text{ H}$$

$$C = 235 \text{ nF/km} \times 0.5 \text{ km} = 117.5 \text{ nF}$$

The R-L-C value of overhead line (L2) can be calculated:

$$R = 0.2426 \text{ ohm/km} \times 5 \text{ km} = 1.213 \text{ ohm}$$

$$L = \frac{X}{2.\pi.f} = \frac{0.3614}{(2)(3.14)(50)} = 0.00115 \text{ H/km} ; 0.00115 \text{ H/km} \times 5 \text{ km} = 0.00575 \text{ H}$$

$$C = 10.12 \text{ nF/km} \times 5 \text{ km} = 50.6 \text{ nF}$$

Length of distribution line (L3) from distribution bus to transformer is 400 m and to each loads/DG units are 100 m (L4). Thus the R-L-C values of L3 and L4 can be obtained:

$$\text{For length 400 m, } R = 0.437 \text{ ohm/km} \times 0.4 = 0.174 \text{ ohm}$$

$$L = \frac{X}{2.\pi.f} = \frac{0.302}{(2)(3.14)(50)} = 9.617e-4 \text{ H/km} ; 9.617e-4 \text{ H/km} \times 0.4 \text{ km} = 3.846e-4 \text{ H}$$

$$C = 10.2 \text{ nF/km} \times 0.4 \text{ km} = 4.08 \text{ nF.}$$

$$\text{For length 100 m, } R = 0.437 \text{ ohm/km} \times 0.1 = 0.0437 \text{ ohm}$$

$$L = 9.617e-4 \text{ H/km} \times 0.1 \text{ km} = 9.617e-5 \text{ H}$$

$$C = 10.2 \text{ nF/km} \times 0.1 \text{ km} = 1.02 \text{ nF}$$

Appendix B. Resistance and Inductance of Transformer

For each winding the per unit resistance and inductance are defined as:

$$R_{pu} = \frac{R(\Omega)}{R_{base}} \quad (6)$$

$$L_{pu} = \frac{L(H)}{L_{base}} \quad (7)$$

The base resistance and base inductance used for each winding are:

$$R_{base} = \frac{(V_n)^2}{P_n} \quad (8)$$

$$L_{base} = \frac{(R_{base})}{2\pi \cdot f_n} \quad (9)$$

For the magnetization resistance R_m and inductance L_m , the p.u values are based on the transformer rated power and on nominal voltage of the winding one.

$$R_{base} = \frac{(20.000/\sqrt{3})^2}{250.000} = 533.33\Omega$$

$$L_{base} = \frac{533.33}{(2)(3.14)(50)} = 1.698H$$

Data from grid reference for $R_1 = 16$ ohm and $X_1 = 94.7$ ohm. Therefore to obtained L_1 :

$$L_1 = \frac{X_1}{2\pi \cdot f} = \frac{94.7}{(2)(3.14)(50)} = 0.3H$$

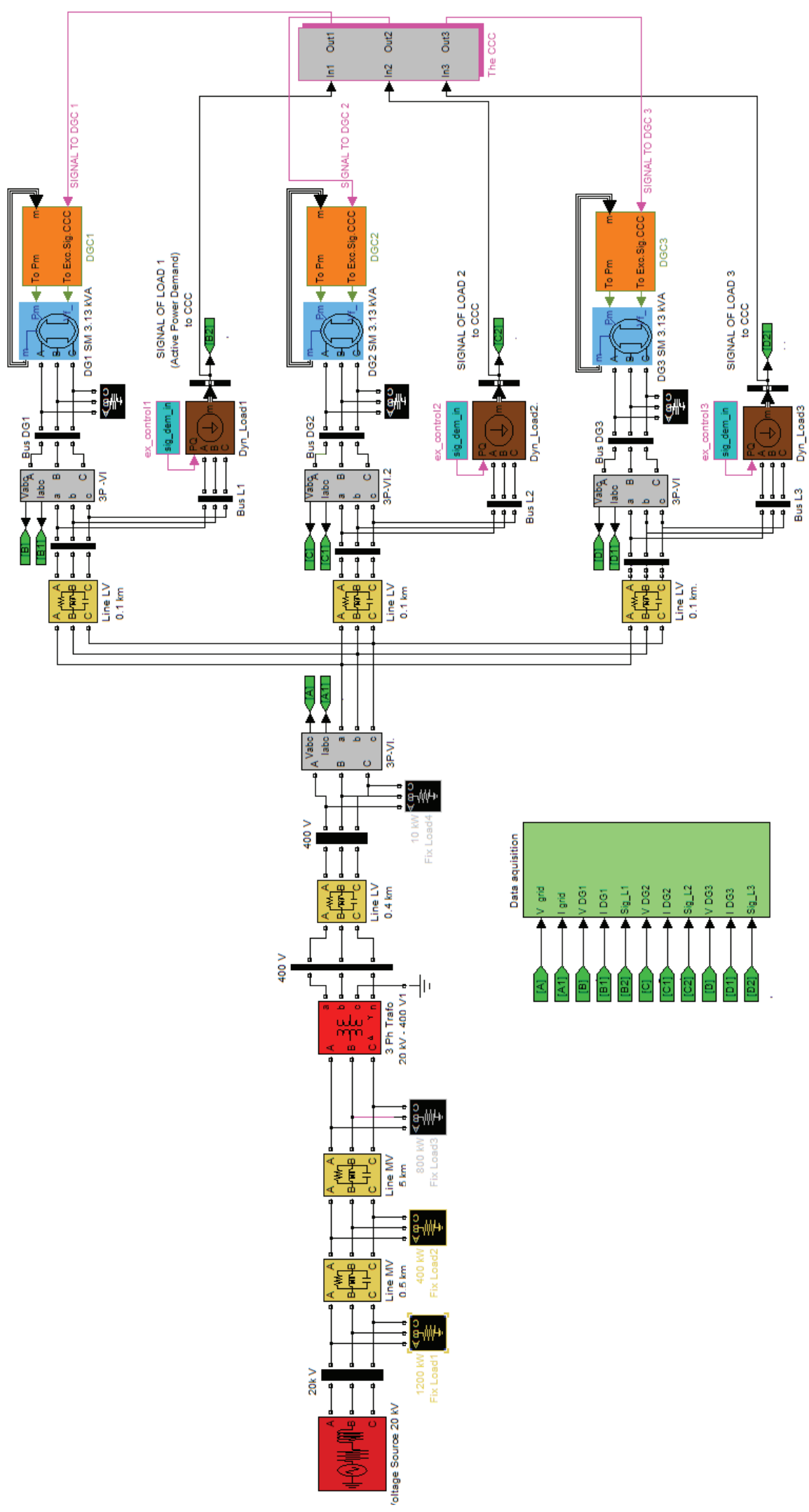
Supposed that the windings transformer (R_1) = 16 ohm and (L_1) = 0.3 H, the corresponding values to be entered in the simulation block are:

$$R_1 = \frac{16\Omega}{533.33\Omega} = 0.03pu$$

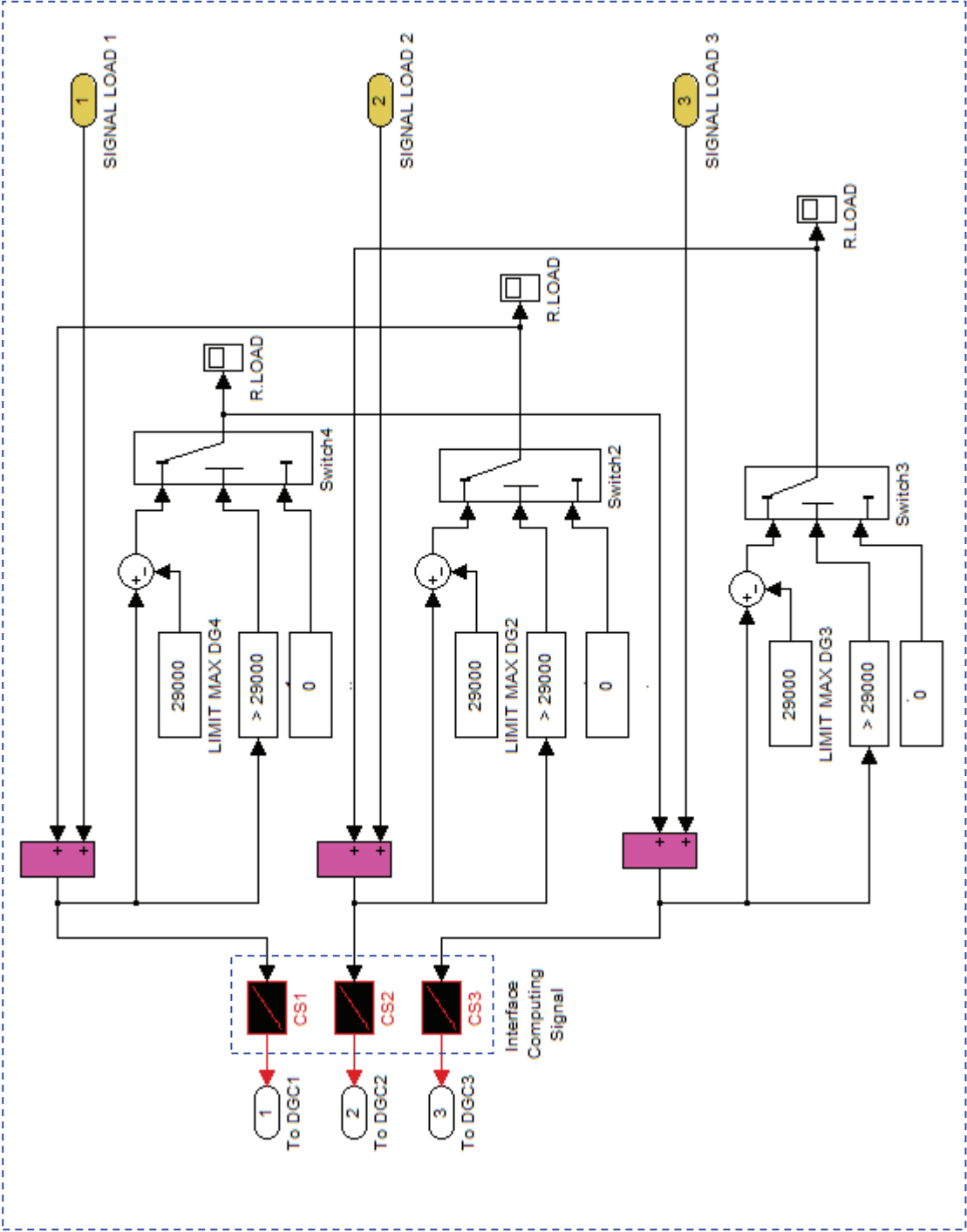
$$L_1 = \frac{0.3H}{1.698H} = 0.177pu$$

To specify a magnetizing current of 0.3% (resistive and inductive) based on nominal current. Thus the per unit values of $1/0.003 = 314$ p.u for resistance and the inductance of the magnetising branch.

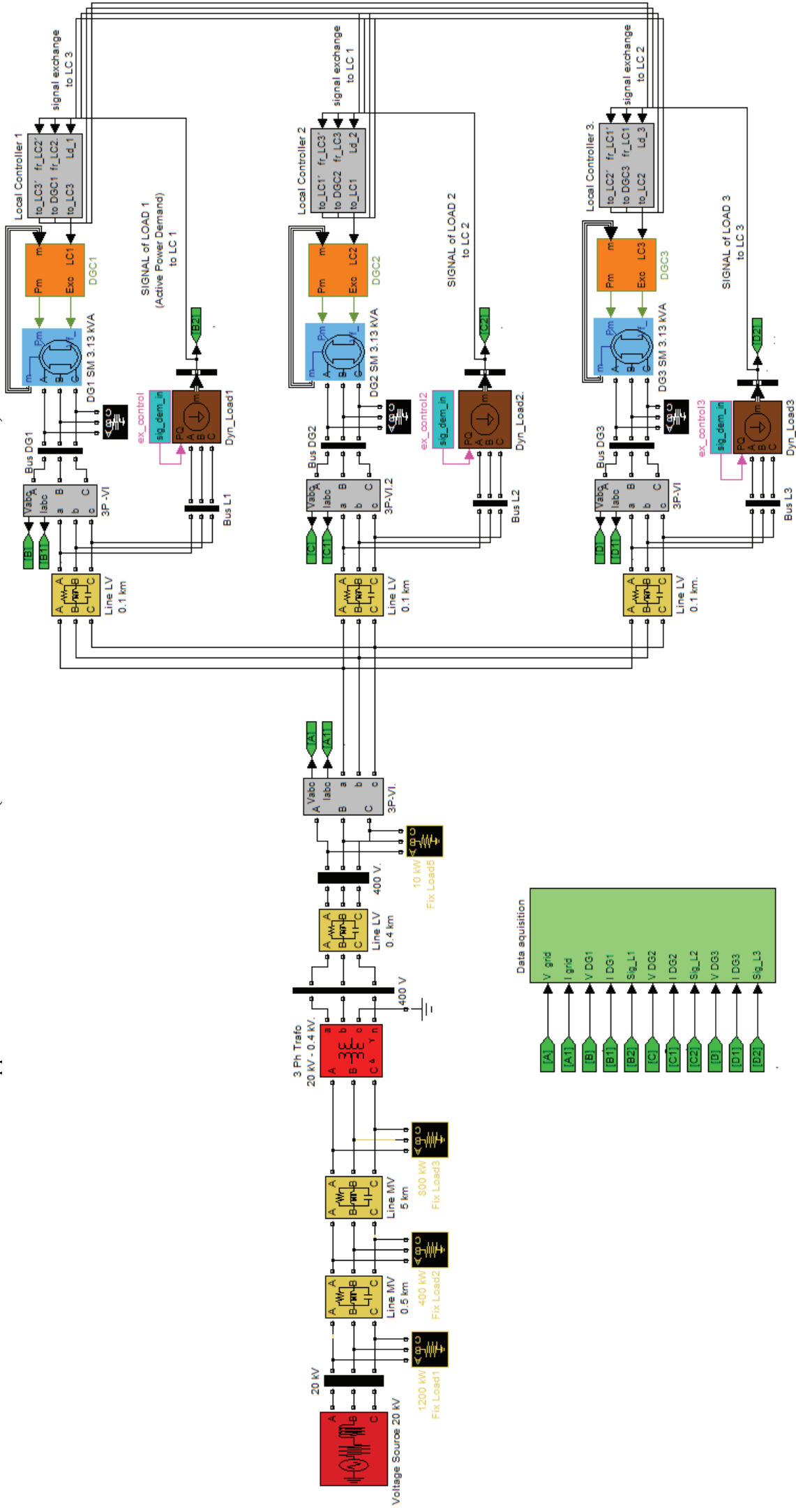
Appendix C. VPP under SAS (MATLAB SIMULINK ENVIRONMENT)



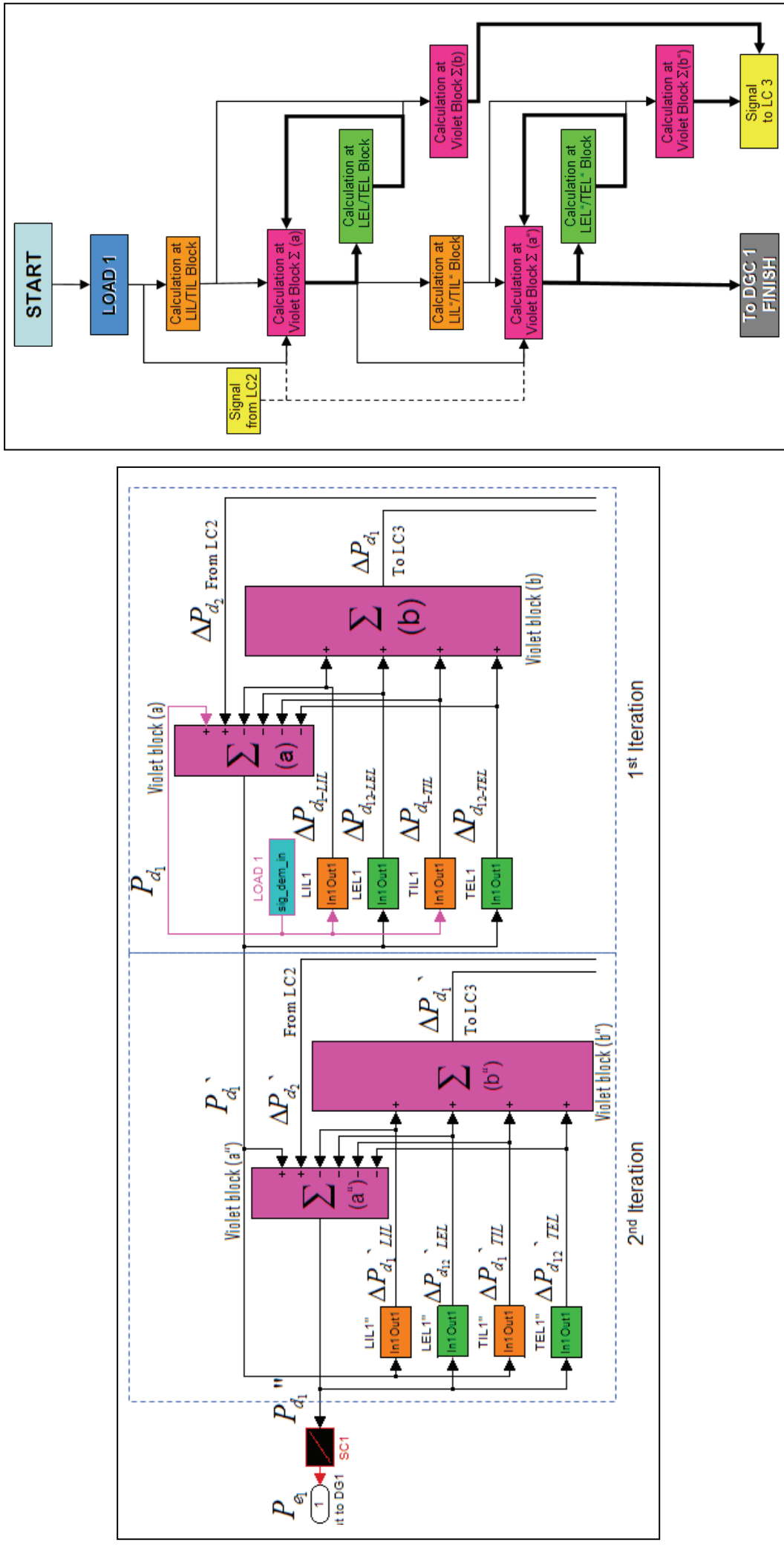
Appendix D. SAS Logic Algorithm (MATLAB SIMULINK ENVIRONMENT)

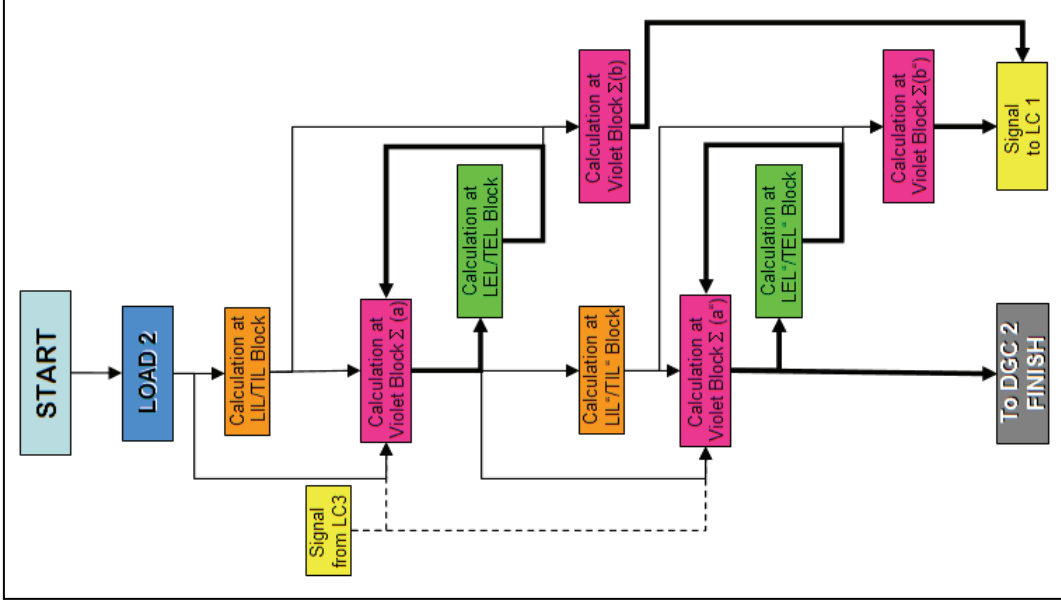
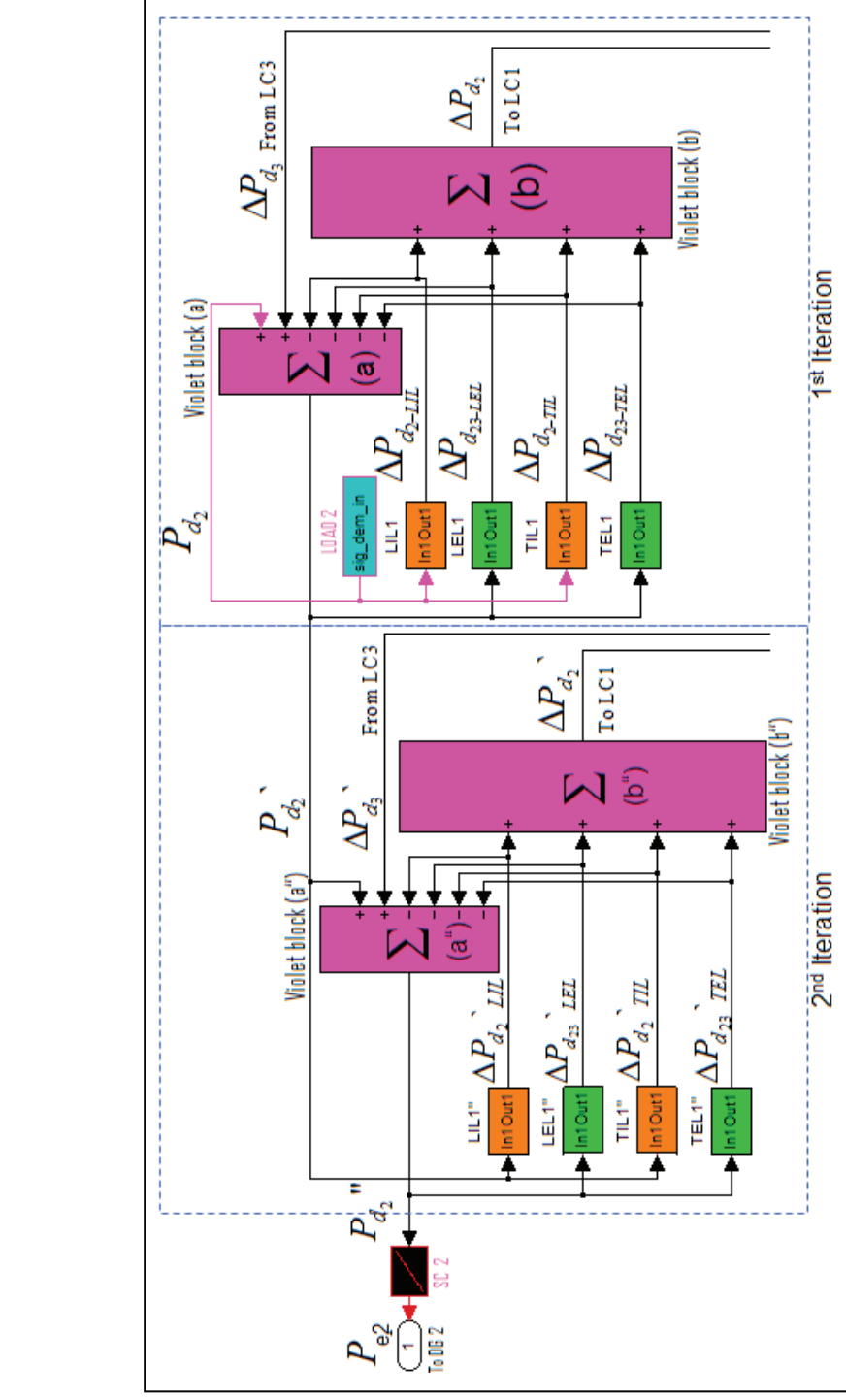


Appendix E. VPP under TEAS (MATLAB SIMULINK ENVIRONMENT)

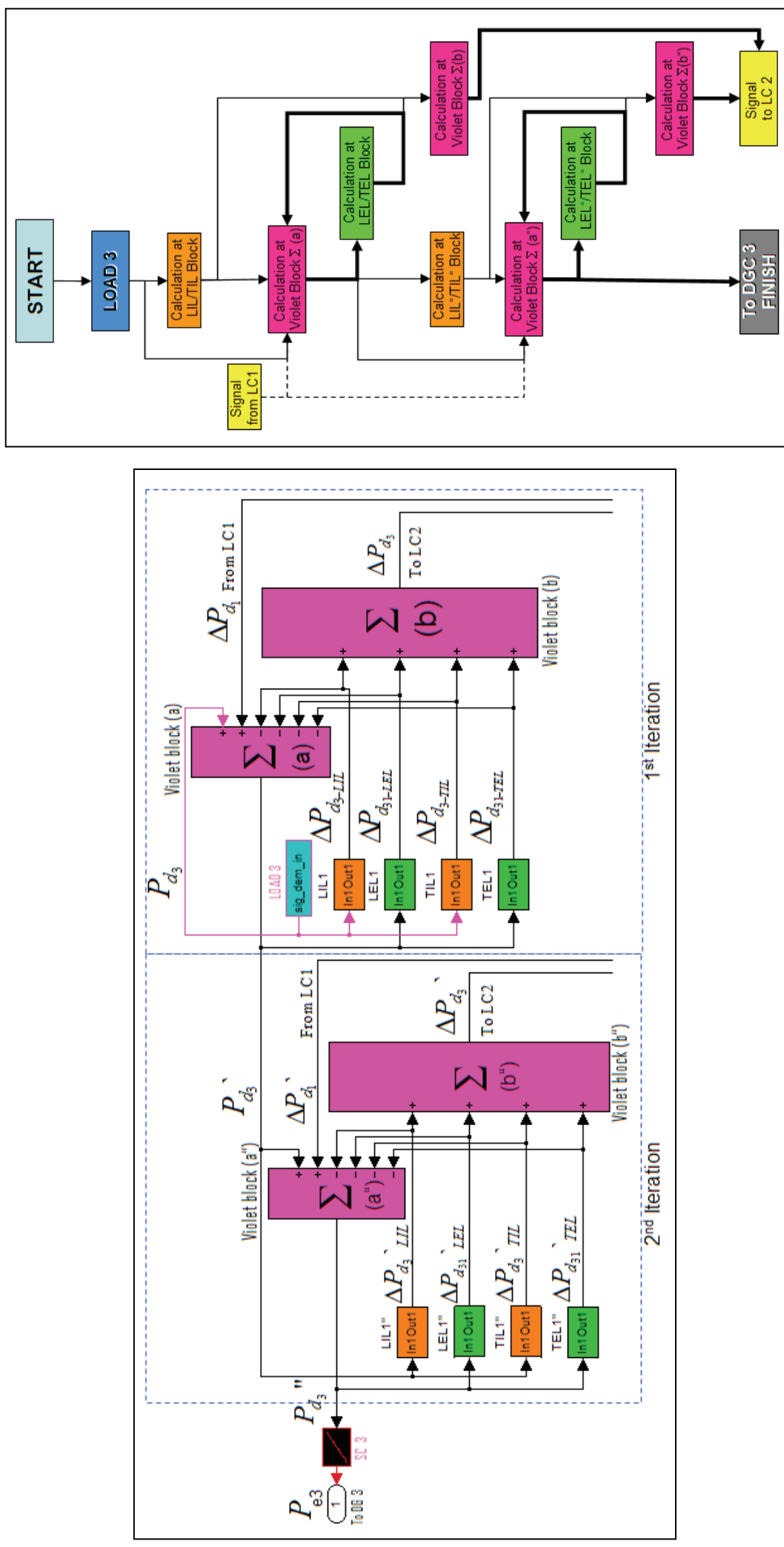


Appendix F. TEAS Logic Algorithm and Flow Chart at LC 1 (MATLAB SIMULINK ENVIRONMENT)





Appendix H. TEAS Logic Algorithm and Flow Chart at LC 3 (MATLAB SIMULINK ENVIRONMENT)



Appendix I. Relation of equation (1),(2),(3) and (4)

$$P_{e(n)} = P_{d(n)} + \sum_{m=1}^i [\Delta P_{d(n+1)}]_{(m)} + \sum_{m=1}^i (-1) \cdot [\Delta P_{d(n)}]_{(m)} \quad \dots(4)$$

Case n=1, m=2

$$P_{e(1)} = P_{d(1)} + [\Delta P_{d(2)}]_{(1)} + [\Delta P_{d(2)}]_{(2)} - [\Delta P_{d(1)}]_{(1)} - [\Delta P_{d(1)}]_{(2)}$$

$$P_{e(1)} = P_{d(1)} - [\Delta P_{d(1)}]_{(1)} + [\Delta P_{d(2)}]_{(1)} - [\Delta P_{d(1)}]_{(2)} + [\Delta P_{d(2)}]_{(2)}$$

$$P_{e_1} = P_{d_1} - \Delta P_{d_{12-LEL}} - \Delta P_{d_{1-TIL}} - \Delta P_{d_{12-TEL}} + \Delta P_{d_2} - \Delta P_{d_1_{LIL}} - \Delta P_{d_{12_{LEL}}} - \Delta P_{d_{1_{TIL}}} - \Delta P_{d_{12_{TEL}}} + \Delta P_{d_2} \quad \dots(1)$$

Case n=2

$$P_{e(2)} = P_{d(2)} + [\Delta P_{d(3)}]_{(1)} - [\Delta P_{d(2)}]_{(1)} + [\Delta P_{d(3)}]_{(2)} - [\Delta P_{d(2)}]_{(2)}$$

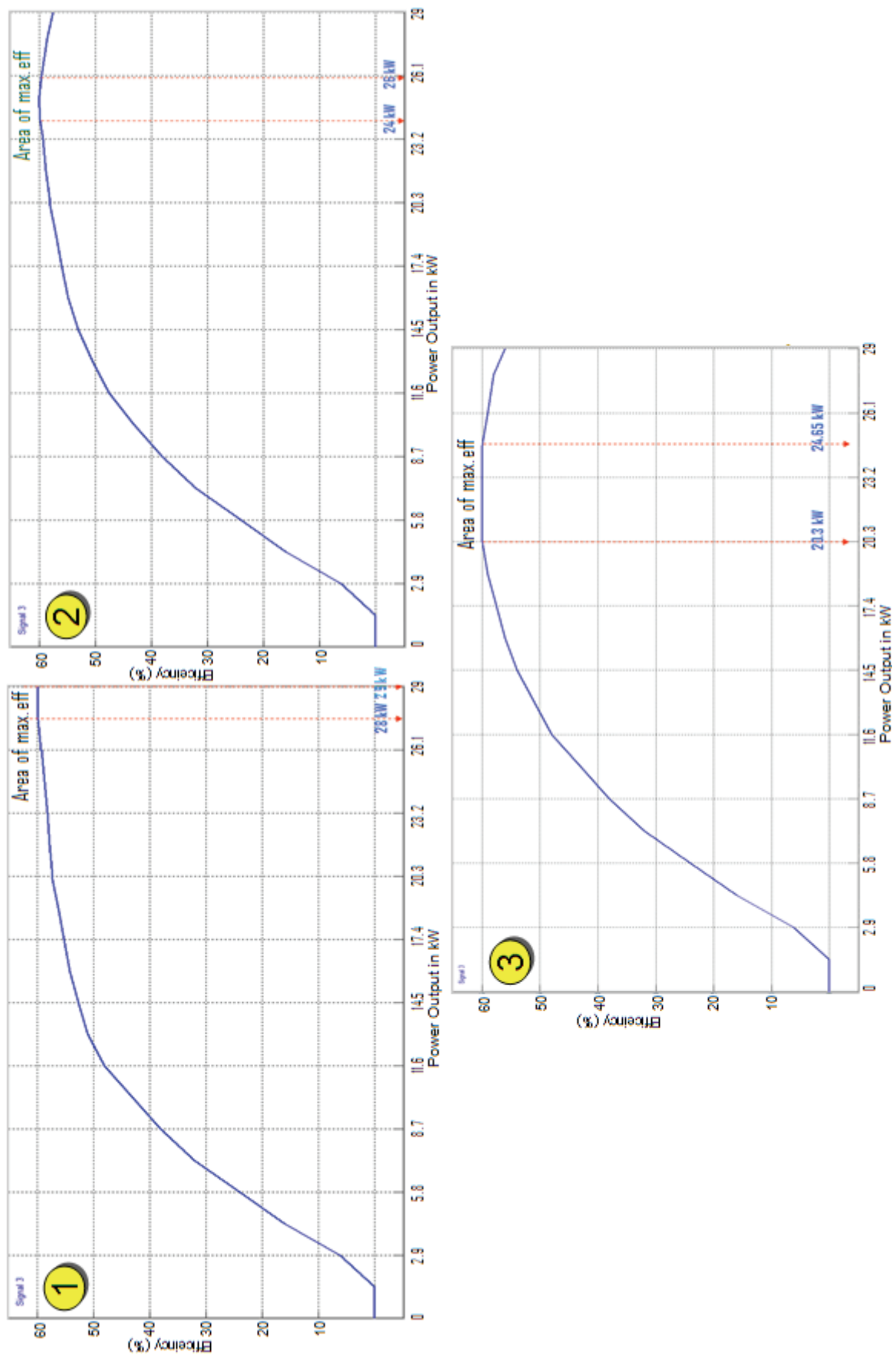
$$P_{e_2} = P_{d_2} - \Delta P_{d_{23-LEL}} - \Delta P_{d_{2-TIL}} - \Delta P_{d_{23-TEL}} + \Delta P_{d_3} - \Delta P_{d_2_{LIL}} - \Delta P_{d_{23_{LEL}}} - \Delta P_{d_{2_{TIL}}} - \Delta P_{d_{23_{TEL}}} + \Delta P_{d_3} \quad \dots(2)$$

Case n=3, k=3

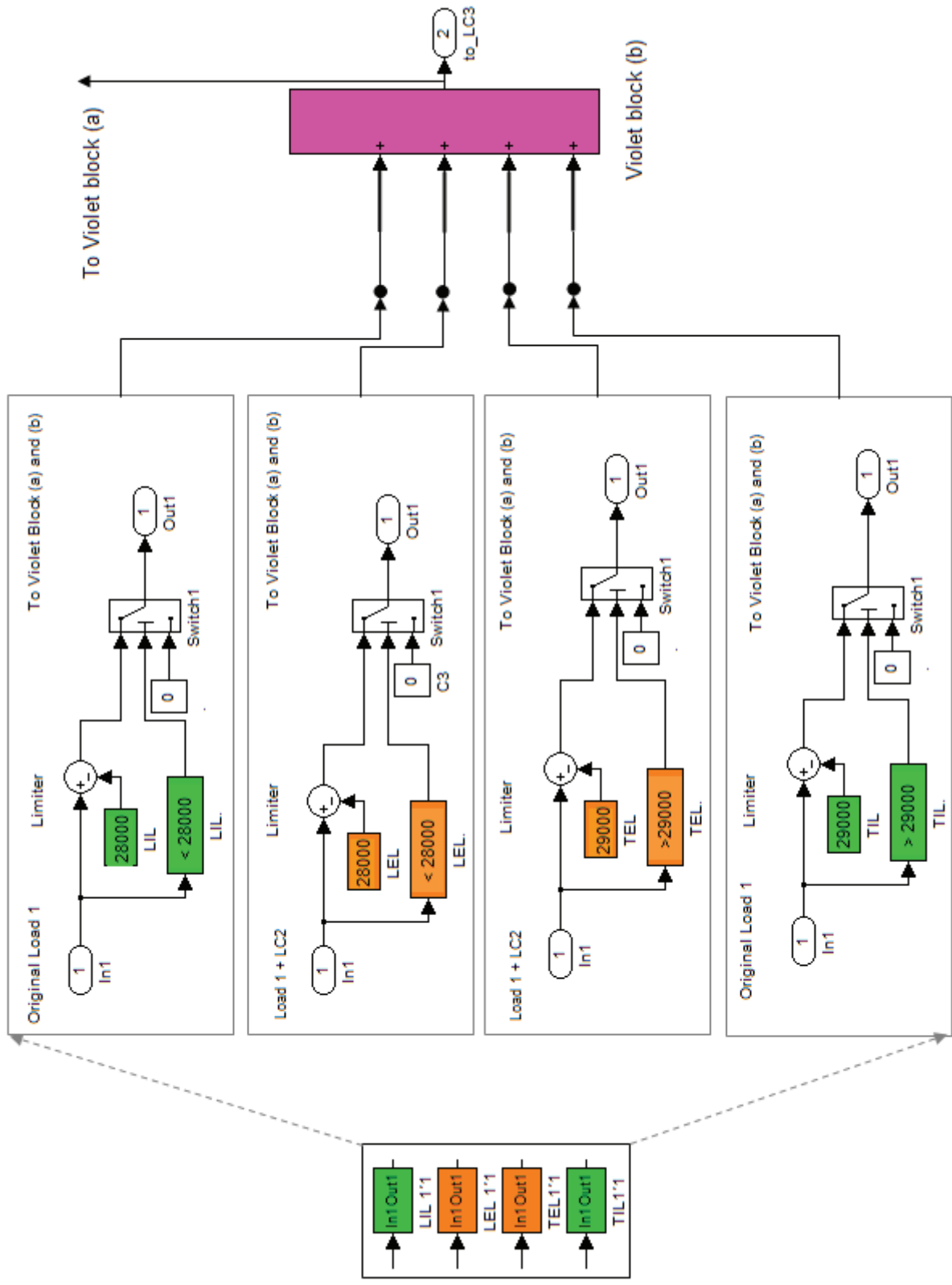
$$P_{e(3)} = P_{d(3)} + [\Delta P_{d(1)}]_{(1)} - [\Delta P_{d(3)}]_{(1)} + [\Delta P_{d(1)}]_{(2)} - [\Delta P_{d(3)}]_{(2)}$$

$$P_{e_3} = P_{d_3} - \Delta P_{d_{31-LEL}} - \Delta P_{d_{31-TIL}} - \Delta P_{d_{31-TEL}} + \Delta P_{d_1} - \Delta P_{d_3_{LIL}} - \Delta P_{d_{31_{LEL}}} - \Delta P_{d_{31_{TIL}}} - \Delta P_{d_{31_{TEL}}} + \Delta P_{d_1} \quad \dots(3)$$

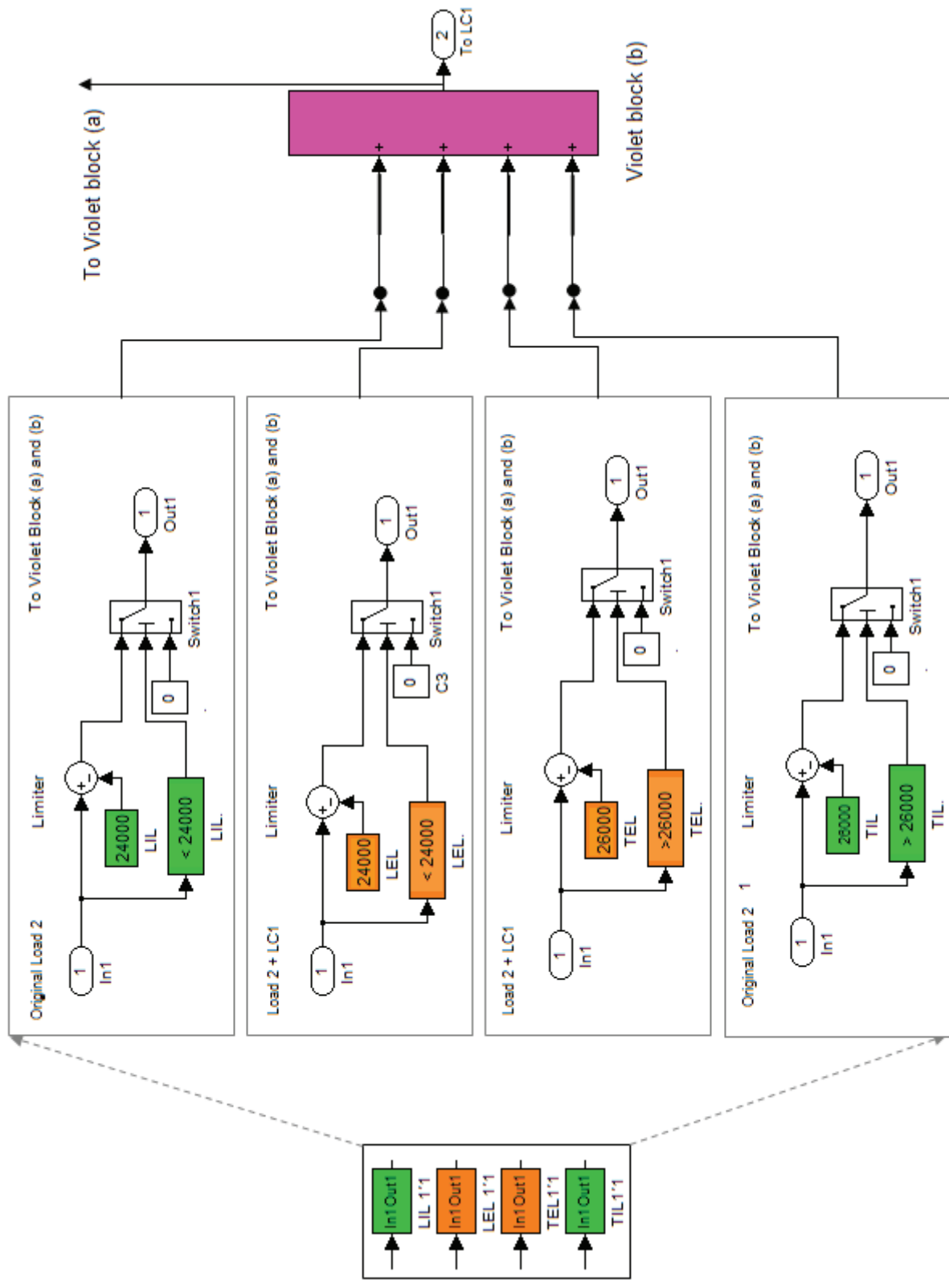
Appendix J. Three DG Units with Three Variation of Efficiency Curves



Appendix K. Setting of DG Power Parameter at LIL, LEL, TIL and TEL blocks (case DG1)



Appendix L. Setting of DG Power Parameter at LIL, LEL, TIL and TEL blocks (case DG2)



Appendix M. Setting of DG Power Parameter at LIL, LEL, TIL and TEL blocks (case DG3)

